

THE UNIVERSITY OF CALGARY

Dynamic Chain Exchange of Diblock Copolymer Micelles

by

Carl K. Smith

A DISSERTATION

SUBMITTED TO THE FACULTY OF GRADUATE STUDIES

IN PARTIAL FULFILLMENT OF THE REQUIREMENTS FOR THE DEGREE OF

DOCTOR OF PHILOSOPHY

DEPARTMENT OF CHEMISTRY

CALGARY, ALBERTA

SEPTEMBER, 1995

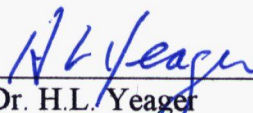
© Carl K. Smith 1995

THE UNIVERSITY OF CALGARY
FACULTY OF GRADUATE STUDIES

The undersigned certify that they have read, and recommend to the Faculty of Graduate Studies for acceptance, a thesis entitled "Dynamic Chain Exchange of Diblock Copolymer Micelles" submitted by Carl K. Smith in partial fulfillment of the requirements for the degree of Doctor of Philosophy.



Dr. G. Liu
Department of Chemistry



Dr. H.L. Yeager
Department of Chemistry



Dr. R. Paul
Department of Chemistry



Dr. J. Gleeson
Department of Physics



Dr. M.C. Williams, External Examiner
Department of Chemical Engineering
University of Alberta

October 17, 1995 Date

ABSTRACT

Two groups of matched diblock copolymers were synthesized by anionic polymerization for experiments measuring the rate of chain exchange of copolymer chains between molecularly dissolved unimers and micelles. They included polystyrene-*b*-poly(hydroxyethyl methacrylate) [PS-PHEMA], and poly(methyl methacrylate)-*b*-poly(methacrylic acid) [PMMA-PMAA]. Each set of copolymers included an unlabelled polymer and a matched polymer labelled with a pyrene chromophore.

Micelles of PS-PHEMA in cyclohexane / THF and PMMA-PMAA in ethyl acetate / methanol were characterized by viscometry and dynamic light scattering to determine the aggregation numbers. PMMA-PMAA micelles were formed in solutions of 80 % or greater ethyl acetate and PS-PHEMA formed micelles in solutions of 20 to 75 % cyclohexane. The critical micelle concentrations (CMC) of PS-PHEMA in 20 % cyclohexane / 80 % THF and of PMMA-PMAA in 85 % ethyl acetate / 15 % methanol and in 90 % ethyl acetate / 10 % methanol were determined by measuring an increase in the fluorescence lifetime of pyrene attached to the end of the core forming block upon the onset of micellization.

Two major goals of this research were to confirm the rate law and to measure the polymer chain exchange constant under various conditions. The kinetics experiments were conducted by mixing a micellar solution of the unlabelled copolymer with that of a solution of a matching pyrene labelled copolymer whose concentration was below its CMC. The incorporation of the labelled copolymer into micelles was following the variation in the fluorescence intensity of pyrene with time. The chain insertion rate

constant (k_p) was determined for PMMA-PMAA at 22 °C in 85 % ethyl acetate and in 90 % ethyl acetate.

Micelle chain exchange experiments were also attempted for PS-PHEMA in 20 % cyclohexane. At room temperature the rate of polymer chain exchange was not detectable after 36 hours, however after heating at 50 °C for one hour 60 % of the labelled chains were incorporated into micelles. The difference in the rate constants was likely due to a greater amount of hydrogen bonding between polymer chains in the cores of the micelles of the PS-PHEMA system.

ACKNOWLEDGMENTS

I would like to thank Dr. G. Liu who suggested diblock copolymer micelles as a research topic and for his guidance and encouragement throughout this project.

I would also like to express my gratitude to:

Dr. H.L. Yeager and Dr. R. Paul who have been mentors and teachers.

Dr. T. Chen and Dr. R. Kydd for their time during my candidacy exam.

Dr. J. Gleeson and Dr. M.C. Williams for taking the time to read my thesis.

Dr. N. Hu for synthesis of PS-PHEMA and PMMA-PHEMA and for teaching me how to synthesize my own polymers.

Dr. J. Tao for providing light scattering data.

Mr. Sean Stewart and Mr. Fred Henselwood for their help in the lab.

Mr. Mike Siewert for going far beyond the call of duty to make sure the instruments worked.

Spencer and Wendy Chambers for their support and understanding.

My parents who have supported and encouraged me in every possible way.

Cathy, my wife and best friend.

Margaret Evelyn for her special smile.

Financial support from the Faculty of Graduate Studies, the Department of Chemistry at the University of Calgary and NSERC is gratefully acknowledged.

TABLE OF CONTENTS

	Page
APPROVAL PAGE	ii
ABSTRACT	iii
ACKNOWLEDGMENTS	v
TABLE OF CONTENTS	vi
LIST OF TABLES	xi
LIST OF FIGURES	xii
LIST OF SYMBOLS AND ABBREVIATIONS	xviii
CHAPTER I. INTRODUCTION	1
I-1. Diblock Copolymer Micelles	1
I-2. Equilibrium Dynamics of Diblock Copolymer Micelles	6
I-3. Research Objectives	11
I-4. Organization of the Thesis	12
CHAPTER II. BACKGROUND	14
II-1. Characterization of Diblock Copolymers	14
II-2. Characterization of Diblock Copolymer Micelles	16
II-2.a. Dilute Solution Viscometry of Copolymer Micelles	16
II-2.b. Light Scattering	20
II-2.b.i. Static Light Scattering by Large Molecules in Solution	20
II-2.b.ii. Dynamic Light Scattering	22
II-2.b.iii. CMC and Micellization Kinetics by Light Scattering	23
II-2.c. X-Ray Scattering	24
II-2.d. Small Angle Neutron Scattering	25
II-2.e. Sedimentation Velocity and Gel Permeation Chromatography	26
II-2.f. Electron Microscopy	27

TABLE OF CONTENTS (continued)

	Page
III-3. Characterization of Diblock Copolymers	57
III-3.a. Characterization of FI-PMMA-H	57
III-3.b. Characterization of FI-PMMA-PHEMA-Py	57
III-3.c. Characterization of the Copolymers of PS-PHEMA	61
III-3.d. Characterization of FI-PMMA-PMAA-Py and PMMA-PMAA	69
III-4. Micelle Formation	76
III-5. Instrumental	76
III-5.a. Viscometry	76
III-5.b. Dynamic Light Scattering	78
III-5.c. Steady State Fluorescence	78
III-5.d. Time Resolved Fluorescence	79
III-5.e. UV-Visible Spectroscopy	79
III-5.e.i. UV-Visible Fluorescent Chromophores Standards	79
III-5.f. NMR	80
III-5.g. Gel Permeation Chromatography	80
 CHAPTER IV. CHAIN EXCHANGE KINETICS of PMMA-PMAA MICELLES	 83
IV-1. Introduction	83
IV-2. Theory	84
IV-2.a. Experimental Procedure	84
IV-2.b. Model of Dynamic Chain Exchange of Diblock Copolymer Micelles	86
IV-3. Experimental	91
IV-3.a. Fluorescence Experimental Results on PMMA-PMAA Micelles	91

TABLE OF CONTENTS (continued)

	Page
IV-3.a.i. Fluorescence Intensity Ratio (I_{Py}/I_{Fl}) to Determine Micellar Solvent Systems	91
IV-3.a.ii. Time Resolved Fluorescence Spectroscopy to Determine CMC	91
IV-3.b. Characterization of Micelles	100
IV-4. Measurement of the Dynamic Chain Exchange Rate	104
IV-4.a. Experimental Procedures and Results	104
IV-5. Summary	110
CHAPTER V. PMMA-PHEMA COPOLYMER MICELLES	111
V-1. Introduction	111
V-2. Results and Discussion	112
V-2.a. Characterization of Micelles by Viscometry and Light Scattering	112
V-2.b. Steady State Fluorescence Experiments on PMMA-PHEMA Micelles	116
V-2.c. Time Correlated Single Photon Counting Fluorescence Spectroscopy	124
V-2.d. Oxygen Quenching of Fluorescence in PMMA-PHEMA Micelles	131
V-3. Summary	133
CHAPTER VI. PS-PHEMA MICELLES	135
VI-1. Introduction	135
VI-2. Theory	136

TABLE OF CONTENTS (continued)

	Page
VI-2.a. Dynamic Chain Exchange Experiments by Pyrene Fluorescence Intensity	136
VI-3. Experimental	136
VI-3.a. Characterization of Micelles	136
VI-3.b. Time Resolved Fluorescence Spectroscopy	137
VI-3.c. Dynamic Chain Exchange Rate Experimental Results	140
VI-3.d. Dynamic Chain Exchange in 10 % Cyclohexane Solution	144
VI-3.e. Micelle Chain Exchange by Energy Transfer	144
VI-4. Summary	145
VI-4.a. PS-PHEMA Micelle Characterization	145
VI-4.b. Dynamic Chain Exchange Experiments	147
 CHAPTER VII. CONCLUSIONS	 149
 BIBLIOGRAPHY	 154

LIST OF TABLES

Table		Page
III-1	Summary of characterization results for PS-PHEMA copolymers.	65
III-2	Summary of characterization results for PMMA-PMAA copolymers.	71
IV-1	Characterization of unlabelled PMMA-PMAA diblock copolymer micelles.	101
IV-2	Characterization of labelled PMMA-PMAA-Py diblock copolymer micelles.	101
IV-3	Dynamic chain exchange results.	109
V-1	Characterization of diblock copolymer micelles of PMMA-PHEMA.	117
V-2	Effect of oxygen on the fluorescence intensity area ratios.	132
V-3	The effect of oxygen on the lifetime of pyrene fluorescence.	132
VI-1	Characterization of unlabelled PS-PHEMA diblock copolymer micelles for polymer VI-3a.	143
VI-2	Characterization of unlabelled PS-PHEMA diblock copolymer micelles for polymer VI-1a.	143

LIST OF FIGURES

Figure		Page
I-1	Aggregation of diblock copolymer chains into spherical micelles.	3
I-2	Schematic representation of the dynamic equilibrium between unimers and diblock copolymer micelles.	5
III-1	Initiation reaction steps for the anionic polymerization of F1-PMMA-PTBMA-Py.	52
III-2	Initiation reaction steps for the anionic polymerization of PMMA-PTBMA.	53
III-3	Propagation steps for the anionic polymerization for the diblock copolymers of PMMA-PTBMA.	54
III-4	The termination step of F1-PMMA-PTBMA-Py.	55
III-5	The hydrolysis of F1-PMMA-PTBMA-Py to F1-PMMA-PMMA-Py.	56
III-6	GPC chromatograms of an esterified sample of F1-PMMA-PHEMA-Py.	59
III-7	UV-VIS absorption spectra of F1-PMMA-PHEMA-Py in THF.	60
III-8	Calibration curve for Waters Styragel HR4 analytical column using polystyrene standards.	62

LIST OF FIGURES (continued)

Figure		Page
III-9	GPC chromatograms of the homopolymer PS, sample extracted with cyclohexane after polymerization of the copolymer PS-PHEMA.	63
III-10	GPC chromatograms of an esterified sample of PS-PHEMA.	64
III-11	NMR of PS ₁₀₀ -PHEMA ₁₀₀ copolymer esterified by cinnamoyl chloride.	66
III-12	Calibration curve for Zorbax 60S, 1000S and 3000S columns using PMMA standards.	72
III-13	GPC chromatogram for labelled and unlabelled PMMA-PMAA.	73
III-14	UV-VIS absorption spectra of F1-PMMA-PMMA-Py in THF.	74
III-15	NMR of unlabelled MMA-TBMA in CDCl ₃ .	75
III-16	UV-visible spectra of 1-pyrenemethanol in THF.	81
III-17	UV-visible spectra of F1(MMA) ₃₅ -H standard in THF.	82
IV-1	Steady state fluorescence spectra of F1-PMMA-PMAA-Py in 90 % ethyl acetate / 10 % methanol and in 50 % ethyl acetate / 50 % methanol.	93

LIST OF FIGURES (continued)

Figure		Page
IV-2	Ratio of the fluorescence intensity areas of pyrene to fluorene chromophores (I_{Py}/I_{F1}) as a function of the solvent composition.	94
IV-3	TCSPC fluorescence emission decay spectra of F1-PMMA-PMAA-Py micelles in 85 % ethyl acetate / 15 % methanol.	95
IV-4	Fluorescence lifetime of pyrene chromophores of F1-PMMA-PMAA-Py as a function of copolymer concentration in 85 % ethyl acetate / 15 % methanol.	96
IV-5	Fluorescence lifetime of pyrene chromophores of F1-PMMA-PMAA-Py in 85 % ethyl acetate / 15 % methanol as a function of copolymer concentration presented on a linear scale.	97
IV-6	Fluorescence lifetime of pyrene chromophores of F1-PMMA-PMAA-Py as a function of copolymer concentration 90 % ethyl acetate / 10 % methanol.	98
IV-7	Fluorescence lifetime of pyrene chromophores F1-PMMA-PMAA-Py in 90 % ethyl acetate / 10 % methanol as a function of copolymer concentration presented on a linear scale.	99
IV-8	Reduced viscosity of PMMA-PMAA (unlabelled) micelles in 90 % ethyl acetate / 10 % methanol versus copolymer concentration.	102

LIST OF FIGURES (continued)

Figure		Page
IV-9	Reduced viscosity of PMMA-PMAA (unlabelled) micelles in 85 % ethyl acetate / 15 % methanol versus copolymer concentration.	103
IV-10	Relative pyrene fluorescence intensity versus time for micelle chain exchange experiment in 85 % ethyl acetate / 15 % methanol.	106
IV-11	Values of $A(t)$ and line kt versus time for chain exchange experiment in 90 % ethyl acetate / 10 % methanol.	108
V-1	Schematic diagram of the micellization of F1-PMMA-PHEMA-Py in ethyl acetate / methanol.	113
V-2	Reduced viscosity as a function of copolymer concentration for F1-PMMA-PHEMA-Py in 95 % ethyl acetate and in 50 % ethyl acetate in methanol.	115
V-3	The overlap of the fluorescence emission of fluorene with the absorption spectra of 1-methanolpyrene.	119
V-4	Steady state fluorescence spectra of F1-PMMA-PHEMA-Py in ethyl acetate / methanol as a function of ethyl acetate content.	120
V-5	Ratio of the fluorescence intensity areas of pyrene to that of fluorene for F1-PMMA-PHEMA-Py in ethyl acetate / methanol as a function of ethyl acetate content.	121

LIST OF FIGURES (continued)

Figure		Page
V-6	Fluorescence intensity ratio (I_{Py}/I_{F1}) for F1-PMMA-PHEMA-Py for copolymer concentrations 0.022 mg/ml, 0.044 mg/ml and 0.110 mg/ml.	122
V-7	The UV-visible absorption spectra of 1-pyrenemethanol in THF and fluorescence emission spectra of F1-PMMA-PHEMA-Py in 1:1 ethyl acetate / methanol.	125
V-8	Fluorescence emission decay curve of pyrene attached to F1-PMMA-PHEMA-Py.	126
V-9	Fluorescence lifetimes of pyrene attached to F1-PMMA-PHEMA-Py in ethyl acetate / methanol as a function of ethyl acetate content.	128
V-10	Pyrene average fluorescence lifetimes vs. ethyl acetate content.	129
V-11	Fluorescence lifetime of pyrene versus F1-PMMA-PHEMA-Py polymer concentration for 95 % ethyl acetate micelle solutions and for 50 % ethyl acetate polymer solutions.	130
VI-1	Intrinsic viscosity versus solvent composition for PS-PHEMA.	138
VI-2	Aggregation number versus solvent composition.	139
VI-3	Average lifetime of pyrene chromophore on polymer I-1b versus solvent composition.	141

LIST OF FIGURES (continued)

Figure		Page
VI-4	Average fluorescence lifetime of pyrene chromophores of polymer VI-1b versus copolymer concentration for 20 % cyclohexane / 80 % THF solutions.	142

LIST OF SYMBOLS AND ABBREVIATIONS

Symbol	Definition
A	energy acceptor
A	monomer
A_2, A_1	pre-exponential factor
A_i	virial coefficient
a_i	pre-exponential factor
A-W	Aniansson and Wall
B	monomer
c	concentration
c^*	critical micelle concentration
c_M^0	initial unlabelled micelle aggregate concentration
c_y^0	initial labelled unimer concentration
CMC	critical micelle concentration
D	energy donor
D_z, D	translational diffusion coefficient
d	doublet
$E(R)$	energy transfer efficiency
EtOAc	ethyl acetate
$F, F(t), F_0$	fluorescence emission intensity
Fl	fluorene

LIST OF SYMBOLS AND ABBREVIATIONS (continued)

Symbol	Definition
f	free energy of micellization
f_0	friction coefficient
$g^{(1)}(\tau)$	normalized autocorrelation function of light scattering intensity
GPC	gel permeation chromatography
H	proton
$I(t), I(q)$	light scattering intensity
$I(t)$	fluorescence emission intensity
I_0	light scattering intensity extrapolated to zero angle
I_λ	donor fluorescence emission intensity
$I_{Py}, I_{Py}(t)$	pyrene fluorescence emission intensity
I_{Fl}	fluorene fluorescence emission intensity
J	overlap integral
K	Mark-Houwink equation constant
K	light scattering optical constant
k	Boltzmann's constant
k_{et}	energy transfer rate constant
k_0	diffusion controlled bimolecular rate constant
k_p	rate constant of unimer incorporation
k_{-p}	rate constant of unimer dissociation
k_q	bimolecular quenching constant

LIST OF SYMBOLS AND ABBREVIATIONS (continued)

Symbol	Definition
LS	light scattering
M	molecular mass
M_m	molecular mass of micelle
M_n, \overline{M}_n	number averaged molecular mass
M_p	micelle aggregate of p polymer chains
M_v	viscosity averaged molecular mass
\overline{M}_w	weight averaged molecular mass
MM, MMA	methyl methacrylate
MPy	micelle with one labelled polymer chain incorporated
MW	molecular weight
m	degree of polymerization
m	multiplet
MeOH	methanol
N	naphthalene
N	number of data points
N	number of particles, molecules etc.
N_0	Avogadro's number
N_A, N_B	repeat number of polymerization of block A, B
NET	non-radiative energy transfer
NMR	nuclear magnetic resonance

LIST OF SYMBOLS AND ABBREVIATIONS (continued)

Symbol	Definition
n	degree of polymerization
n	refractive index
\bar{n}_w	weight average repeat number
ns	nanosecond (10^{-9} s)
nm	nanometer (10^{-9} m)
dn/dc	specific refractive increment
PCEMA	poly(cinnamoyl ethyl methacrylate)
PHEMA	poly(2-hydroxyethyl methacrylate)
PMAA	poly(methacrylic acid)
PMMA	poly(methyl methacrylate)
PS	polystyrene
Py	pyrene
$\sim\sim$ Py	pyrene labelled unimer chain
p	aggregation number of micelle
\bar{p}	average aggregation number
Q	fluorescence quencher species
q	scattering vector
R	gas constant
R	distance

LIST OF SYMBOLS AND ABBREVIATIONS (continued)

Symbol	Definition
R	radius
ΔR	excess Rayleigh ratio
R_g	radius of gyration
R_h	hydrodynamic radius
R_0	critical resonance energy transfer distance
RI	refractive index
S	styrene
s	singlet
$(\overline{s^2})_z$	z-averaged square of the radius of gyration
SANS	small angle neutron scattering
SAXS	small angle X-ray scattering
T	temperature
TBMA	<i>t</i> -butyl methacrylate
TCSPC	time correlated single photon counting
TEM	transmission electronic microscopy
THF	tetrahydrofuran
t	time
t	triplet
t	viscometer flow time of polymer solution
t_0	viscometer flow time of solvent

LIST OF SYMBOLS AND ABBREVIATIONS (continued)

Symbol	Definition
U	unimer chain or species
UV-VIS	ultraviolet-visible
V	volume
w_i	weight fraction
α	Mark-Houwink equation exponential factor
Γ	characteristic decay rate
γ	quenching efficiency
ϵ	molar absorptivity
ϵ_λ	acceptor molar absorptivity
η	viscosity
$[\eta]$	intrinsic viscosity
η_0	solvent viscosity
η_{20}	viscosity of water at 20 °C
η_T	viscosity of water at temperature T
η_r	relative viscosity
η_{red}	reduced viscosity
η_s	solution viscosity
η_{sp}	specific viscosity
κ	instrument constant for steady state fluorimeter
κ'	modified instrument constant for steady state fluorimeter

LIST OF SYMBOLS AND ABBREVIATIONS (continued)

Symbol	Definition
κ^2	rotation constant
λ	wavelength
μm	micrometers (10^{-6} m)
Π	osmotic pressure
ρ	density of polymer solution
ρ_0	density of solvent
σ	variance
τ_D	intrinsic fluorescence lifetime of donor
τ_0	fluorescence lifetime in the absence of quenchers
τ	fluorescence lifetime
$\tau_i \tau_1 \tau_2$	relaxation time for multiexponential decay equation
$\langle \tau \rangle$	average fluorescence lifetime
φ_0	concentration of the soluble block in the corona sphere
φ_D	fluorescence quantum yield of energy donor
φ_{DA}	fluorescence quantum yield of energy donor in the presence of acceptor
φ_m	fluorescence quantum yield of pyrene in micelle aggregates
φ_u	fluorescence quantum yield of pyrene in unimer phase
φ_v	volume fraction of solute spheres
χ	fluorescence quenching efficiency
χ^2	error function

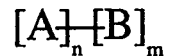
LIST OF SYMBOLS AND ABBREVIATIONS (continued)

Symbol	Definition
$\chi_{BS}, \chi_{AS}, \chi$	polymer-solvent interaction constant

CHAPTER I. INTRODUCTION

I-1. Diblock Copolymer Micelles

Diblock copolymers consist of two homopolymer chains bonded to one another in a head-to-tail fashion. A diblock copolymer consisting of a sequence of n units of monomer A and m units of monomer B can be represented by:



In solutions of selective solvents block and graft copolymers show unique colloidal behavior. A selective solvent is capable of dissolving one of the constituent blocks but at the same time is also a poor solvent for the other block. The poorly solvated polymer blocks aggregate together and the well solvated blocks are dissolved in the solvent. Many different types of microphase segregated structures are possible, including lamellar, cylindrical and spherical micelles. Spherical micelles will be the focus of this project. A spherical micelle (Figure I-1, pg. 3) consists of an aggregation of the poorly solvated polymer block, called the micelle core, surrounded by well solvated polymer chains, called the micelle corona. It is the corona that is responsible for maintaining the dispersion of the micelle particles in solution.

The factors which affect the process of micellization and the physical attributes of the micelles include the chemical composition¹, structure² and molar mass³ of the

copolymer, the strength of the interaction between the copolymer blocks and the solvent system^{4,5}, copolymer concentration, and temperature⁶.

Micelles are in equilibrium with molecularly dispersed polymer chains, called unimers (Figure I-2, pg. 5). There are two models for association: closed and open association. Open association of block copolymers results in micelles that have a continuum of aggregation numbers⁷. Soap micelles in hydrocarbon media can approach this behavior. The usual case for block copolymers is for micelles to be formed in selective solvents where the aggregates have a narrow size distribution and this is called closed association⁷.

Thus it is normally assumed for simplicity, that there is one aggregation (or association) number for the block copolymer micelles and that the process can be represented by:



where U represents the unimers units and M_p the micellar aggregation of p polymer units.

The above system represents a state of dynamic equilibrium between the micelle aggregates and molecularly dissolved polymer chains (or unimers). Generally, this

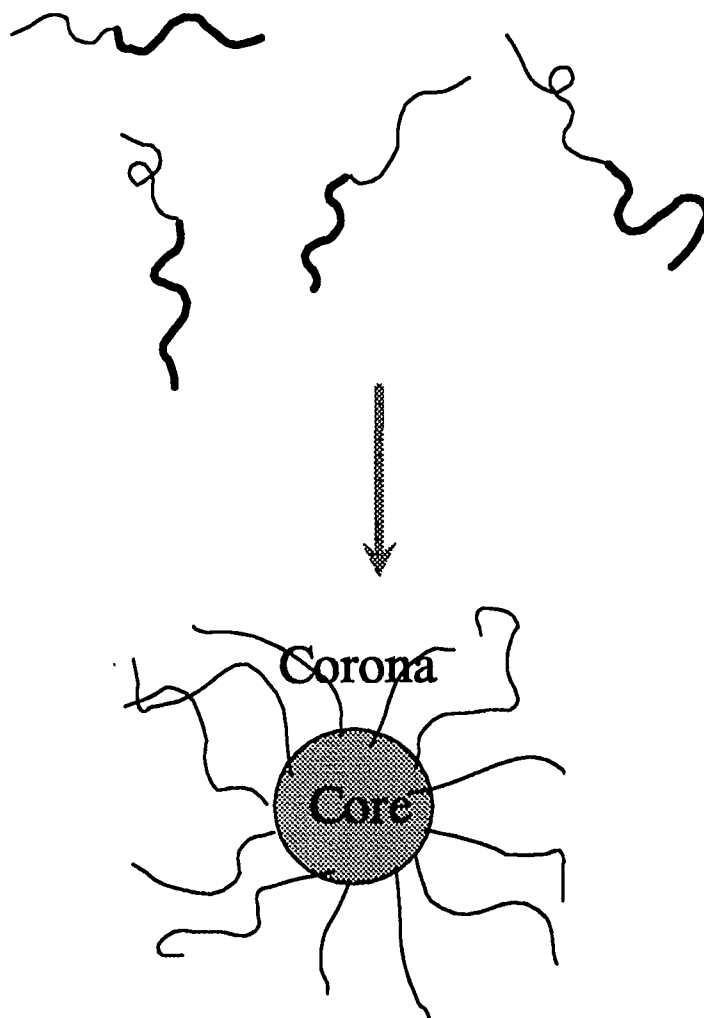


Figure I-1. Aggregation of diblock copolymer chains into spherical micelles.

involves the incorporation and expulsion of single chains from the micelle aggregations. Thus the narrow size distribution is maintained. It is also possible that micelles could be formed by fission of micelles and by fusion of smaller aggregates. The energy barriers for fusion and fission would be much higher since fission would involve the simultaneous disentanglement of many polymer chains and fusion of two smaller aggregates would have to overcome a large energy of repulsion.

The properties of copolymer micelles resemble those of soap dispersions in water. Diblock copolymer micelles consist of many polymer chains that have aggregated reversibly together. Diblock copolymer micelles are able to dissolve otherwise insoluble substances and stabilize dispersions of colloidal particles. For example, most dyes used in industrial processes are only sparingly soluble in water. Dyes can be made soluble in water with the addition of diblock copolymers and the application of these dyes to other materials is less problematic.

Block copolymers have important applications in materials used for coatings, adhesives, and thin films. In these applications, if one of the blocks has an amphiphilic nature, adsorption of the block copolymers can change the surface wetting properties of the solid. Generally one of the blocks of the copolymer will coat out on the solid surface from a solvent if it is a poor solvent for one of the blocks. The result is a polymer brush which resembles micelles in so far as there is microheterogeneous phase separation of the two copolymer blocks.

The adsorption of diblock copolymers at a surface interface will also be influenced by the formation of micelles in the solvent which occurs at polymer concentrations above

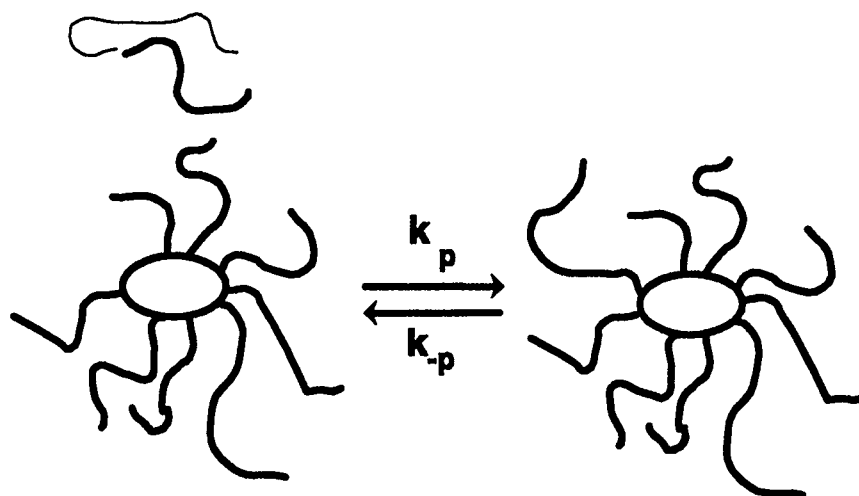


Figure I-2. Schematic diagram of the dynamic equilibrium between unimers and diblock copolymer micelles. The forward reaction is the adsorption of an unimer chain into a micelle (see equation I-2)

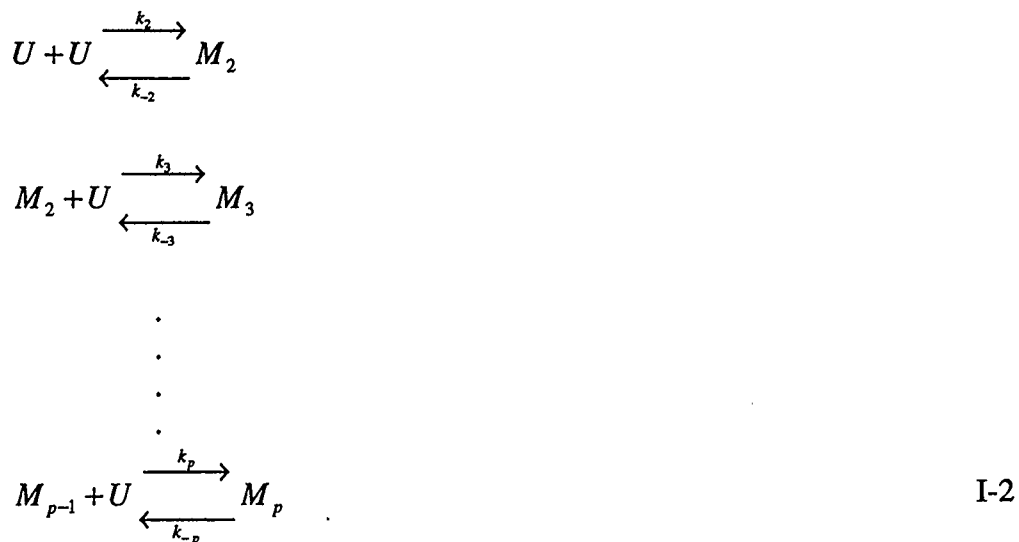
the critical micelle concentration (CMC). Micelle formation will affect the kinetics of surface adsorption of diblock copolymers^{8,9}.

The self-assembly of diblock copolymers could provide a relevant model for some aspects of the self-assembly of proteins, lipids and cell membranes. In cell biology these molecules perform transformations between micelles, vesicles and bilayer membranes and there are subtle physical changes that guide the form and the function of the structures¹⁰. To some extent the factors which govern their organized aggregation have been delineated¹¹. However a full understanding of the thermodynamics and kinetics of self assembly of these types of molecules in aqueous and in organic media has not been achieved and the physical chemistry of diblock copolymer micelle formation may be instructive.

I-2. Equilibrium Dynamics of Diblock Copolymer Micelles

In a micellar system, chain exchange between the unimer pool and micelles, the breakdown of larger micelles into smaller ones (fission), and the formation of larger micelles from smaller ones (fusion) may all occur simultaneously^{12,13}. Of all these processes, micelle chain exchange is the most fundamental.

Aniansson and Wall assumed that association and dissociation proceeds in unitary steps and in the general case:



where M_{p-1} and M_p are micelles with $p-1$ and p chains, respectively; U denotes a unimer chain; and k_p and k_{-p} are unimer incorporation and dissociation rate constants. Under equilibrium conditions, all of the individual step reactions (at each value of p) will also be at equilibrium and hence all k_p and k_{-p} are related by:

$$\frac{d[M_p]}{dt} = k_p[U][M_{p-1}] - k_{-p}[M_p] = 0$$

and therefore

$$k_p [M_{p-1}][U] = k_{-p} [M_p]
 \tag{I-3}$$

The magnitude of the rate constants k_p and k_{-p} determines the relaxation rate of a diblock micelle system when it is subjected to an external perturbation. This becomes especially true if the chain exchange process is much faster than the micelle fusion and fission processes, a case generally applicable to diblock copolymer micelles¹⁴. The magnitudes of k_p and k_{-p} also shed light on the rate of diblock copolymer brush buildup as polymer brushes¹⁵⁻¹⁸, which are self-assembled structures of diblock copolymers at a solid substrate / solution interface. Polymer brushes have a close resemblance to the structure of diblock micelles.

Despite the fundamental importance of k_p and k_{-p} , the study of micelle chain exchange kinetics has been rare in the past. Halperin and Alexander¹⁵ have recently derived scaling relations between k_p and the lengths of two blocks of a diblock copolymer. Some experimental studies have been carried out on diblock copolymer micelles and the results have been analyzed in the spirit of the Aniansson and Wall (A-W) theory¹⁹⁻²¹, which was developed for small-molecule surfactant micelles. According to the A-W theory, the concentration of unimers or micelles or their equivalents should relax after a “perturbation” to their new equilibrium values with two relaxation times τ_1 and τ_2 where $\tau_1 < \tau_2$. Assuming that the chain exchange process is much faster than the micelle fusion and fission processes, Aniansson and Wall related τ_1 and τ_2 to k_{-p} , k_p and to micelle parameters such as the average aggregation number \bar{p} and the variance σ in \bar{p} .

Some experimenters have initiated studies into the equilibrium dynamics of chain exchange for diblock copolymer micelles. Bednar *et al.*²² have followed the association

and dissociation kinetics of polystyrene-*b*-poly(hydrogenated isoprene) in 1,4 dioxane / heptane mixtures. In their experiments they first formed micelles in a solvent mixture and then added an equal amount of good solvent and monitored the dissociation of micelles by measuring the decrease in the intensity of scattered light from a laser source. Bednar also measured the rate of formation of micelles by adding an amount of poor solvent to a solution of well solvated polymer and measuring the increase in the intensity of scattered light from the laser source. The light scattering intensity data for the micelle formation experiment was fitted to the equation $I(t) = a_1 e^{-t/\tau_1} + a_2 e^{-t/\tau_2}$ and that of the micelle dissociation experiment was fitted to $I(t) = I_0(1 - a_1 e^{-t/\tau_1} + a_2 e^{-t/\tau_2})$. No correlation could be implied between the experimental relaxation times and any mechanism of relaxation under equilibrium conditions as the perturbations used in these experiments were too large.

Prochazka *et al.*²³ studied the micellization kinetics of polystyrene-*b*-poly(hydrogenated isoprene) labelled with carbazole or anthracene in solutions containing various ratios of 1,4-dioxane and heptane. Non-radiative energy transfer (NET) between the two fluorescent chromophores was observed upon the onset of micellization. Separate micellar solutions of the diblock copolymer were made with anthracene and carbazole labels. These solutions were mixed and the increase in the amount of NET was measured with respect to time. The unimer-micelle chain exchange rate was observed by an increase in the amount of NET. The data was analyzed using a double exponential decay (or growth) in the fluorescence intensity. Using this approach it was not possible to obtain

the chain exchange rate directly because with the passage of time the distribution of the chromophore labels within the micelles becomes more complex. For example the efficiency of energy transfer from the donor to the energy acceptor may change in a complicated way as the number of acceptors in a micelle changes. Prochazka did show that the diblock copolymer micelle exchange rate was at least two orders of magnitude slower than that exhibited by detergents.

Wang *et al.*²⁴ performed a similar experiment with polystyrene-*b*-poly(oxyethylene) labelled at the block junction with either a naphthalene or pyrene chromophore in methanol / water solutions. They proposed an analysis of the fluorescence emission intensity data based on a model of chain exchange that transfers between micelles via unimers. They included the model of Duhamel *et al.*²⁵ to account for the varying amounts of fluorescence quenching arising from the evolving distribution of the donor and acceptor molecules within the micelles. The fluorescence emission intensity data of the energy donor $I(t)$ was fitted to the equation $I(t) = A_1 e^{-t/\tau_1} + A_2 e^{-t/\tau_2}$. However, their numerical analysis did not produce a fit that could relate their values for the double exponential decay to τ_1 and τ_2 of Aniansson and Wall and therefore they were not able to accurately calculate a value for k_p . Wang concluded that the mechanism for chain exchange was more complex than chain expulsion from micelles to unimers followed by acquisition of a unimer into a micelle. They suggested that the exchange process included a mechanism where polymer chain transfer also occurred during the collision of

two micelle aggregates in addition to the expulsion / inclusion mechanism. To date no experimental data has been provided to support or contradict this proposed mechanism.

Although the relaxation kinetics of diblock micelles has been found to follow a two stage mechanism in agreement with the A-W theory, rate constants such as k_p have so far not been obtained. The difficulty has been in establishing the equivalence between the experimentally determined τ_1 and τ_2 and the relaxation times discussed by Aniansson and Wall, due to complications from the techniques used for monitoring the relaxation of a micellar system.

In addition to the aforementioned complication, most of the previous studies utilized large perturbations. The use of large perturbations, such as the sudden change in solvent composition²⁶ or temperature²⁷ to cause micelle formation from a solution without micelles or vice versa, makes the experimental detection of the relaxation process easier but renders the A-W theory inapplicable to the experimental results.

I-3. Research Objectives

This project was concerned with the determination of the kinetic properties of chain exchange of diblock copolymer micelles. The chain exchange rate was measured by monitoring the rate of incorporation of labelled diblock copolymer into micelles of the unlabelled diblock copolymer. The exchange rate should be directly proportional to the concentration of the unimer chains and to the micelle particles. Two major goals of this research were to confirm the rate law and to measure the polymer chain exchange constant

under various conditions. The changes in the rate constant were related to the properties of the micelle system.

Three diblock copolymers were used in this study, poly(methyl methacrylate)-*b*-poly(methacrylic acid) (PMMA-PMAA), poly(styrene)-*b*-poly(hydroxyethylmethacrylate) (PS-PHEMA), and poly(methyl methacrylate)-*b*-poly(hydroxyethylmethacrylate) (PMMA-PHEMA). These polymers were synthesized by the anionic polymerization method to ensure monodisperse samples and a well defined structure.

Fluorescence techniques, such as steady state energy transfer, time resolved fluorescence, and steady state anisotropy have been used in this project to measure the onset of micellization and to measure the critical micelle concentration (CMC). Techniques such as light scattering and viscometry have been used to characterize the overall radius and aggregation number of micelles of the three polymers mentioned above. Steady state fluorescence intensity measurements were then used to measure the exchange rate between unimer chains and micelles of PMMA-*b*-PMAA and of PS-*b*-PHEMA in selective solvent systems.

I-4. Organization of the Thesis

Chapter II provides a background for all the experimental procedures for characterization of diblock copolymers, followed by the methods of characterization of diblock copolymer micelles. A review of viscometry, light scattering and other scattering techniques, and of gel permeation chromatography (GPC), amongst other standard

techniques, is provided. Fluorescence techniques and their application to diblock copolymer micelles are also reviewed. Finally experiments reported to date on the measurements of the kinetics of micelle chain exchange are reviewed. Chapter III details the synthesis of all the polymers used in this thesis and characterizes all of the copolymers and standards used in this project. Chapter IV details the characterization of PMMA-PMAA micelles in ethyl acetate / methanol solutions and measures the chain exchange rate of these micelles with the use of fluorescence techniques. Chapter V examines micelles formed by PMMA-PHEMA in ethyl acetate / methanol. These micelles are characterized and some fluorescence properties of the chromophore labels are detailed. This chapter includes an examination of the effect of dissolved oxygen on the fluorescence of pyrene. Chapter VI characterizes and examines micelles formed by PS-PHEMA in cyclohexane / THF. Kinetic studies were attempted at room temperature and at elevated temperatures. Chapter VII provides conclusions and suggestions for future work.

CHAPTER II: BACKGROUND

II-1. Characterization of Diblock Copolymers

Studies of the properties of diblock copolymers require that the polymers have a well defined structure and a narrow molecular weight distribution. To date this usually requires that diblock copolymers are synthesized by anionic polymerization techniques²⁸⁻³¹. Diblock copolymers can be characterized by viscometry³²⁻³⁴, NMR³⁵, gel permeation chromatography^{36,37} (GPC) and light scattering techniques^{38,39} (LS). If chromophore labels have been attached it is also possible to characterize the polymers with UV-VIS absorption spectroscopy. Other methods also include membrane and vapour pressure osmometry, ebulliometry and cryoscopy. All of the above methods are standard and are well known.

The differing nature of the two diblocks complicates the interpretation of tests such as viscometry, light scattering and GPC. For viscometry, it is not usually possible to have a set of standard polymers to calibrate the viscometer for the Mark-Houwink equation⁴⁰:

$$[\eta] = KM_v^\alpha \quad \text{II-1}$$

Where $[\eta]$ is the intrinsic viscosity, K and α are constants for a particular polymer-solvent pair at a particular temperature and M_v is the viscosity average molecular weight. For

diblock copolymers the values of K and α would be an averaged value for the two blocks. Viscometry is not commonly used for the determination of the overall molecular weight of diblock copolymers.

The same situation holds for GPC where the elution time is related to the effective hydrodynamic radius of the polymer which again is an averaged result of differing contributions from the two blocks with the overall polydispersity of the polymer also measured. It is possible to take a sample of the first block during the synthesis and measure its size and polydispersity by GPC. The number averaged size of the second block can be related to that of the first by NMR spectroscopy.

The weight averaged molecular weight of the polymers can be determined by static light scattering. As with GPC and viscometry it is an apparent molecular weight that is determined from the experiment^{41,42}. The average chemical composition of the copolymers can be found by NMR though it must be pointed out that there is generally a fairly broad distribution in the chemical composition even for a polymer with a narrow molecular weight polydispersity.

The best method for the characterization of diblock copolymers is to obtain a sample of the first block during synthesis and to fully characterize this block by GPC, to obtain the polydispersity, and by light scattering to find the weight average molecular weight. The diblock copolymer is fully characterized by GPC to find the polydispersity of the whole polymer and by NMR to derive the number ratio of the two blocks and hence the molecular weight.

II-2. Characterization of Diblock Copolymer Micelles

Many methods have been used to characterize micelles formed from diblock copolymers and these include light scattering techniques, dilute solution viscometry, small angle neutron scattering, electron microscopy, ultracentrifugation, gel permeation chromatography, small angle X-ray scattering, and fluorescence spectroscopy.

II-2.a. Dilute Solution Viscometry of Copolymer Micelles

In a dilute solution, solvated polymer chains will increase the viscosity of the solvent. The amount of this increase was considered by Einstein⁴³. In the case where the polymer solute is treated as a collection of rigid non-draining spheres dispersed in the solvent, Einstein found the viscosity of a polymer solution to be:

$$\eta_s = \eta_o (1 + 2.5\phi_v) \quad \text{II-2}$$

where ϕ_v is the volume fraction of the solute spheres, η_s is the viscosity of the solution, and η_o is the viscosity of the solvent. Polymer coils or micelles are considered as non-draining spheres that have a hydrodynamic radius R_h . The hydrodynamic radius can be related to the volume fraction of the solvated spheres to obtain:

$$\eta_s = \eta_o \left(1 + \frac{10}{3} \frac{N}{V} \pi R_h^3\right) \quad \text{II-3}$$

The intrinsic viscosity $[\eta]$ is defined as :

$$[\eta] = \lim_{c \rightarrow 0} \frac{\eta_s - \eta_0}{c\eta_0} \quad \text{II-4}$$

where c is the polymer concentration. By inserting equation II-3 into II-4 the relationship between the molar mass and the intrinsic viscosity is obtained⁴⁴:

$$[\eta] = \frac{10\pi}{3M_m} N_0 R_h^3 \quad \text{II-5}$$

where N_0 is Avogadro's number and the substitution for the concentration $c = M_m \frac{N}{V}$ has been made. Rearranging we obtain:

$$M_m = \frac{10\pi}{3[\eta]} N_0 R_h^3 \quad \text{II-6}$$

M_m is the molecular mass of any non-draining spherical particles including diblock copolymer micelles. Thus the molecular mass of these micelles can be obtained after the hydrodynamic radius is established. The hydrodynamic radius is determined from dynamic light scattering experiments. The aggregation number (p) of diblock copolymer micelles

can be found by dividing the measured molecular mass of the micelles (M_m) by the molecular mass of the diblock copolymer M .

$$p = \frac{M_m}{M} \quad \text{II-7}$$

The molecular mass of single polymer chains can be found independently. Substituting into equation II-7 for the value of M_m in equation II-6 the value of p becomes:

$$p = \frac{10\pi}{3[\eta]M} N_0 R_h^3 \quad \text{II-8}$$

In experiments on copolymer micelles the intrinsic viscosity is determined from a set of measurements of relative viscosity at several polymer concentrations at a fixed solvent composition. The relative viscosity is defined as:

$$\eta_r = \frac{\eta}{\eta_0} \quad \text{II-9}$$

where the viscosity of the solvent η_0 and of the polymer solution η are measured with a

Ubbelohde viscometer. The relative viscosity is related to the measured flow times as:

$$\eta_r = \frac{\rho t}{\rho_0 t_0} \quad \text{II-10}$$

where ρ is the density of the polymer solution and ρ_0 is the density of the solvent and t is the flow time of the polymer solutions and t_0 is that of the solvent.

The specific viscosity η_{sp} is then defined as:

$$\eta_{sp} = \eta_r - 1 \quad \text{II-11}$$

The reduced viscosity η_{red} is obtained by dividing η_{sp} by the concentration of the polymer in the solution:

$$\eta_{red} = \frac{\eta_{sp}}{c} \quad \text{II-12}$$

The reduced viscosity of the polymer-solvent system is measured at several polymer concentrations. The reduced viscosity is extrapolated to zero polymer concentration to arrive at the intrinsic viscosity:

$$[\eta] = \lim_{c \rightarrow 0} (\eta_{red}) \quad \text{II-13}$$

The molecular mass of the copolymer is found as discussed above, the hydrodynamic radius of the copolymer micelle is measured, as discussed below, by dynamic light scattering techniques.

II-2.b. Light Scattering

Light scattering has been used in this project to determine the hydrodynamic radius of diblock copolymer micelles. Light scattering techniques have the advantage over other methods, such as gel permeation chromatography, in that they are absolute techniques. The basis for the scattering of light by polymer chains is the difference in the refractive indices between the polymer segments and the solvent. There are two types of light scattering experiments, static and dynamic light scattering. In general the molecular weight of a diblock copolymer can be determined by static light scattering however in practice it is difficult to obtain accurate measurements of dn/dc , the specific refractive index, in mixed solvent systems. Small variations in the solvent system composition will result in large errors in the measured values of dn/dc . In mixed solvent systems dynamic light scattering experiments can be used to measure the copolymer hydrodynamic radius.

I-2.b.i. Static Light Scattering by Large Molecules in Solution

Static light scattering experiments in a single solvent from a laser source can give the weight average molecular weight. The scattered intensity of the source is a function of the wavelength of the source, the angle of measurement, and the concentration of the

polymer solution amongst other factors. The equation of the scattering for a polydisperse sample is^{38,39,45}:

$$\frac{Kc}{\Delta R_{\theta}} = \left[\frac{1}{M_w} + 2A_2c + 3A_3 + \dots \right] \left[1 + \left(\frac{16\pi^2 \eta_0^2 \sin(\theta/2)}{3\lambda^2} \right) (\overline{s^2})_z \right] \quad \text{II-14}$$

where K is the optical constant and is a function of the refractive index of the solvent, the value of dn/dc , and the wavelength of the incident monochromatic light. The concentration of the polymer is c , A_i are virial coefficients, ΔR is the excess Rayleigh ratio.

The z averaged square of the radius of gyration is $(\overline{s^2})_z$.

In the limit of zero polymer concentration and zero angle of measurement the weight averaged molecular weight is determined:

$$\left(\frac{Kc}{\Delta R_{\theta}} \right)_{\substack{c \rightarrow 0 \\ \theta \rightarrow 0}} = \frac{1}{M_w} \quad \text{II-15}$$

This evaluation is usually done with a Zimm plot.

II-2.b.ii. Dynamic Light Scattering

The hydrodynamic radius of diblock copolymer micelles in mixed solvent systems can be obtained by dynamic light scattering. The basis of dynamic light scattering is the measurement of the real-time fluctuations in the intensity of the scattered light. The decay of the normalized autocorrelation function of the intensity $g^{(1)}$ with respect to the correlation time τ for a monodisperse sample is given by:

$$g^{(1)}(\tau) = \exp(-\Gamma\tau) \quad \text{II-16}$$

where Γ is the characteristic decay rate which is related to the translational diffusion coefficient, D , of the solute by:

$$\Gamma = q^2 D \quad \text{II-17}$$

where q is the scattering vector as defined in equation II-21. For polydisperse samples the z-average value of the translational diffusion coefficient D_z is obtained.

The value of D is related to the frictional coefficient f_0 by the Einstein equation:

$$D = kT/f_0 \quad \text{II-18}$$

and the hydrodynamic radius of the solute is obtained from Stokes equation⁴⁶

$$D = kT/6\pi\eta_0 R_h \quad \text{II-19}$$

If the value of the diffusion coefficient is the z-average value then the hydrodynamic radius is also the z-average of the hydrodynamic radius.

II-2.b.iii. CMC and Micellization Kinetics by Light Scattering

The critical micelle concentration of micellization can be determined since the intensity of the scattered light increases greatly upon micellization of diblock copolymers, typically by a factor of 50 at the CMC⁶.

Static light scattering has been used for the determining the weight averaged molecular weight and the CMC of diblock copolymer micelles in both pure and in mixed solvent systems⁴⁷⁻⁴⁹. The experiments with mixed solvent systems can be more complicated, again because it is necessary to find dn/dc for the diblock in the mixed solvent system (see Section II-2.b.). This source of error can be minimized by choosing solvent pairs that are isorefractive. This problem can also carry over to the experiment itself over the range of polymer concentrations used if the solvent mixtures used are not carefully matched. This problem does not present itself in dynamic light scattering experiments.

II-2.c. X-Ray Scattering

X-ray scattering techniques have been used to characterize copolymer micelles. Small angle X-ray scattering has the advantage of a larger value of the scattering vector q due to the shorter wavelength of light that is employed. It is possible to determine the core radius as well as the overall micelle radius and the micelle aggregation number. The Guinier relationship dictates the intensity of the scattering:

$$I(q) = I_0 \exp\left(-\frac{q^2 R_g^2}{3n_0^2}\right) \quad \text{II-20}$$

where

$$q = \frac{4\pi n_0 \sin(\theta / 2)}{\lambda} \quad \text{II-21}$$

and where θ is the angle of measurement, λ is the wavelength of the incident radiation, n_0 is the refractive index of the solvent and I_0 is the intensity of the scattered light extrapolated to zero angle. Where $qR_g / n_0 < 1.3$ a plot of $\ln(I(q))$ against q^2 will yield the radius of gyration of the scatterers.

In the case of X-ray scattering, where the electron density of the corona polymer chains is similar to that of the solvent, the scattering of radiation will be mostly due to

micelle cores. In most systems there is some contribution from both the cores and from the corona⁵⁰⁻⁵³.

II-2.d. Small Angle Neutron Scattering

Neutron scattering has the potential to provide contrast between the micelle core and the corona by the method of selective deuteration. It is also possible to determine the configuration of a single chain within a micelle structure due to the large contrast provided by deuteration. Small angle neutron scattering (SANS) has been used to study the multiphase structure of poly(styrene)-*b*-poly(oxyethylene) copolymer in water⁵⁴.

The wavelengths of X-rays are typically 0.1 nm, that of neutrons 0.1 to 2 nm, compared to the wavelengths used in light scattering experiments (450-650 nm). The wavelengths used for X-ray and neutron scattering are much smaller and therefore these two methods are able to provide information of size on a much smaller scale than is possible using light scattering. However because of interference effects detection must be at small angles only for these two methods. The Guinier expression limits the range of useful dimensions that can be measured. For small angle X-ray scattering (SAXS) the maximum value of $\langle s^2 \rangle_z^{1/2}$ is about 5 nm, for SANS it is about 20 nm, and for light it is about 200 nm.

II-2.e. Sedimentation Velocity and Gel Permeation Chromatography

Sedimentation velocity⁴⁷ and GPC can in principle be used to determine the mass distribution of diblock copolymer micelles and information on equilibrium between unimers and micelles. Tuzar et al^{55,56}. have looked at the distribution of micelles of styrene-butadiene-styrene block copolymers in THF / allyl alcohol by sedimentation velocity and have been able to separate unimers and micelle aggregations. The micelle aggregations had reasonably narrow mass distributions and were well segregated from the unimers, all of which supports the closed association model of diblock copolymer association.

Experiments on polystyrene-*b*-polyisoprene in N,N-dimethyl-acetamide systems using GPC^{57,58} were successful in detecting micelles. In this set of experiments the temperature was raised and this changed the ratio of unimers to micelles which was successfully detected. The reverse flow method of correction was used to obtain a polydispersity of mass distribution of micelles of 1.02. In general, the separation of the micelles from the unimers can be less sensitive because the mode of separation is by the differences in the hydrodynamic radius. This does not change as much in going from unimers to micelles as does the molecular weight. Hence this method is much less sensitive than sedimentation velocity.

In both cases the peaks are broadened according to Gilbert's theory⁵⁹ due to the dynamic nature of the unimer-micelle equilibrium. Micelle aggregations were continuously disturbed and re-established as the experiment proceeded and this resulted in the

broadening of the peak at elution volumes below that of the unimers. This effect is minimized if the CMC of the polymer is much lower than the concentration of the sample used in the experiment and if the rate of dissociation of the micelles to free chains is very low.

II-2.f. Electron Microscopy

Direct information of the formation, the size and the shape of copolymer micelle has been obtained with the use of electron microscopy⁶⁰. For example Price *et al.* have used transmission electron microscopy to observe polystyrene-*b*-poly(ethylene/propylene) in *n*-decane. TEM micrographs showed the micelles formed comprised of dense spherical cores of polystyrene surrounded by chains of poly(ethylene/propylene). They also showed that the size distribution of the micelles was narrow. The method of preparation of micelles for electron microscopy removes the solvent in all cases and this must have disturbed the characteristics of the micelles. Thus, it was possible to obtain or confirm the shape of the micelles and the size distribution of the micelles but it was not possible to obtain an accurate measurement of the dimensions of the micelles in its undisturbed state in solution.

II-2.g. Osmometry

Membrane osmometry has been used to measure the CMC and obtain the thermodynamic parameters of micellization for polystyrene-*b*-poly(ethylene/propylene) in *n*-decane⁶⁰. The measured osmotic pressure varies as:

$$\frac{\Pi}{c} = \frac{RT}{M_n} + A_2c \quad \text{II-22}$$

where A_2 is the second virial coefficient. At the CMC the value of M_n increases greatly and thus the value of $\frac{\Pi}{RTc}$ is greatly reduced. The values of the CMC were measured as a function of the temperature from which the values of the enthalpy, free energy and entropy change of micellization were deduced. The values of the CMC were measured to be between 2.5 and 0.3 g/L (2.5×10^{-5} to 3×10^{-6} M) range. It was however necessary to assume that the aggregation number of the micelles formed did not change over the temperature range used. This assumption was not validated.

II-2.h. Fluorescence Spectroscopy

The most important methods used in this study of the properties of diblock copolymer micelles were fluorescence spectroscopic techniques. Many experiments have already been done using fluorescence techniques^{23,25,61-69} due to the techniques sensitivity. Fluorescence spectroscopy is more sensitive than other spectroscopic techniques primarily due to the lifetime of the excited states of the chromophores. Generally⁷⁰, the lifetimes of

chromophores is in the range of 10 ns. This is in the time scale in which chromophore molecules are able to rotate and also is in the time frame in which fluorescence quenchers are able to migrate to excited chromophores in solvents (but not usually in solids). This makes fluorescent chromophores sensitive probes to changes in its environment. An important property of fluorescent chromophores that can change significantly with a change in the environment is the average fluorescence lifetime.

II-2.h.i. Time Resolved Fluorescence Emission Spectra

The time correlated single photon counting (TCSPC) method has been utilized to measure the fluorescence lifetime of excited chromophores⁷¹. Some of the factors that influence the lifetime are the natural or intrinsic fluorescence lifetime of the chromophore, the number and efficiency of fluorescence quenchers available to the chromophore during the fluorescence lifetime, and the environment that the chromophore. In the case of chromophores attached to diblock copolymers fluorescent probes can be found at the ends on either of the constituent blocks, or at the junction between the blocks. Also, the chromophores could be located randomly on either of the blocks. Generally, the time resolved fluorescence experiments in this study are conducted under atmospheric conditions and hence there is dissolved oxygen in the samples that can quench excited chromophores. The experiment consists of measuring the fluorescence decay profile and then determining the average fluorescence lifetime by the weighted sum of the exponential

decay. The average lifetime is determined by:

$$\langle \tau \rangle = \sum_i^n a_i \tau_i \quad \text{II-23}$$

where a_i is the pre-exponential factor or a multi-exponential fit to the decay curve with lifetimes of τ_i . In our study, fluorescent chromophores will be attached to diblock copolymers in some advantageous fashion and the fluorescence properties of the chromophore both in and out of micelles will be measured.

II-2.h.ii. Energy Transfer

Energy transfer is the process by which excitation energy of one chromophore (energy donor D) is transferred to another (energy acceptor A) via the dipole-dipole mechanism. The general reaction is represented by the equation:



The mechanism involves dipole-dipole coupling between the donor and the acceptor. A necessary condition for energy transfer to occur by the non-radiative (dipole-dipole) mechanism is that the fluorescence emission spectra of the energy donor overlap with that of the absorption of the acceptor molecule. Trivial energy transfer, which occurs

when the donor emits a photon which is subsequently reabsorbed by the energy acceptor can be minimized by keeping the concentration of the chromophores low.

The rate of energy transfer is given by :

$$k_{et} = \frac{1}{\tau_D} \left(\frac{R_0}{R} \right)^6 \quad \text{II-25}$$

where τ_D is the fluorescence lifetime of the energy donor and R the distance between the two chromophores. R_0 is a characteristic distance called the critical resonance energy transfer distance. The efficiency of non-radiative energy transfer $E(R)$ is given by⁷²:

$$E(R) = \frac{R_0^6}{R_0^6 + R^6} \quad \text{II-26}$$

If the distance of the two chromophores is equal to the critical distance then the efficiency of energy is 50 %. In general, the value of R_0 for most useful chromophore pairings is in the 20 to 50 angstrom range. It should also be noted that the two chromophores need not be different and where the two chromophores are the same the transfer of energy is called energy migration.

The critical energy transfer (or Forster) distance, can be calculated from the overlap between the light absorption spectra of the energy acceptor and the fluorescence

emission spectra of the energy donor. It has been derived by Forster as:

$$R_0 = \sqrt[6]{\frac{9000 \ln(10) \kappa^2 \phi_D J}{128 \pi^5 n^4 N_0}} \quad \text{II-27}$$

where ϕ_D is the donor chromophore fluorescence quantum yield in the absence of energy transfer, n is the refractive index of the solvent at the excitation wavelength, N_0 is Avogadro's number, J is the overlap integral between the normalized donor fluorescence intensity I_λ and the acceptor molar absorptivity, ϵ_λ .

$$J = \int_0^\infty \lambda^4 I_\lambda \epsilon_\lambda d\lambda \quad \text{II-28}$$

where λ represents the wavelength and the fluorescence intensity I_λ has been normalized:

$$\int_0^\infty I_\lambda d\lambda = 1 \quad \text{II-29}$$

κ^2 is a measure of the relative orientation of the donor and the acceptor. If the pair of chromophores are rotating at a rate much greater than that of energy transfer then its value is 2/3.

In the current study the energy donors were limited to fluorene derivatives and the energy acceptors limited to pyrene derivatives.

II-2.h.iii. Fluorescence Quenching

Fluorescence quenching is the term used for any process that decreases the fluorescence intensity of a chromophore and it can be the result of either excited state reactions, energy transfer, complex formation, and collisional quenching. In this study, the two modes of quenching that will be encountered are collisional (or dynamic) quenching and energy transfer. Collisional quenching is the result of encounters between an excited fluorophore and a quencher. The quencher must diffuse to the chromophore in the lifetime of the excited state and upon collision the chromophore returns to the ground state without emission of a photon. Oxygen is a common and very efficient quencher of almost all fluorophores. Collisional quenching of fluorescence is described by the Stern-Volmer equation:

$$\frac{F_0}{F} = 1 + k_q \tau_0 [Q] \quad \text{II-30}$$

where F_0 and F are the fluorescence intensities in the absence and presence of the quencher, k_q is the bimolecular quenching constant and τ_0 is the lifetime of the fluorophore in the absence of the quencher, and $[Q]$ is the concentration of the quencher.

The amount of quenching is also reflected in the measured lifetime of the fluorophore :

$$\frac{F_0}{F} = \frac{\tau_0}{\tau} \quad \text{II-31}$$

where τ is the measured lifetime of the fluorophore in the presence of the quencher. The value of k_q is related to the rate of collision by:

$$k_q = \gamma k_0 \quad \text{II-32}$$

where k_0 is the diffusion-controlled bimolecular rate constant, and γ is the quenching efficiency.

The Smoluchowski equation⁷³ gives the relationship between the sum of the collision radii of the two chromophores R , the sum of the diffusion coefficients of the two chromophores D , and the value of k_0 .

$$k_0 = \frac{4\pi RDN_0}{1000} \quad \text{II-33}$$

Therefore the amount of fluorescence intensity quenching (or equivalently, the decrease in the fluorescence lifetime) is related to the sum of the diffusion coefficients of

the fluorophore and the quencher. Oxygen quenching of a chromophore is one type of quenching that will be exploited in this study. Energy transfer from an energy donor to an energy acceptor is another form of fluorescence quenching of the energy donor. The quenching efficiency χ is defined as:

$$\chi = 1 - \frac{\phi_{DA}}{\phi_D} \quad \text{II-34}$$

where ϕ_{DA} is the quantum yield of the donor in the presence of the energy acceptor and ϕ_D is the quantum yield of the donor without the energy acceptor present.

II-3. Diblock Copolymer Micelles and Fluorescence Spectroscopy

Fluorescence spectroscopy has been used to monitor the properties of diblock copolymers in solution, mostly to determine the onset of micellization. These experiments include fluorescence quenching⁶², steady state and time dependent fluorescence depolarization⁶⁵, time resolved fluorescence^{48,63,79}, excimer fluorescence spectroscopy^{63,69} and non-radiative energy transfer^{23,25,61,66-68} (NET).

Prochazka *et al.*⁶³ monitored the onset of micellization of polystyrene-*b*-poly(*tert*-butyl methacrylate) in 1,4 dioxane / methanol mixtures by monitoring changes in the formation of naphthalene excimer formation. With an increase in the methanol content micelles were formed with polystyrene cores to which were attached naphthalene chromophores. Upon micellization, the fluorescent properties changed. When the

polymer was dissolved molecularly, the naphthalene chromophores were able to form excimers. This was not the case for the micelles and the naphthalene excimer fluorescence band disappeared upon micellization. At the same time, due to a reduction in fluorescence quenching by excimer formation, the fluorescence lifetime of naphthalene increased upon micellization.

Yeung and Frank⁶⁹ studied the onset of micellization and the free chain-micelle equilibrium of polystyrene-*b*-poly(ethylene/polypropylene) in heptane by measuring the amount of styrene excimer formation. In micelle cores it was found that the phenyl rings were able to orient themselves to form excimers and hence the intensity of excimer to phenyl fluorescence increased.

Prochazka *et al.*⁶⁴ used time resolved fluorescence anisotropy decay of attached anthracene or carbazole to measure the onset of micellization of polystyrene-*b*-poly(hydrogenated isoprene) in heptane-dioxane solvent mixtures. The chromophores were attached to the styrene blocks and upon micellization the residual anisotropy of the time resolved fluorescence experiments became significantly greater than zero. This result was interpreted to be due to a reduction in the mobility of the attached chromophores once micelle cores are formed.

The fluorescence lifetime of fluorescent chromophores in micelles or on the interface of micelle cores was found to increase significantly upon the onset of micellization. Kiserow *et al.*⁴⁸ measured the lifetimes of naphthalene chromophores on naphthalene-polystyrene-*b*-poly(methyl methacrylate) (N-S-MM) and polystyrene-

naphthalene-*b*-poly(methyl methacrylate) (S-N-MM) in 1,4 dioxane / methanol. The average lifetime of naphthalene in N-S-MM increased upon the onset of micellization. An easy interpretation is made somewhat more difficult by the fact that upon micellization naphthalene excimer fluorescence ceases to occur. The excimer formation in the well solvated case would quench monomeric naphthalene fluorescence and hence reduce its average fluorescence lifetime. The drop in the naphthalene excimer fluorescence intensity is attributed to a reduced segmental rotation movement of the naphthalene groups within the micelles. S-N-MM did not form excimers in the well solvated case and Kiserow reports that there was only a small change in the fluorescence lifetime of naphthalene upon the onset of micellization.

Watanabe and Matsuda^{67,68} studied the micellization properties of a graft copolymer of polystyrene- *graft* -fluorene-poly(methyl methacrylate)-pyrene (PS- *graft* -Fl-PMMA-Py) that was labelled at the junction point with a fluorenyl group (energy donor) and at the end of the PMMA block with pyrene (energy acceptor). This polymer was well solvated in THF and formed micelles upon the addition of cyclohexane greater than 80 % or upon the addition of acetonitrile of greater than 80 %. THF is a good solvent for both blocks, while cyclohexane is a poor solvent for PMMA and acetonitrile is a poor solvent for PS. In both cyclohexane rich and acetonitrile rich solutions the amount of energy transfer from fluorene to pyrene increased greatly upon micellization as measured by the steady state fluorescence intensity ratios.

Watanabe also observed an increase in the fluorescence lifetime of pendant pyrene chromophores from 27 ns to 105 ns upon the onset of micellization in acetonitrile. This is a curious result since acetonitrile is selectively poor for polystyrene and the pyrene chromophores were at the end of the well solvated micelle corona chains. The data for solvent systems that include the pyrenes in the micelle cores was not complete in this regard due to the insolubility of the polymer shortly after the micelles were formed. The data however did show an increase in the fluorescence lifetime of pyrene from 27 to 37 ns at the onset of micellization before phase separation took place. Thus for pyrene the onset of micellization was concurrent with an increase in the average fluorescence lifetime of pyrene. Watanabe speculated that the reason for the increase in the fluorescence lifetime of pyrene was due to a reduced oxygen quenching efficiency of pyrene fluorescence in the micelles both in the corona, which has a higher concentration of polymer chains in the immediate vicinity and in the micelle cores.

Non-radiative energy transfer (NET) has been used to determine the onset of micellization and the micelle chain exchange kinetics between micelle particles. Major *et al.*⁶¹ synthesized styrene-isoprene diblock copolymer end labelled with a carbazoyl (energy donor) or a naphthyl (energy acceptor) group. The polymers labelled with the energy donor and acceptor pair constituted a matched set. Micelles were formed by the addition of heptane to a well solvated solution containing polymer labelled with carbazoyl and with anthracene in cyclohexane. In systems where the polymers were well solvated little or no energy transfer was observed. Upon the onset of micellization the amount of energy

transfer increased greatly. This was due to the close proximity of energy donors and acceptors in the micelle cores. The steady state fluorescence intensity ratio of anthracene to carbazoyl was measured using an excitation wavelength that is selective for carbazoyl. Major reported that the fluorescence lifetime of the anthracene group in going from cyclohexane to 90 % heptane solvent mixture remained the same within experimental error.

II-4. The Dimensions of Diblock Copolymer Micelles

The most obvious aspect of the dimensions of diblock copolymer micelles is that they are composed of a core of the insoluble polymer block and a corona of solvent swollen polymer chains of the other block. In a mixed solvent system there may be preferential solvent absorption into the micelle core^{74,75}. The dimensions of the micelle corona depend heavily on the amount of overlap there is between the chains of the corona. In the case of "crew cut" micelles where the well solvated chains are short enough that they do not interact with each other, then in a good solvent the corona dimensions will scale as N_A^v , where v is $2/3$ for a good solvent and $1/2$ for a theta solvent, N_A is the number of repeat units of the corona forming polymer block⁷⁶. The radius of the core will scale as $N_B^{2/3}$, where N_B is the number of repeat units of the core forming polymer block.

Where the amount of overlap between the corona polymer chains becomes increasingly greater the predictions as to the scaling of the size of the corona and the aggregation numbers becomes more complicated until the regime that occurs when the

size of the corona chains (N_A) is much greater than that of the core forming chains. At this point ($N_A \gg N_B$) the influence of the core is minimal and perturbation caused by chain interaction in the corona is also minimal and is restricted to near the core-corona-interface. This is called the “hairy” micelle model. The radius of the micelle for the “hairy” micelle case scales as $R \propto N_A^{3/5} N_B^{4/25}$.

II-5. Micellization Model

Modelling of diblock copolymer micelles has been attempted by several groups^{8,9,77,78,80-84}. In our study it is the variation in the aggregation number with respect to the solvent quality and the polymerization number of the two blocks that is of interest.

Munch and Gast⁸ have presented a model that attempts to account for all the thermodynamic parameters. In their treatment, they have simplified their treatment by assuming that the interaction between the solvent and the corona block was athermal (i.e. $\chi_{AS} = 0$). Then the free energy, f , of micellization per chain is:

$$\begin{aligned} \frac{f}{kT} = & 4\pi \left(\frac{3N_B}{4\pi} \right)^{2/3} \left(\frac{\chi_{BS}}{6} \right)^{1/2} p^{-1/3} \\ & + \frac{3}{2} \left[\left(\frac{3p}{4\pi N_A^{1/2}} \right)^{2/3} \left(\frac{1}{\alpha^{1/3}} + \left(\frac{1+\alpha\phi_0}{\phi_0} \right)^{1/3} - \alpha^{1/3} \right)^2 \right] + \left(\frac{4\pi N_A^{1/2}}{3p} \right)^{2/3} \left[\alpha^{1/3} + \left(\left(\frac{1+\alpha\phi_0}{\phi_0} \right)^{1/3} - \alpha^{1/3} \right)^{-2} \right] \\ & + \frac{\beta}{1+\alpha} \frac{1-\phi_0}{\phi_0} \ln(1-\phi_0) \end{aligned}$$

where p is the aggregation number, N_A is the number of segments of the soluble block, N_B is the number of segments of the insoluble block, χ_{BS} is the Flory interaction parameter for the insoluble block and the solvent, α is the ratio of N_A / N_B , ϕ_0 is the concentration of the soluble block in the corona sphere (volume fraction) and β is the ratio of the ratio of the total degree of polymerization to that of the size of the solvent (N / N_s). The aggregation number expected is then obtained by differentiating the free energy with respect to p , the aggregation number and then setting $df/dp = 0$. A complex relationship between χ_{BS} and p emerges. If one can arrive at reasonable estimates of all the parameters in the differential equation then an accurate description of the variation of p can be obtained as both the solvent quality and the degree of polymerization are changed.

Nagarajan and Ganesh⁸⁵ also considered this problem and they arrived at scaling relationship for the aggregation number with respect to the degrees of polymerization for both of the blocks. For polystyrene-*b*-polybutadiene in heptane they arrived at the following scaling relationships:

$$p \propto N_B^{1.10} N_A^{-0.24}$$

CHAPTER III: SYNTHESIS and PROCEDURES

III-1. Introduction

The next sections describe the synthesis of the polymers used in this project. Diblock copolymers used for studies of micellization in dilute solution require copolymers that have well known architectures and low polydispersities. This necessitates the use of ionic polymerization techniques. The polymers used in this study are:

- 1) Fluorene-poly(methyl methacrylate)-*b*-poly(methacrylic acid)-pyrene,
[FI-PMMA-PMAA-Py].
- 1a) Poly(methyl methacrylate)-*b*-poly(methacrylic acid), [PMMA-PMAA].
- 2) Fluorene-poly(methyl methacrylate)-*b*-poly(hydroxyethylmethacrylate)-pyrene,
[FI-PMMA-PHEMA-Py].
- 3) Poly(styrene)-*b*-poly(hydroxyethylmethacrylate), [PS-PHEMA].
- 3a) Poly(styrene)-pyrene-*b*-poly(hydroxyethylmethacrylate), [PS-Py-PHEMA].

The equipment used in the characterization of the diblock copolymers and in experimental studies of copolymer solution and of copolymer micelle solutions are also described.

III-2. Synthesis of Diblock Copolymers

III-2.a. Materials

Fluorene. Fluorene (Aldrich, 98 %) was recrystallized three times from methanol and three times from hexane.

Lithium chloride. Anhydrous material from Aldrich (99.99 %) was dried under vacuum prior to use.

n-Butyllithium - 1.6 M in hexanes (Aldrich) under argon or nitrogen in Sureseal bottles. They were titrated in 2,5 dimethylbenzyl alcohol indicator in freshly distilled tetrahydrofuran (THF). An amount (~.17 ml) of the indicator is added to THF under argon and cooled to 0° C. *n*-butyllithium is added by syringe with vigorous stirring until the first sign of colour change to brown.

s-Butyllithium - 1.2 M in cyclohexane (Aldrich) under argon or nitrogen in Sureseal bottle. Sample is titrated as per *n*-butyllithium.

Tetrahydrofuran (THF) - THF used for polymerization reactions was refluxed over potassium metal until dry according to benzophenone indicator. Benzophenone turns from yellow to purple when dry.

Methyl methacrylate (MMA)- MMA (Aldrich, 99 %) was first washed three times with 10 % sodium hydroxide aqueous solution in order to remove the inhibitor and then three times with distilled water. The monomer was dried over MgSO₄. The MMA was then distilled over CaH₂ and then distilled over triethylaluminium just before use.

tert-Butyl methacrylate (TBMA)- TBMA (Polysciences, 99 %) was washed three times with 10 % sodium hydroxide aqueous solution and then four times with distilled water. The monomer was then dried over Na_2SO_4 overnight. The monomer was then filtered through Brockmann I aluminium oxide and then distilled over CaH_2 just prior to polymerization.

2-[(Trimethylsilyl)oxy]ethyl Methacrylate. The conversion of 2-hydroxyethyl methacrylate (HEMA) to the product has been described previously⁸⁶. To 2-hydroxyethyl methacrylate (Aldrich, 97 %, 24 g, 0.18 mol) was added dropwise 1,1,1,3,3,3-hexamethyldisilazane (Aldrich, 98 %, 30 g, 0.18 mol) over 20 minutes. The temperature was maintained at 0 °C. A catalytic amount of trimethylsilyl chloride was then added and the reaction mixture was warmed to room temperature and stirred overnight. The product was obtained by distillation under reduced pressure from the mixture and stored over CaH_2 . The monomer was distilled from CaH_2 and then from triethyl aluminium under reduced pressure just prior to polymerization.

Styrene. Styrene (Aldrich, 99 %) was filtered through an alumina column and then stirred with benzylmagnesium chloride at room temperature for 3 hours. The monomer was distilled under reduced pressure just before polymerization.

III-2.a.i. Synthesis of 1-Bromomethyl Pyrene

The first step⁸⁷ to the target product was 1-pyrenemethanol which was obtained by reduction of 1-pyrenecarboxaldehyde (Aldrich, 99 %). Sodium borohydride (0.6 g) was

added to a mixture of 1-pyrenecarboxaldehyde (5.0g), ethanol (100 ml) and 10 ml of 0.05 M NaOH solution and allowed to react at room temperature for five hours. The reaction was quenched with a dilute solution of sulphuric acid. Ethanol was removed by rotoevaporation and another 100 ml of water was added to the mixture. The product was extracted with three portions of diethyl ether. The ether layer was then washed with three portions of 10 % w/w sodium bicarbonate and then with three aliquots of distilled water. The ether solution was then dried with sodium sulphate, filtered, and then the ether was removed by rotoevaporation. 1-Pyrenemethanol was recrystallized from cyclohexane three times to obtain the pure product.

1-Pyrenemethanol (1.9 g) was dissolved in CCl₄ (125 ml) to which PBr₃ (0.4 ml) was added. The reaction was allowed to proceed for 2 hours at 55-60 °C. The reaction was terminated with methanol (1 ml). The CCl₄ solution was then washed three times with 10 % NaHCO₃ solution, three times with distilled water and once with a saturated NaCl solution. The organic layer was then dried over Na₂CO₃ after which the solution was filtered and the solvent then removed. The product was recrystallized from a mixture of CCl₄ and hexane. 1-Bromomethylpyrene is stable for months if refrigerated.

III-2.a.ii. Synthesis of Fluoreneacetic Anhydride

1.0 g of 9-fluoreneacetic acid (Aldrich, 99 %) was dissolved in 10 mls of dry benzene and 1.0 mls (3 equivalents) of thionyl chloride was added. The reaction⁸⁸ was monitored by TLC plates. The solution was refluxed for 11 hours with a calcium chloride

drying column and then was cooled to room temperature. The solvent, along with the thionyl chloride, hydrochloric acid, and benzene were removed under reduced pressure. A green coloured oil was left over. The product was purified first by filtering a benzene solution through Celite 454 and then by recrystallization from a benzene / hexane mixture. The product was a white crystalline solid and was confirmed with IR (1810,1743,1450,1403,1050,1037 cm^{-1}) and NMR (7.27-7.90, 8H, m; 4.37, 1H, t; 2.92, 2H, d).

III-2.a.iii. Synthesis of 1-Pyrenebutyric Anhydride

1-Pyrenebutyric acid chloride was provided courtesy of Dr. N. Hu, synthesized by the treatment of 1-pyrenebutyric acid with thionyl chloride. To synthesize 1-pyrenebutyric anhydride, 225 mg of 1-pyrenebutyric acid chloride was added to 220 mg of 1-pyrenebutyric acid and dissolved in about 10 mls of dry pyridine under argon. The yellow solution developed an orange colour during the first hour. The reaction was allowed to proceed for six hours. The solvent was then removed by vacuum pump. The crude product was then dissolved in benzene. A white solid was left behind and the solution was removed by pipette. The product was purified by recrystallization from hot benzene / hexane. The product was confirmed by IR (1814, 1743, 1053 cm^{-1}).

II-2.a.iv. Synthesis of 1-Phenyl-1-(1'-pyrenyl) Ethylene

This compound was prepared by Dr. N. Hu from 1-pyrene-carboxyaldehyde according to the literature procedure⁸⁹. The pure product was obtained by recrystallization from ether twice.

III-2.b. Polymerization Reactions

All polymerization reactions were carried out in glass flasks, which were carefully cleaned, under positive argon pressure. The polymerization flasks were dried under high vacuum and flame dried three times. The transfer of initiators and monomers were done by syringes that were carefully cleaned and then dried under vacuum.

III-2.b.i. Polymerization Reaction for FI-(MMA)₃₅-H

This polymer was used as a standard for UV-Visible spectroscopy to obtain a realistic value of the molar absorptivity of fluorene attached to PMMA and was synthesized by anionic polymerization. A polymerization flask was dried under high vacuum overnight with periodically baking. After charging the flask with argon, fluorene (0.1295 g) was added into the flask and dried under high vacuum for 30 minutes. The flask was charged with argon again and then THF (20 ml) was added. Into the THF solution was added *n*-butyllithium (1.6 M, 0.46 μ l) at 0 °C. After stirring for 5 minutes the solution was cooled to -78 °C. Distilled methyl methacrylate (1.6 ml) was then added in one portion to the initiator solution. The polymerization was carried out at this

temperature for 60 minutes. The reaction was terminated with methanol and then the reaction mixture was raised to room temperature. The polymer was reprecipitated from methanol three times. Spectroscopic grade solvents were used for the purification.

III-2.b.ii. Polymerization Reaction for FI-PMMA-PHEMA-Py

This polymer was made by sequential anionic polymerization⁸⁶ by Dr. N. Hu. A polymerization flask was charged with lithium chloride⁹⁰ (10 mg) and dried under high vacuum overnight with periodically baking. After charging the flask with argon, fluorene (35.0 mg) was added into the flask and dried under high vacuum for 30 minutes. The flask was charged with argon again and then THF (50 ml) was added. Into the THF solution *n*-butyllithium (1.6 M, 0.1 ml) was added at 0 °C. After stirring for 5 minutes the solution was cooled to -78 °C. Distilled methyl methacrylate (1.7 ml) was then added in one portion to the initiator solution. The polymerization of methyl methacrylate was carried out at this temperature for 20 minutes. Into the living polymer solution was added dropwise and slowly 2-[(trimethylsilyl)oxy]ethyl methacrylate (3.4 ml). The polymerization of the second block was continued for an additional 1.0 hour. The living polymer was terminated with 1-bromomethylpyrene. The termination reaction was allowed to proceed for 4 hours and then the polymer was treated with methanol and allowed to warm to room temperature. The polymer was then treated with methanol (2.0 ml) and 10 % HCl aqueous solution (0.3 ml) at room temperature for 30 minutes to hydrolyze the second block to HEMA. The polymer was poured into water and collected by filtration

and dried under vacuum. The polymer was redissolved in THF-MeOH (9:1) and precipitated three times from ether by the reverse precipitation technique in order to remove excess 1-bromomethylpyrene.

III-2.b.iii. Polymerization Reaction for PS-Py-PHEMA and PS-PHEMA

These copolymers were synthesized by Dr. N. Hu. A clean and dry polymerization flask was charged with THF (50 ml) and the flask was cooled to -78 °C in a dry ice and acetone bath. *s*-Butyllithium (Aldrich, 1.2 M) was added as an initiator. Three drops of styrene were added into this solution, which was allowed to react for 1 minute. The remainder of the styrene was then added in one portion. The polymerization was carried out at this temperature for 30 minutes. Into the living polymer solution was added 1,1-diphenylethylene (3 equivalents of the initiator) in THF. After stirring for 30 minutes the second monomer, 2-[(trimethylsilyl)oxy]ethyl methacrylate was added dropwise over 20 minutes. The stirring continued for another hour. The living polymer was quenched with methanol and the polymer solution was warmed to room temperature.

The second block was subsequently hydrolyzed to HEMA by treating it with a solution of methanol (2.0 ml) and 10 % HCl aqueous solution (0.3 ml) at room temperature for 30 minutes. The polymer solution was poured into water and collected by filtration, and then dried under vacuum. The copolymer was redissolved in THF-MeOH (9:1) and reprecipitated from ether three times.

The synthesis of PS-Py-PHEMA follows the procedure is the same as that presented above with the exception that 1-phenyl-1-(1'-pyrenyl) ethylene was used to cap the polymerization of the first block (polystyrene), which was followed by the addition of the second block (2-[(trimethylsilyl)oxy]ethyl methacrylate).

The copolymer was purified to remove the byproducts and then the polystyrene homopolymer was removed by heating a suspension of the solid polymer in cyclohexane at about 50 °C for four hours. Cyclohexane is a theta solvent for polystyrene and a non-solvent for PHEMA. The solid diblock copolymer was filtered and the dissolved homopolymer was recovered for analysis of size and polydispersity.

Two sets of matched copolymers, with and without the pyrene labels, of approximately 100 and 300 repeat units per block were synthesized. The complete analysis of the characterization is shown in Table III-1.

III-2.b.iv. Labelling of PS-(Py)-PHEMA with Fluorene Chromophores

PS-(Py)-PHEMA diblock copolymer was randomly labelled with fluorene chromophores on the HEMA block by reacting the copolymer with 9-fluoreneacetic anhydride in dry pyridine at room temperature for 24 hours. The polymers were collected by reverse precipitation from 15 % diethyl ether in pentane. The pure polymers were obtained by three precipitations from ether-pentane (1:1). The labelling densities were determined by UV-VIS spectroscopy using fluorene acetic acid (Aldrich, 99%) as a standard [$\epsilon(304 \text{ nm}) = 7771 \text{ cm}^{-1} \text{ M}^{-1}$].

III-2.b.v. Polymerization Reaction for FI-PMMA-PMAA-Py and PMMA-PMAA

The precursor polymer [fluorene-poly(methyl methacrylate)-*b*-poly(*tert*-butyl methacrylate)-pyrene] was synthesized by sequential anionic polymerization. Fluorenyl lithium was prepared by reacting equal molar amounts of fluorene and *n*-butyllithium (1.6 M, 0.1 ml) at 0 °C in THF. Lithium chloride was added to improve the polydispersity⁹⁰. The reaction mixture was cooled to -78 °C and methyl methacrylate was added, followed half an hour later by the addition of *tert*-butyl methacrylate. The polymerization of the second block proceeded for six hours and was terminated with 1-bromomethylpyrene (1.5 equivalents). The excess terminator was removed by reverse precipitation by pentane from THF. The unlabelled polymer was initiated by *n*-butyllithium and diphenylethylene and was terminated by the addition of methanol but otherwise followed the same polymerization procedure as above.

The conversion of the *tert*-butyl methacrylate block to the product has been described previously⁹¹. The polymers were dissolved in dry dichloromethane. The *tert* - butyl group was hydrolyzed by the addition of trimethylsilyl iodide to this solution under argon and at room temperature for 45 minutes. The solvent was then removed under anhydrous conditions and under reduced pressure. Toluene was added to the polymer and then evaporated to remove *tert* - butyl iodide completely. The polymer was then dissolved in THF and the polymer solution was poured slowly into methanol containing a catalytic amount of 10 % HCl solution. After stirring for 10 minutes the polymer was precipitated from Na₂S₂O₅ aqueous solution. The colourless polymer was collected and dried under

INITIATION

a) Labelled copolymer

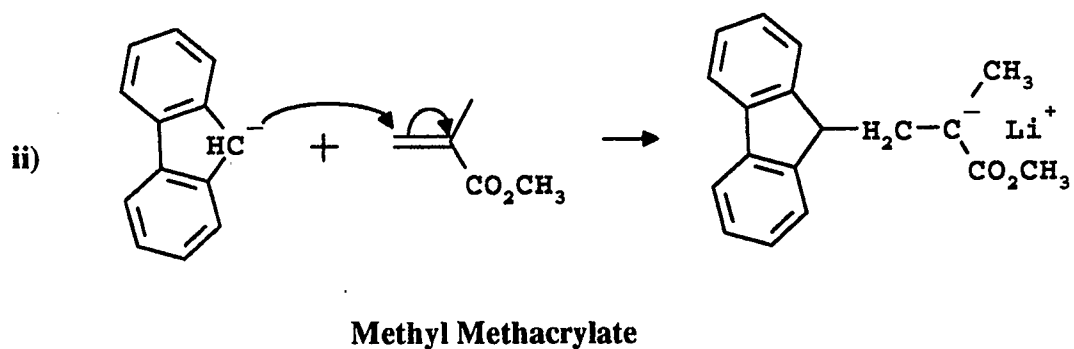
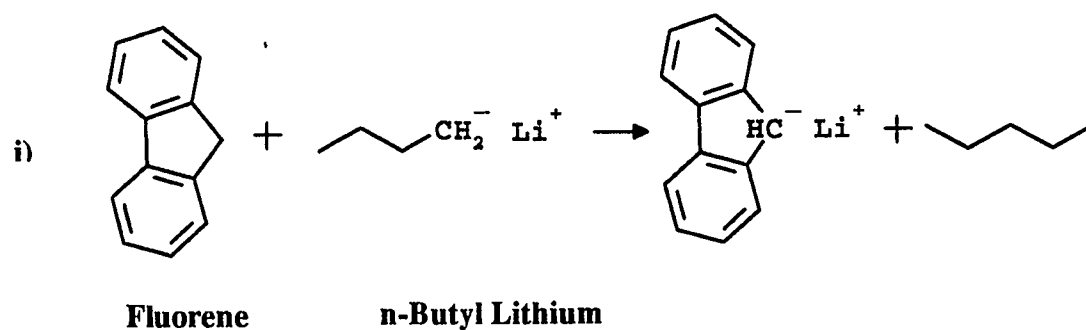


Figure III-1. Initiation reaction steps for the anionic polymerization of FI-PMMA-PTBMA-Py. The first step is extraction of the most acidic proton from fluorene by *n*-butyllithium. The second step is a Micheal reaction of the fluorenyl anion with a molecule of methyl methacrylate.

INITIATION

b) Unlabelled copolymer

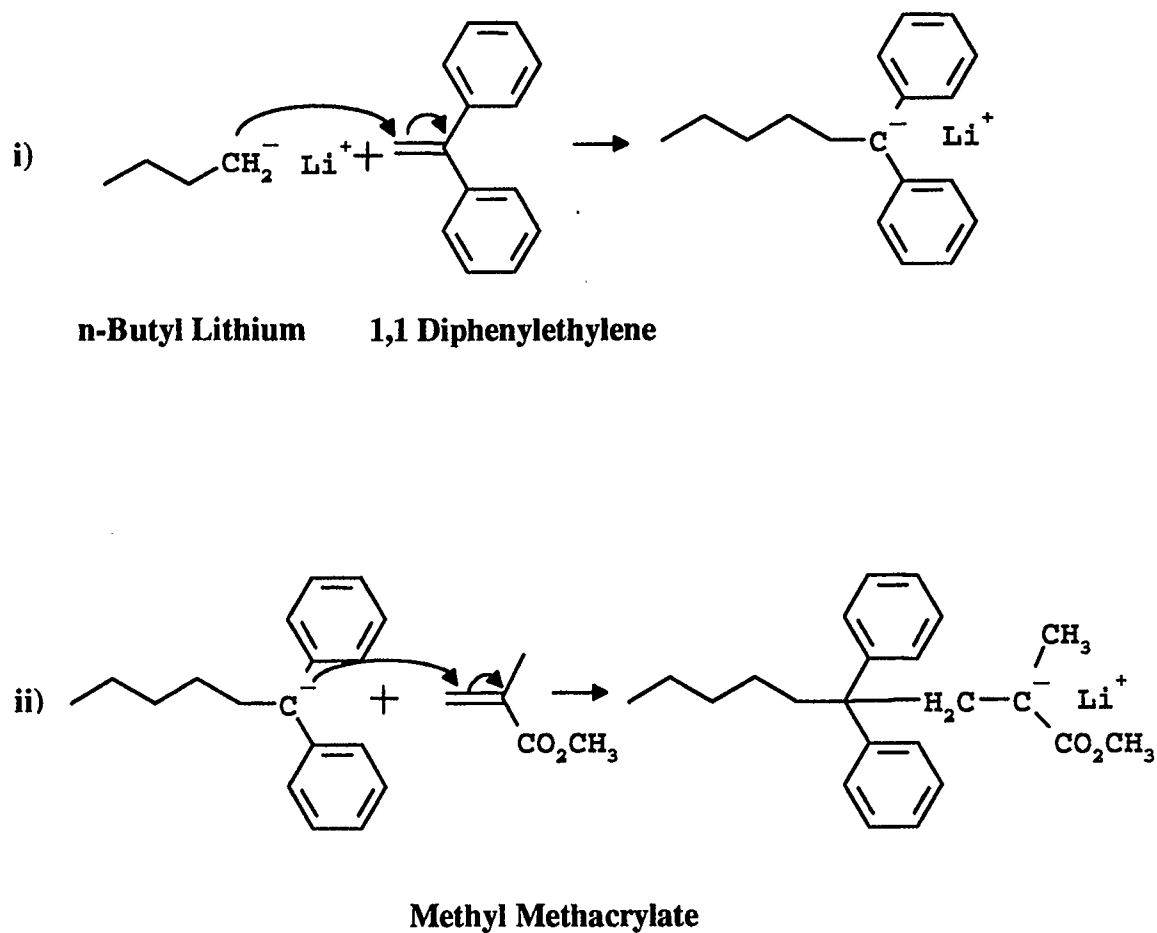


Figure III-2. Initiation reaction steps for the anionic polymerization of PMMA-PTBMA. The first step is a Micheal reaction by *n*-butyllithium with diphenylethylene to eliminate the reaction of the anion with the carbonyl group of the methacrylate. The second step is a Micheal reaction of the diphenylethylene anion with a molecule of methyl methacrylate.

PROPAGATION

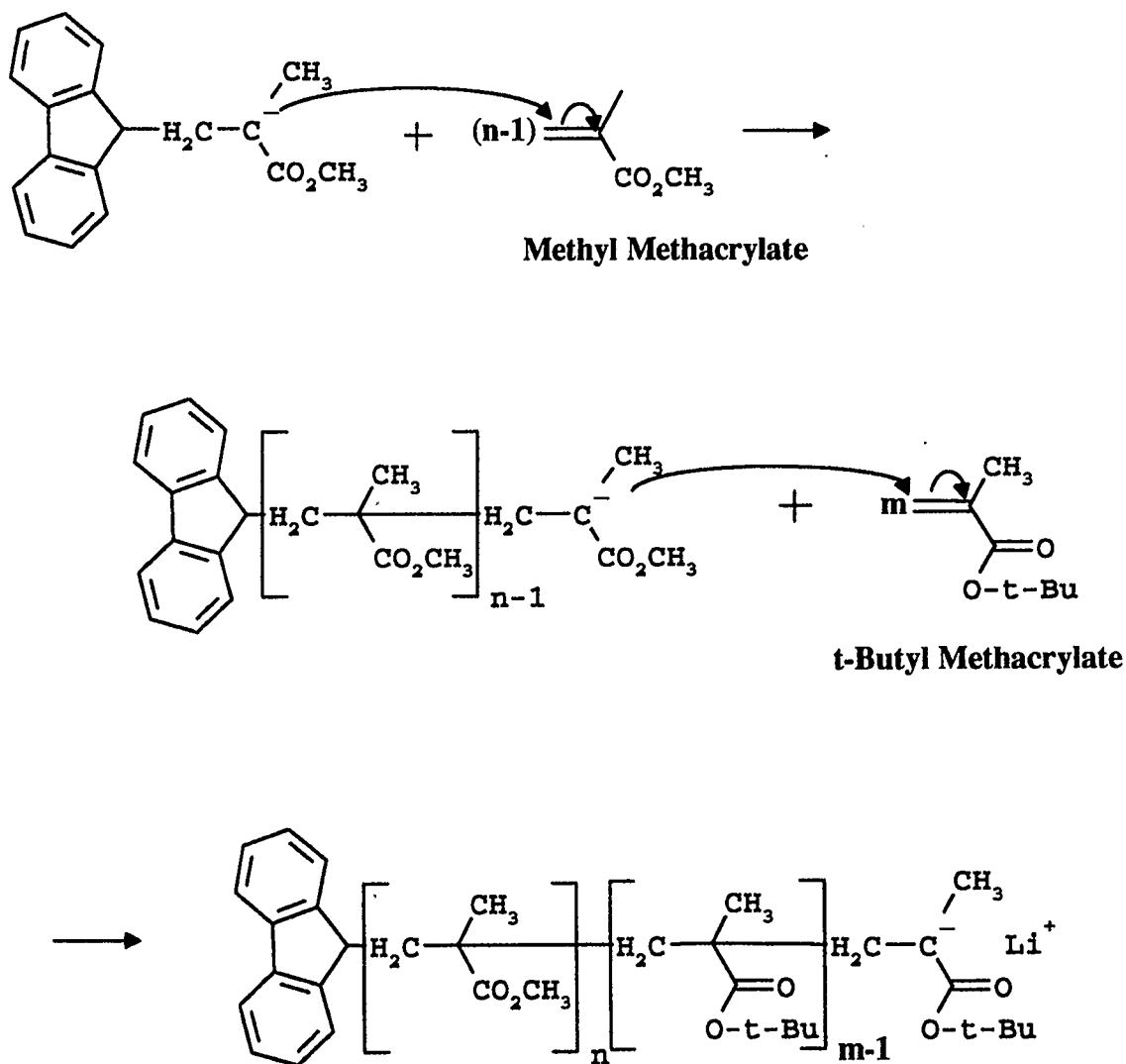


Figure III-3. Propagation steps for the anionic polymerization for the diblock copolymers of PMMA-PTBMA. Both blocks are methacrylates and polymerize by sequential Michael additions to the anions. The labelled copolymer is shown here, however the mechanism for the polymerization of the unlabelled copolymer is the same.

TERMINATION

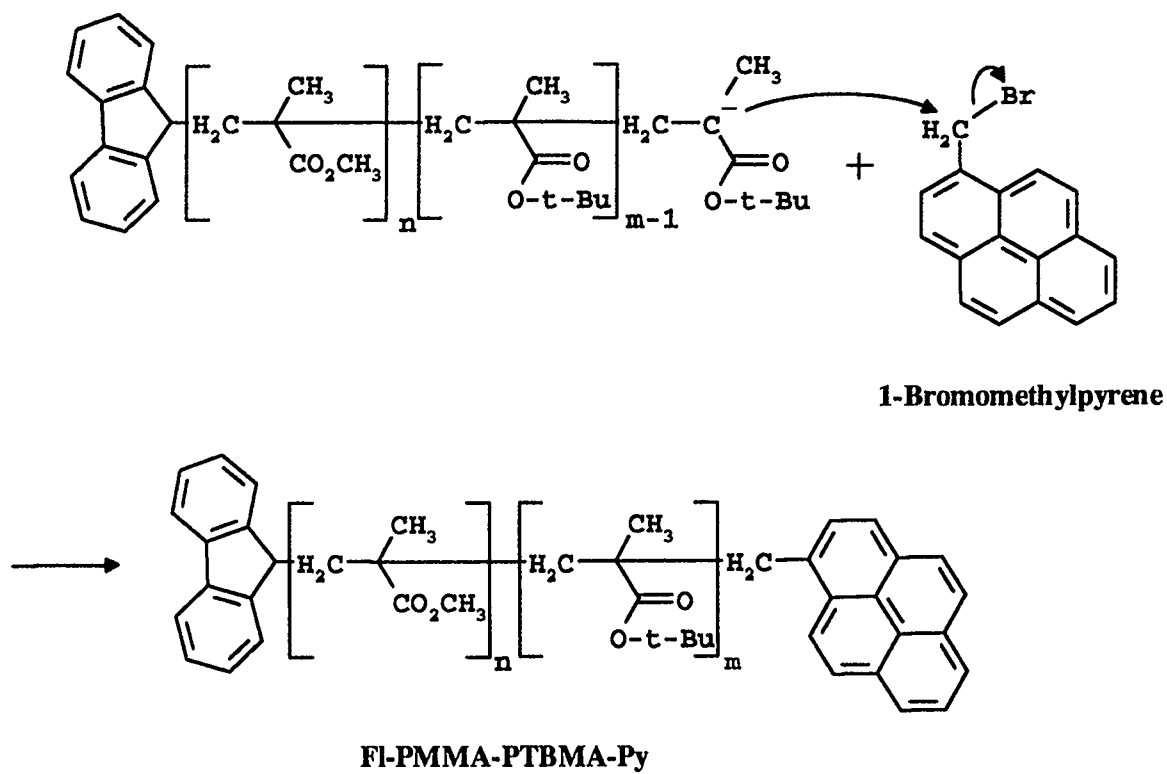


Figure III-4. The termination step of FI-PMMA-PTBMA-Py. This step proceeds by nucleophilic substitution of the bromide by the living polymer anion. Termination unlabelled copolymer polymerization reaction is achieved by the addition of methanol.

HYDROLYSIS

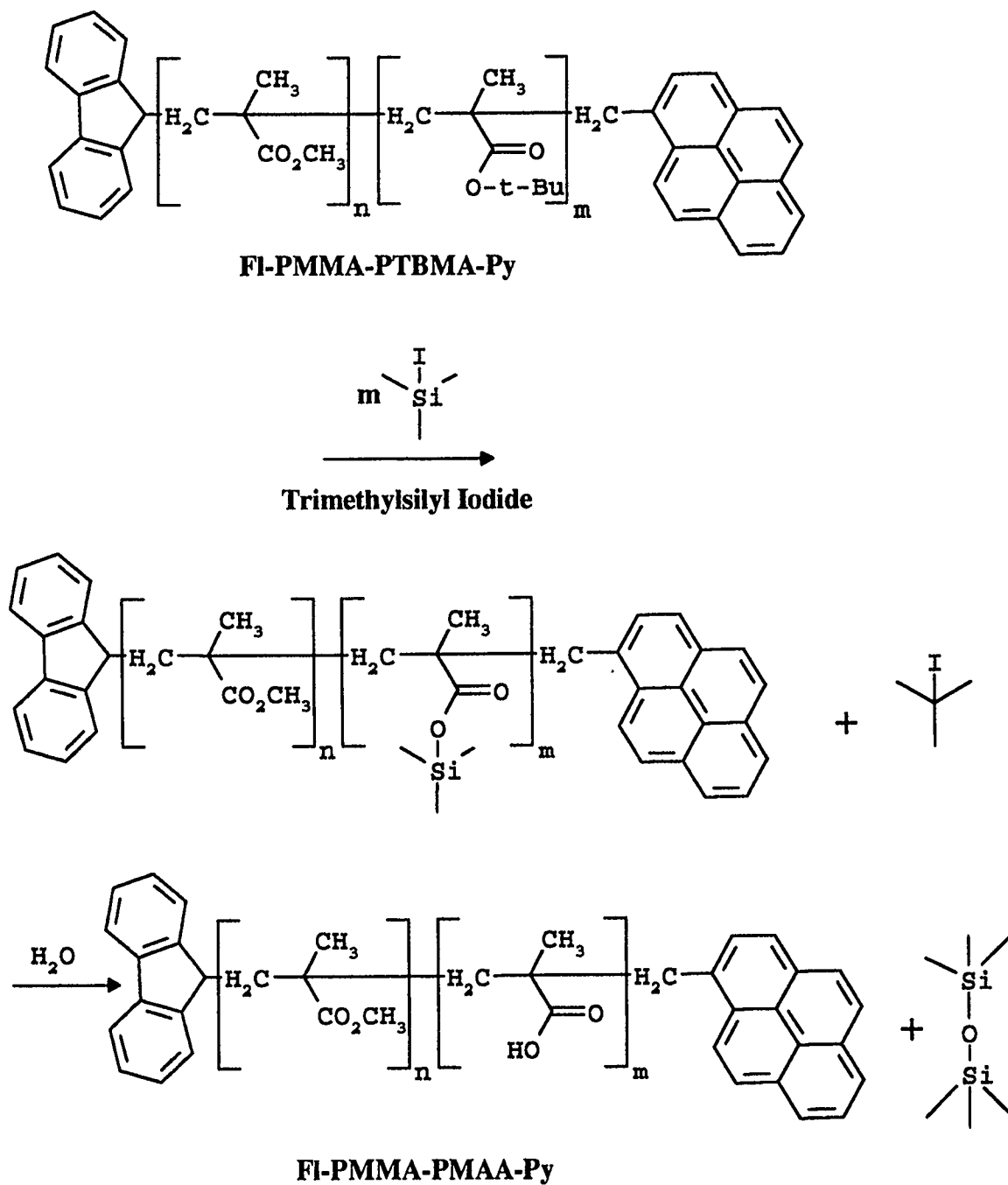


Figure III-5. The hydrolysis of FI-PMMA-PTBMA-Py to FI-PMMA-PMAA-Py. Trimethylsilyl iodide selectively hydrolyzes the *t*-butyl rather than the methyl group.

vacuum. The polymer was redissolved in methanol-ethyl acetate (1:1) and precipitated from ether by reverse precipitation. The polymer was collected and dried under vacuum. A small amount of the hydrolyzed polymers were esterified⁹² with 3 methyl-1-p-tolyltriazene (Aldrich, 98%, 20 % molar excess) in benzene at 40°C for four days for molecular weight determination by GPC.

III-3 Characterization of Diblock Copolymers

III-3.a. Characterization of FI-PMMA-H.

FI-(MMA)₃₅-H was characterized by NMR (CD₂Cl₂) using a 20 second delay time between pulses. Aromatic fluorene peaks (8H, 8.0-7.3 ppm) were ratioed against the methyl ester peaks (3H, singlet, 4.2-3.2 ppm), the methylene peaks (2H, 2.6-1.7 ppm) and the methyl peaks (3H, 1.4-0.7 ppm). The average of these ratios was used for the repeat number of the polymer and was found to be 34.93 to 1.00. This polymer was then used to obtain the molar absorptivity of fluorene (see Section III-5.e.i.).

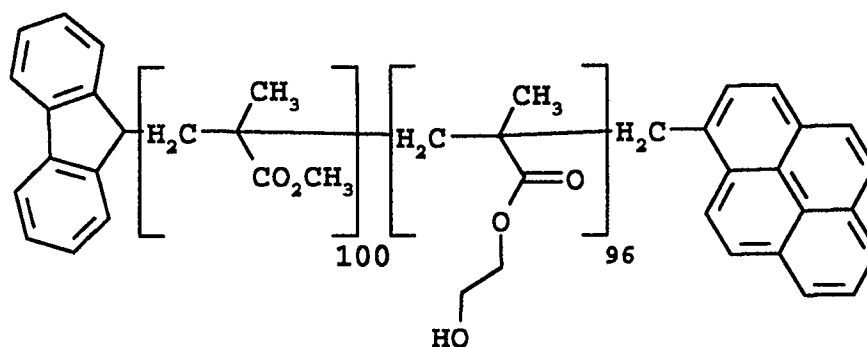
III-3.b. Characterization of FI-PMMA-PHEMA-Py

FI-PMMA-PHEMA-Py was analyzed by GPC, to find the polydispersity of the whole polymer, by proton NMR, to establish the ratio of the block repeat numbers, and by UV-VIS absorption spectroscopy, to determine the molecular weight of the copolymer.

For analysis by gel permeation chromatography (GPC) FI-PMMA-PHEMA-Py was esterified by reacting the polymer with acetic anhydride in dry pyridine. The esterified

polymer was found to have a polydispersity of 1.10 by GPC (Waters HR4 column, Ethyl acetate solvent, refractive index (RI) and UV-VIS detectors, see Figure III-1).

^1H NMR ($\text{CDCl}_3 / \text{CD}_3\text{OH}$, 20 s pulse delay) was used to establish that the ratio of the blocks was 1 PMMA : 0.96 PHEMA. The polymer was not esterified and a mixed deuterated solvent was used to dissolve the polymer. The block ratio was established by integrating the peak areas of the HEMA block ethylene protons (3.4-3.9 ppm, 2 broad peaks, 4H) to that of methyl ester protons of the MMA block (3.39-3.27 ppm, singlet, 3H). UV-VIS absorption spectroscopy of fluorene (Figure III-2) showed the molecular weight (M_n) of the polymer to be $22900 \text{ g/mol} \pm 10 \%$. The molar absorptivity of fluorene for this polymer was assumed to be the same as that fluorene-poly(methyl methacrylate) and at 304 nm was equal to $6844 \text{ cm}^{-1} \text{ M}^{-1}$. The absorbance of pyrene at 304 nm was subtracted from the total absorbance by using the ratio of the molar absorptivities at 342 nm ($4.34 \times 10^4 \text{ M}^{-1} \cdot \text{cm}^{-1}$) and 304 nm ($1.05 \times 10^4 \text{ M}^{-1} \cdot \text{cm}^{-1}$) for 1-pyrenemethanol (Figure III-16). This molecular weight corresponded to a block size of 100 units for the PMMA block and of 96 for the PHEMA block.



Polymer V-1 FI-PMMA-PHEMA-Py

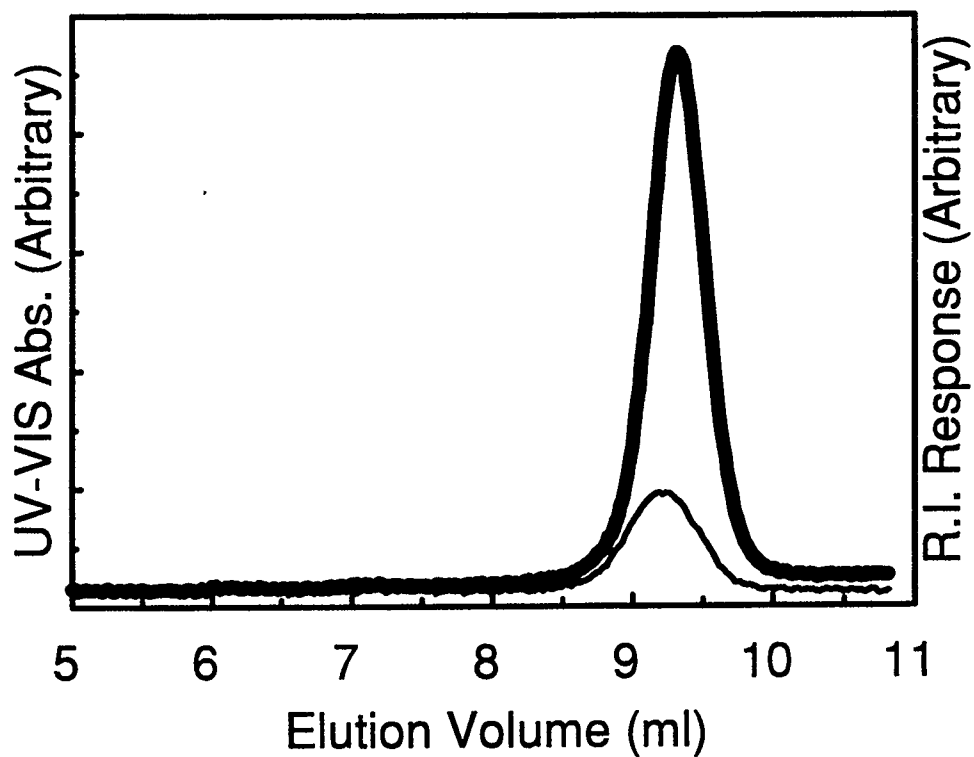


Figure III-6. GPC chromatograms of an esterified sample of FI-PMMA-PHEMA-Py. The eluent was ethyl acetate at a flow rate of 1.0 ml/min. $M_w / M_n = 1.10$. Poly(methyl methacrylate) standards were used. Both an RI (dark line) and UV-VIS (lighter line, $\lambda = 343$ nm) detectors were used.

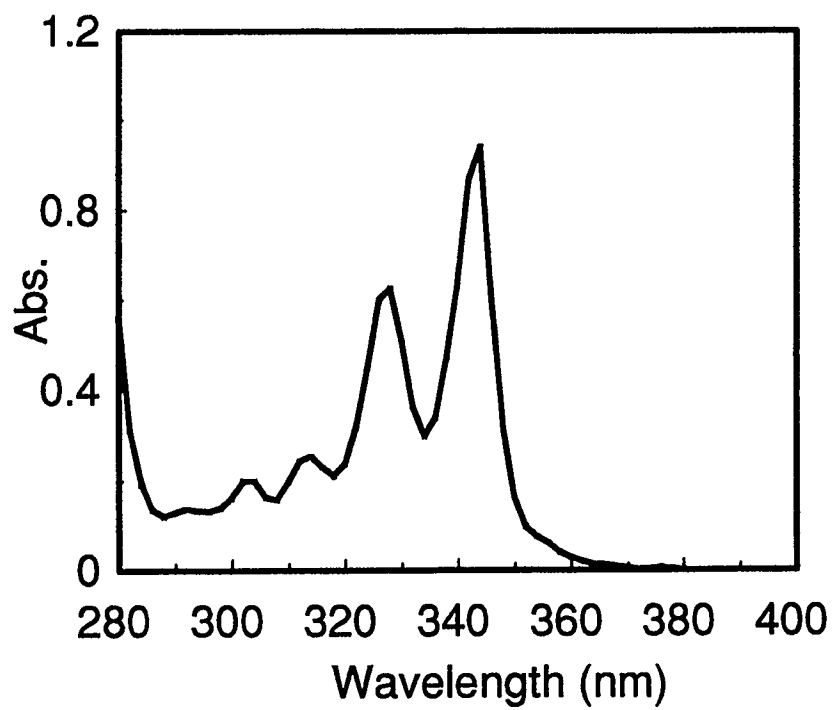


Figure III-7. UV-VIS absorption spectra of FI-PMMA-PHEMA-Py in THF (0.373 mg/ml).

III-3.c. Characterization of the Copolymers of PS-PHEMA.

These copolymers were characterized by proton NMR, GPC, and by UV-VIS spectroscopy. After the synthesis of the diblock copolymer, the homopolymer impurity was removed by heating in cyclohexane. The extracted sample was used for the characterization of the polystyrene block by GPC and light scattering (LS). The first block and the entire copolymer were analyzed by GPC. The molecular weight and polydispersity of the polystyrene block were obtained by running the samples against polystyrene standards (Polysciences). The molecular weight of the first block was calculated using the equation:

$$\text{Log}(MW) = -0.7934(t) + 12.2265 \qquad \text{Correlation} = 0.9994 \qquad \text{III-1}$$

obtained from the calibration curve of the polystyrene standards (Figure III-8). The results are summarized in Table III-1.

Prior to both the NMR and GPC experiments on the diblock copolymer the HEMA block was esterified with cinnamoyl chloride in dry pyridine. The ratio of the block sizes was obtained from proton NMR and when this data was combined with that of the GPC of the PS block the size of the PHEMA block was determined. The entire copolymer was also analyzed by GPC to obtain the overall polydispersity.

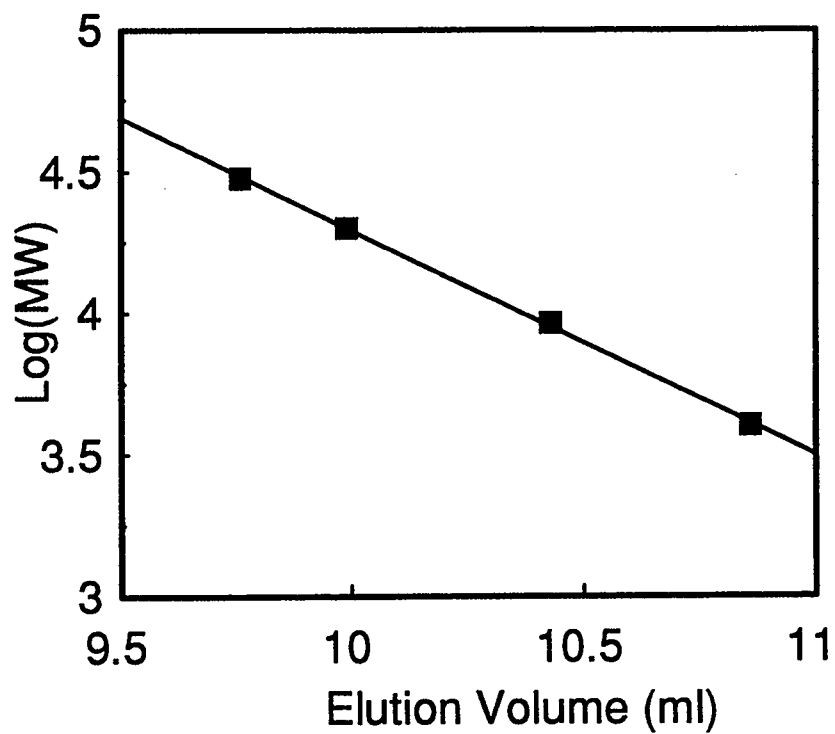


Figure III-8. Calibration curve for Waters Styragel HR4 analytical column using polystyrene standards. The eluent used was ethyl acetate.

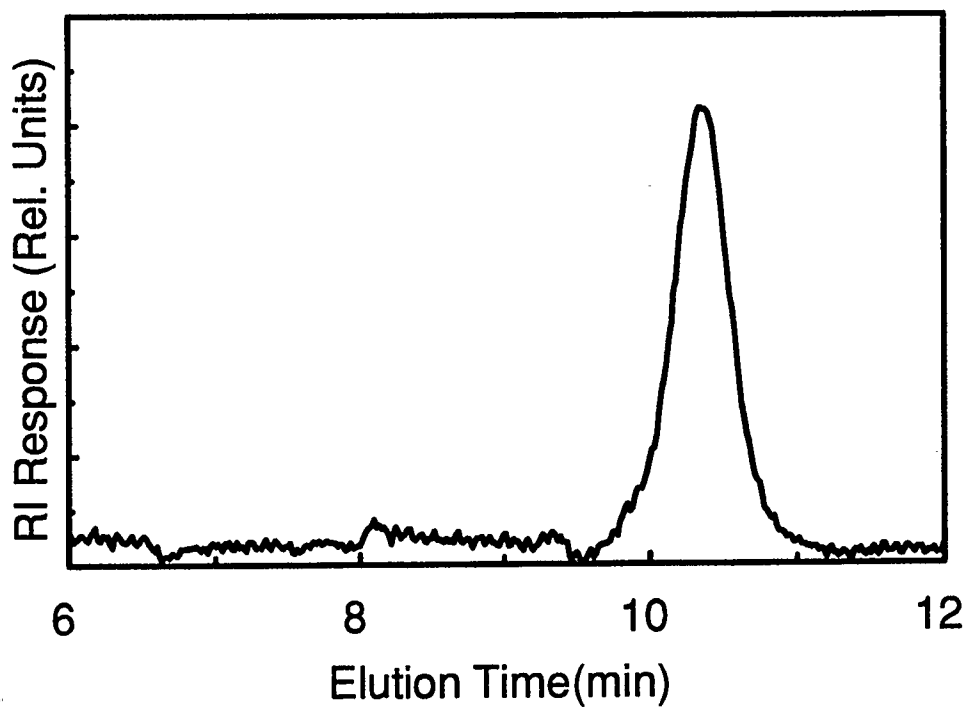


Figure III-9. GPC chromatograms of the homopolymer PS, sample extracted with cyclohexane after polymerization of the copolymer PS-PHEMA. The eluent was ethyl acetate at a flow rate of 1.0 ml/min. $M_w/M_n = 1.08$. Polystyrene standards were used.

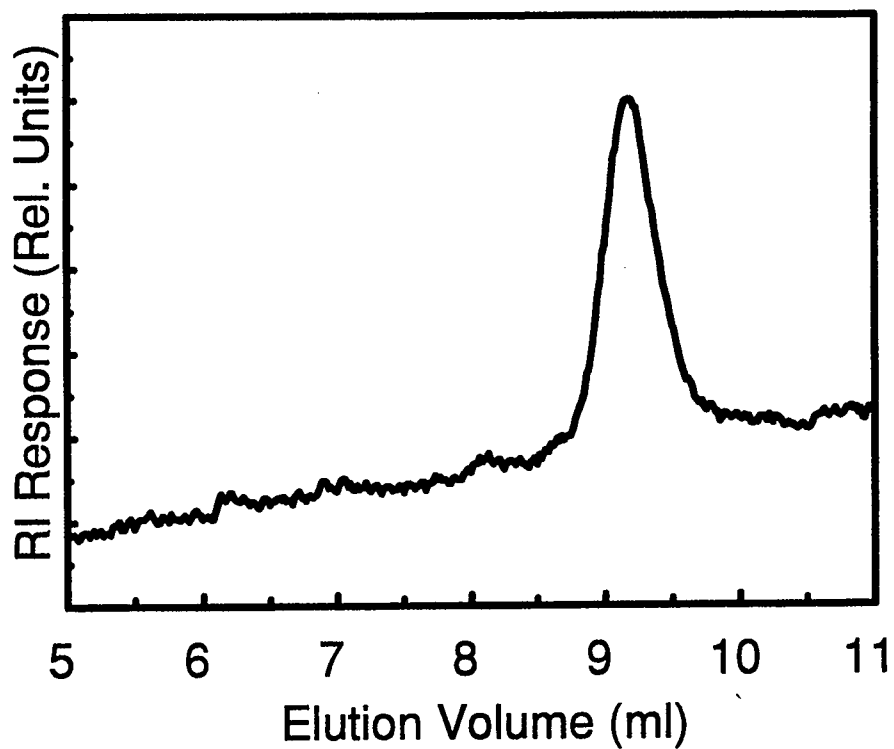


Figure III-10. GPC chromatograms of an esterified sample of PS-PHEMA. The eluent was ethyl acetate at a flow rate of 1.0 ml/min. $M_w / M_n = 1.09$. Polystyrene standards were used.

Table III-1. Summary of characterization results for PS-PHEMA copolymers.

Polymer	PS block (GPC)				Dibloc Copolymer		
	\overline{M}_w g/mole	\overline{M}_n g/mole	\overline{n}_w ^b LS & NMR	$\overline{M}_w/\overline{M}_n$	$\overline{M}_w/\overline{M}_n$ GPC ^a	\overline{M}_w g/mole LS ^a	n/m NMR
VI-1a	.90x10 ⁴	.84x10 ⁴	92	1.08	1.09	3.2x10 ⁴	1.07
VI-1b	.97x10 ⁴	.90x10 ⁴	99 ^c	1.08	1.17		0.93
VI-2a	3.5x10 ⁴	3.1x10 ⁴	305	1.13	1.09	12.6x10 ⁴	0.93
VI-2b	3.2x10 ⁴	2.7x10 ⁴	249 ^d	1.21	1.13		0.83

^a: PS-*b*-PHEMA was esterified using cinnamoyl chloride and then analyzed.

^b: These represent the weight-average numbers of repeat units for PS.

^c: Estimation based on the \overline{n}_w value of Polymer VI-1a and the comparison of the GPC data of Polymers VI-1a and VI-1b.

^d: Estimation based on the \overline{n}_w value of Polymer IV-2a and the comparison of the GPC data of Polymers VI-2a and VI-2b.

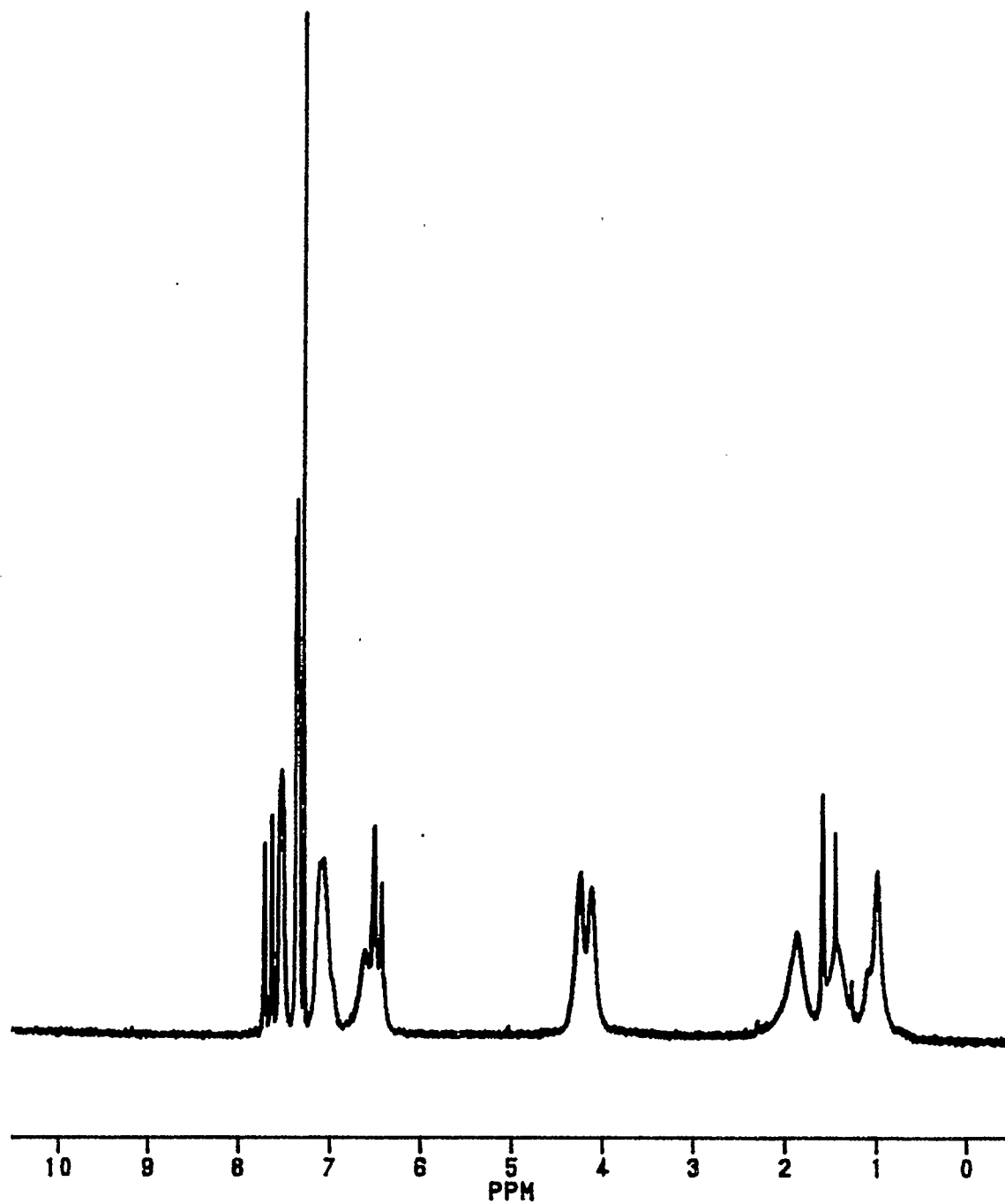
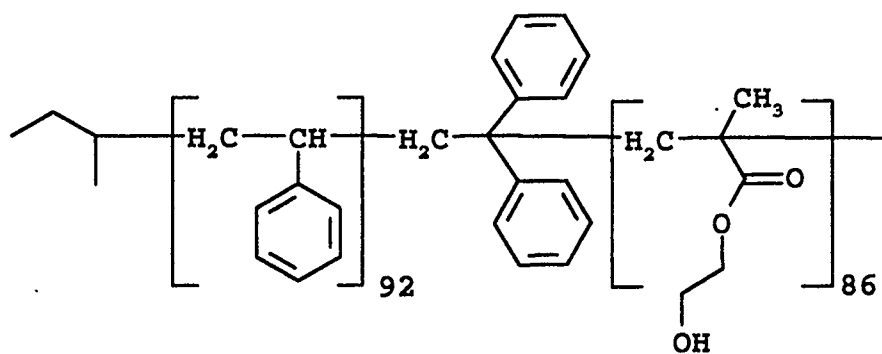
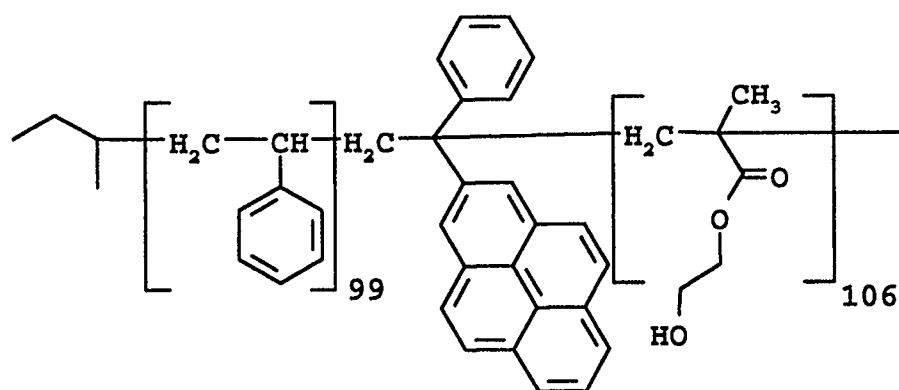


Figure III-11. NMR of PS₁₀₀-PHEMA₁₀₀ copolymer esterified by cinnamoyl chloride. Results of the NMR analysis of all the PS-PHEMA copolymers are shown in Table III-1.

Schematic diagrams of the PS-PHEMA(100) diblock copolymers characterized in Table III-1 are shown above:

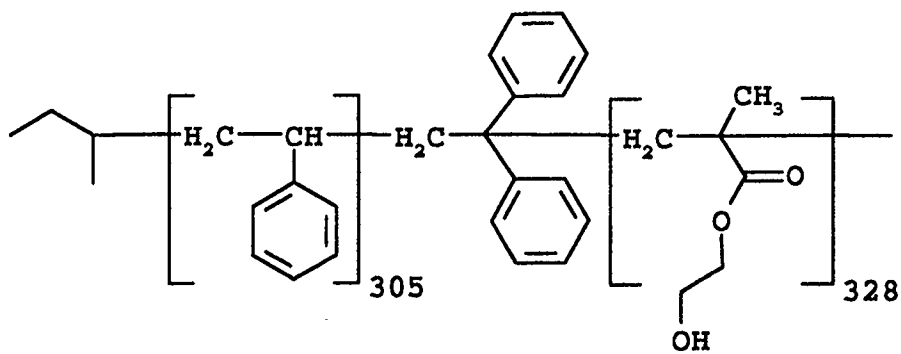


Polymer VI-1a

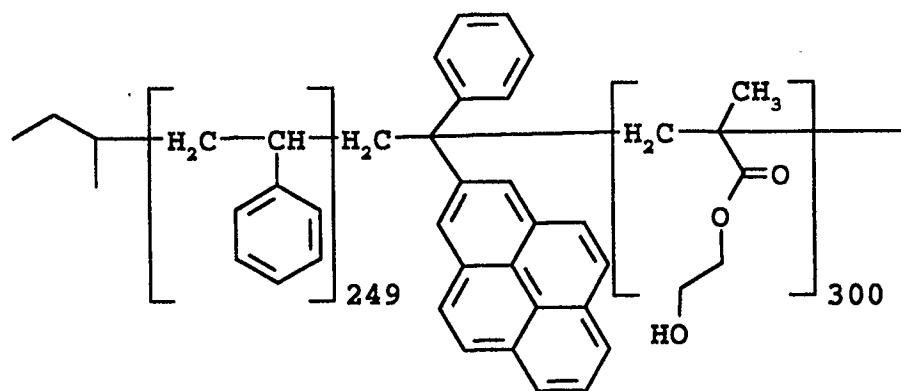


Polymer VI-1b

Schematic diagrams of the PS-PHEMA(300) diblock copolymers characterized in Table III-1 are shown above:



Polymer VI-2a



Polymer VI-2b

III-3.d. Characterization of FI-PMMA-PMAA-Py and PMMA-PMAA

FI-PMMA-PMAA-Py and PMMA-PMAA were characterized by GPC, UV-VIS spectroscopy, and ^1H NMR. The polydispersity of the polymers were found by GPC after methylation of the acid groups to the methyl ester with 3-methyl-1-p-tolyltriazene in benzene⁹². The esterified copolymers were analyzed versus PMMA standards (Polysciences) with a Zorbax 60S, 1000S, and 3000S columns using THF as an eluent and monitored by a Varian Aerograph refractive index detector. The total number of polymer repeat units were obtained as well as the polydispersity of the whole polymers (see Table III-2).

The molecular weight of the methylated copolymer was calculated from the calibration curve equation generated from poly(methyl methacrylate) standards (see Figure III-12):

$$\text{Log}(MW) = 12.175 - 0.5896(t(\text{min})) \quad \text{Correlation} = 0.9980 \quad \text{III-2}$$

The gel permeation chromatograms of the two methylated copolymer samples are shown in Figure III-13. The calculated molecular weights are shown in Table III-2. The overall weight of the methylated samples varies between the two samples by about 21 % which also translates into a difference of 21 % in the molecular weight of the labelled and the unlabelled samples of MMA-MAA.

The $^1\text{H-NMR}$ of both MMA-TBMA copolymers were done in CDCl_3 with a delay time between pulses of 20 seconds. The relative amounts of the two blocks were established from the ratio of the amounts of the methyl ester group of MMA (3H, singlet, 3.91 - 3.50 ppm) to the *t*-butyl group (9H, 1.75 - 1.41 ppm). The NMR of MMA-MAA polymers were done in CD_3OD also with a 20 second delay time between pulses. The degree of hydrolysis was determined from the ratios of the integrated areas of the methyl ester protons (3H, singlet, 3.91 - 3.53 ppm) to that of the remaining *t*-butyl groups (1.42 - 1.49 ppm). The block ratio calculations and the hydrolysis efficiencies are summarized in Table III-2. The extent of hydrolysis for both polymers was about 94 %.

The labelling efficiency of 1-bromomethylpyrene was determined by UV-VIS absorption spectroscopy using 1-methanolpyrene as a standard. 1.53 mg/ml of copolymer was dissolved in THF and an absorbance of 0.9188 was measured at 342 nm. This corresponds to a labelling efficiency of 49.4 %.

Table III-2. Summary of characterization results for PMMA-PMAA copolymers.

Polymer	\overline{M}_n g/mole GPC ^a	$\overline{M}_w / \overline{M}_n$ GPC ^a	n/m NMR	n ^b GPC & NMR	Percent hydrolysis TBMA ^c	M.W. g/mole
IV-1	2.88×10^4	1.12	1.11	146	93.9 %	2.72×10^4
IV-2	3.48×10^4	1.09	1.05	173	94.6 %	3.29×10^4

^a: PMMA-*b*-PMAA was methylated using 3-methyl-1-p-tolyltriazene and then analyzed against PMMA standards.

^b: These represent the average number of repeat units for the PMMA block.

^c: Based on the NMR analysis of PMMA-PTBMA and PMMA-PMAA

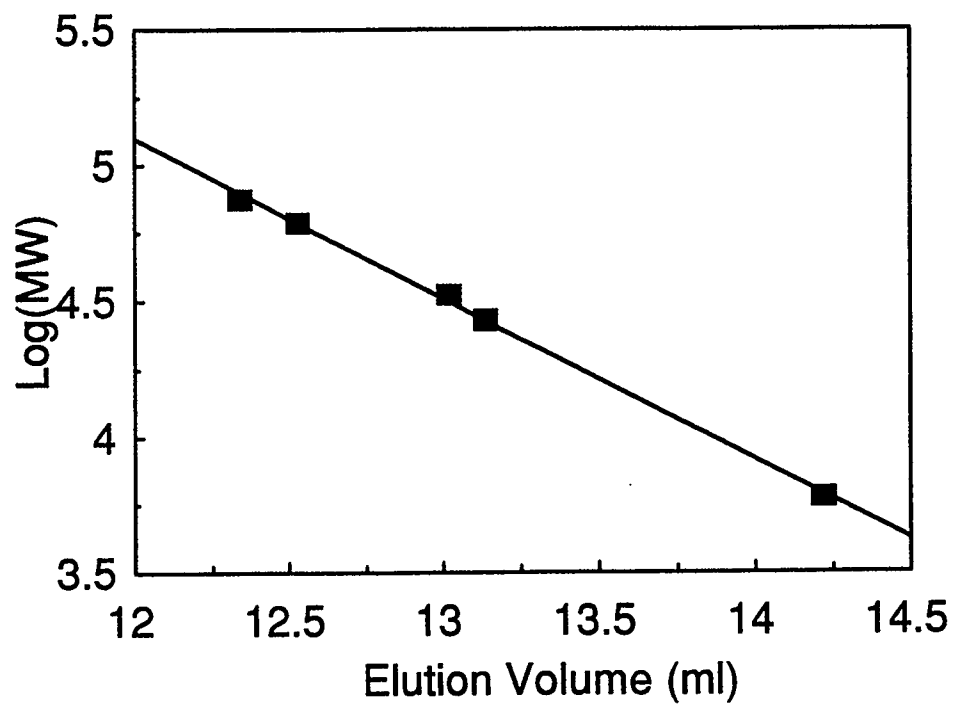


Figure III-12. Calibration curve for Zorbax 60S, 1000S, and 3000S columns using PMMA standards. The eluent was THF.

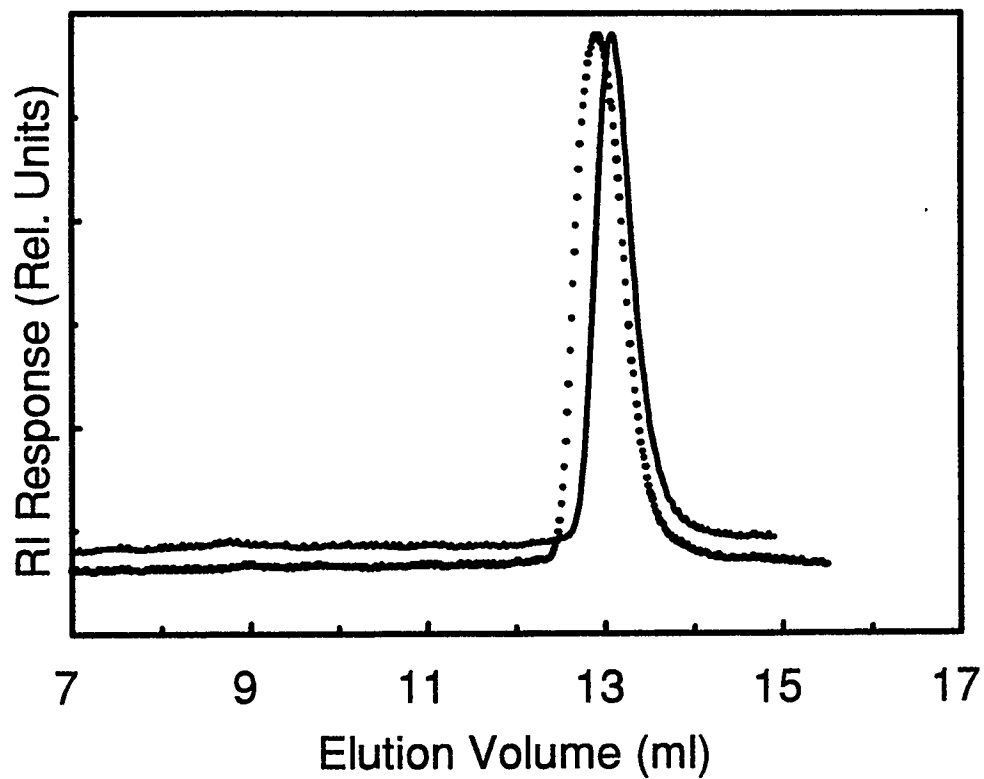


Figure III-13. GPC chromatograms for labelled (dots) and unlabelled (line) PMMA-PMAA. The copolymers were methylated before analysis to form methyl methacrylate. Refractive index detector response is shown.

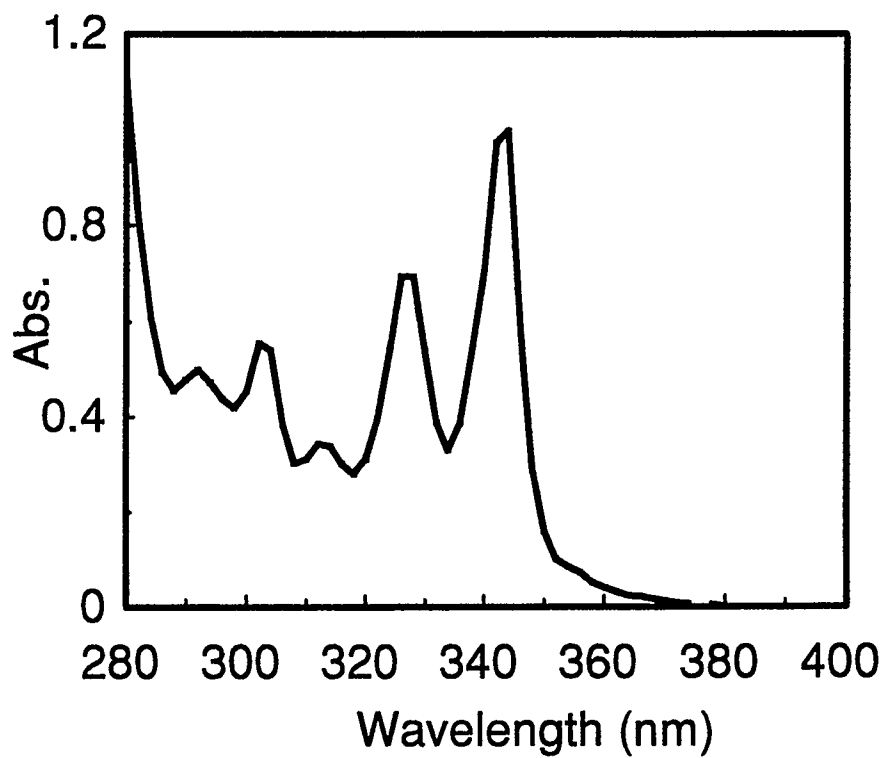


Figure III-14. UV-VIS absorption spectra of Fl-PMMA-PMAA-Py in THF (1.53 mg/ml)

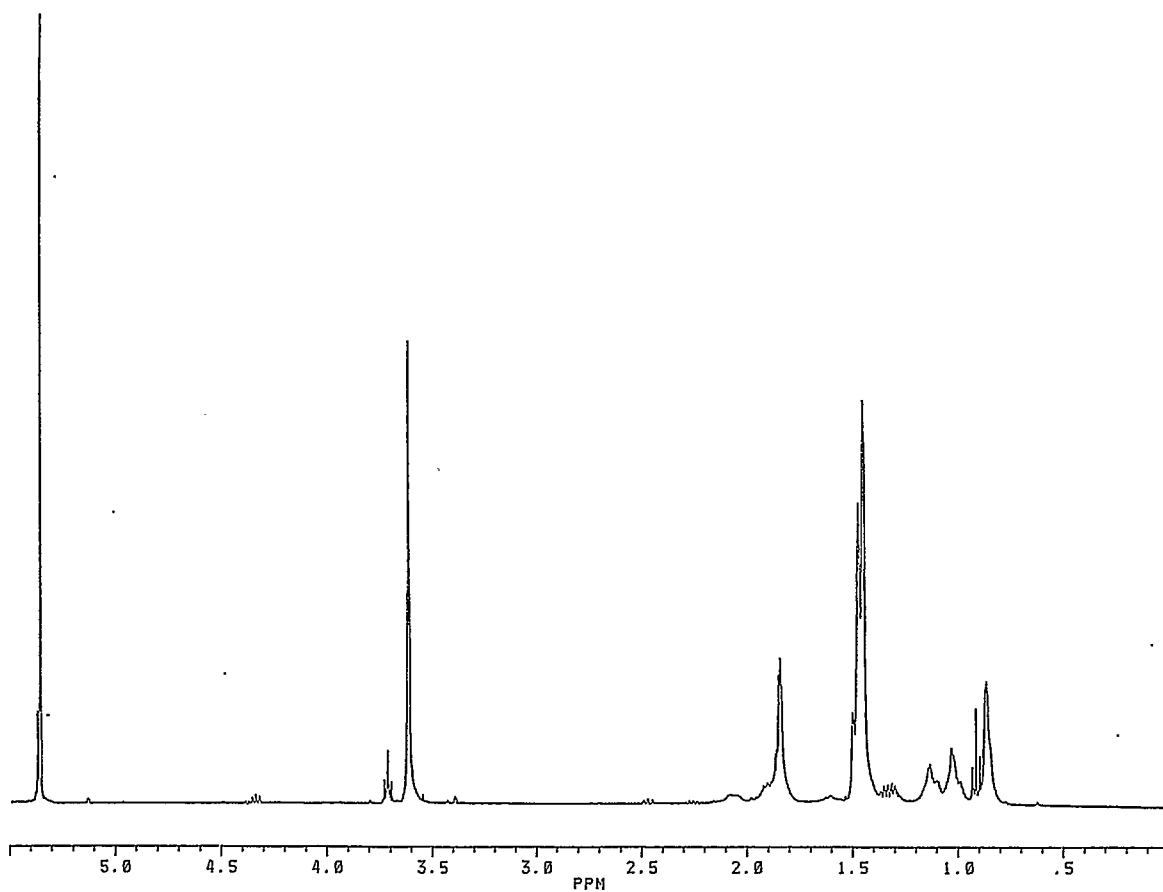


Figure III-15. NMR of unlabelled PMMA-PTBMA in CD_2Cl_2 .

III-4. Micelle Formation

PMMA-PMAA. - Micelles were formed by the slow dropwise addition of ethyl acetate to a solution of PMMA-PMAA polymer in a mixture of methanol and ethyl acetate (v/v = 1:1), under vigorous stirring. Micelle solutions were sealed in glass ampoules and stirred at 40-45 °C for four hours before any physical measurements.

PS-PHEMA. - Micelles were formed by dissolving the copolymer in THF and then adding the required amount of cyclohexane under vigorous stirring. The samples were then sealed in ampoules and then heated 40-45 °C for at least 4 hours with stirring.

PMMA-PHEMA. - Micelles were formed by the slow dropwise addition of ethyl acetate to a solution of PMMA-PHEMA polymer in a mixture of methanol and ethyl acetate (v/v = 1:1), with vigorous stirring. These micelle solutions were stirred at 30-35 °C for four hours before any physical measurements.

III-5. Instrumental

III-5.a. Viscometry

The flow times of solvents, polymer solutions, and copolymer micelle solutions were measured using a Cannon-Ubbelohde type viscometer immersed in a water bath equilibrated at 22.0 °C. All copolymer, copolymer micelle and solvent solutions were passed through a 0.5 µm filter before viscometry measurements. The viscosity of a solution or of solvent were assumed to be linearly proportional to its flow time. The

reduced viscosity η_{red} of a solution is then calculated using

$$\eta_{red} = \frac{t - t_0}{t_0 c} \quad \text{III-3}$$

where t and t_0 are the flow times of the solution and of the solvent respectively. The solvent viscosities were determined by comparing flow times to that of water in the same viscometer. The viscosity of water was calculated by the equation of

$$\log_{10} \left(\frac{\eta_T}{\eta_{20}} \right) = \frac{1.3272(20 - T) - 0.001053(T - 20)^2}{T + 105} \quad \text{III-4}$$

where⁹³ $\eta_{20} = 1.002$ cp.

The density of water at the experimental temperature was calculated by extrapolating the density values⁹³ of water between 20 °C (.99862 g/ml) and 25 °C (.99707 g/ml).

The density of the solvent mixtures of ethyl acetate / methanol and of cyclohexane / THF were calculated as a linear combination of the densities of the two constituent liquids. The calculated densities of 1:1 mixtures of both ethyl acetate / methanol and of THF / cyclohexane were measured in 100 ml volumetric flasks as a check and the results corresponded to the calculated densities within the experimental error of the volumetric flasks used (1 %).

III-5.b. Dynamic Light Scattering

All light scattering experiments reported in this thesis were done by Dr. J. Tao. The hydrodynamic radii R_h of micelles were determined at 22 ± 0.5 °C by photon correlation spectroscopy using an ALV spectrometer equipped with an ALV-5000 full digital correlator (280 channels) over the time range from 10^{-7} to 10^3 s. The laser source was an Addas Nd-YAG laser with emission at 532 nm. The incident beam and the scattered beam were polarized vertical to the scattering plane. The intensity autocorrelation function was analyzed by inverse Laplace transformation using the Contin program to obtain the distribution $g^{(1)}(\tau)$.

When binary solutions solvent mixtures were used, the refractive indices were calculated by using the formula: $\frac{n-1}{\rho} = \frac{w_1}{\rho_1}(n_1-1) + \frac{w_2}{\rho_2}(n_2-1)$ where n is the refractive index of the mixed solvent and is a calculated value from the refractive indices n_1 and n_2 of the individual components, w_i is the weight fractions of the two solvents and ρ_i is the density of the component solvents.

III-5.c. Steady State Fluorescence

Steady state fluorescence measurements were made on a Photon Technologies Alphascan instrument with a xenon lamp operated at 70 W. The steady state spectra were not corrected. The ratio of the fluorescence intensity of pyrene to that of fluorene (I_{Py}/I_{Fl}) was measured by selectively exciting fluorene at 290 nm. Fluorescence emission was

monitored from 300 nm to 500 nm. The slit widths were 1-2 mm and the PMT was operated at -630 V.

For the kinetic experiments, pyrene was excited at 326 nm and the pyrene emission was measured at 387 nm. The slits were opened from 2.5 - 3.5 mm and the PMT was operated at -620 to -630 V.

III-5.d. Time Resolved Fluorescence

Fluorescence lifetimes measurements were taken on a Photon Technologies LS1 time-correlated single photon counting spectrometer. The samples were excited with a hydrogen flash lamp operated at 5 kHz. Pyrene was excited at 326 or 343 nm and the fluorescence emission was monitored at 387 nm. The fluorescence experiments, except where noted, were done under ambient atmospheric conditions.

III-5.e. UV-Visible Spectroscopy

UV measurements were carried out on a Hewlett-Packard 8452A Diode Array single beam spectrophotometer or on a Perkin - Elmer Lambda Array 3840 single beam spectrometer with photodiode array detector. 1 cm quartz cells were used at all times.

III-5.e.i. UV-Visible Fluorescent Chromophores Standards

The labelling efficiency of 1-bromomethylpyrene, of 1-pyreneacetic anhydride and of 9-fluoreneacetic anhydride as well as the molecular weight determination of

FI-PMMA-PHEMA-Py were determined by using standards. 1-Pyrenemethanol and fluorene-poly(methyl methacrylate) [FI-(MMA)₃₅-H] were used. The UV-VIS spectra of 1-pyrenemethanol is shown in Figure III-16 [$\epsilon(342)=4.34 \times 10^4 \text{ cm}^{-1} \cdot \text{M}^{-1}$].

III-5.f. NMR

NMR spectra were obtained on either the Bruker ACE 200 MHz or the Bruker AM 400 MHz instruments using the 5 mm probes.

II-5.g. Gel Permeation Chromatography

Gel permeation chromatography (GPC) were done with Zorbax 60S, 1000S and 3000S columns or with a Waters HR4 styragel column. A Varian Model 5000 Liquid Chromatography instrument was used as a pump. The samples were monitored by a Varian Aerograph refractive index detector and/or a Varian Vari-Chrom UV-Visible detector. Poly(methyl methacrylate) or polystyrene (Polysciences, Inc.) standards were used.

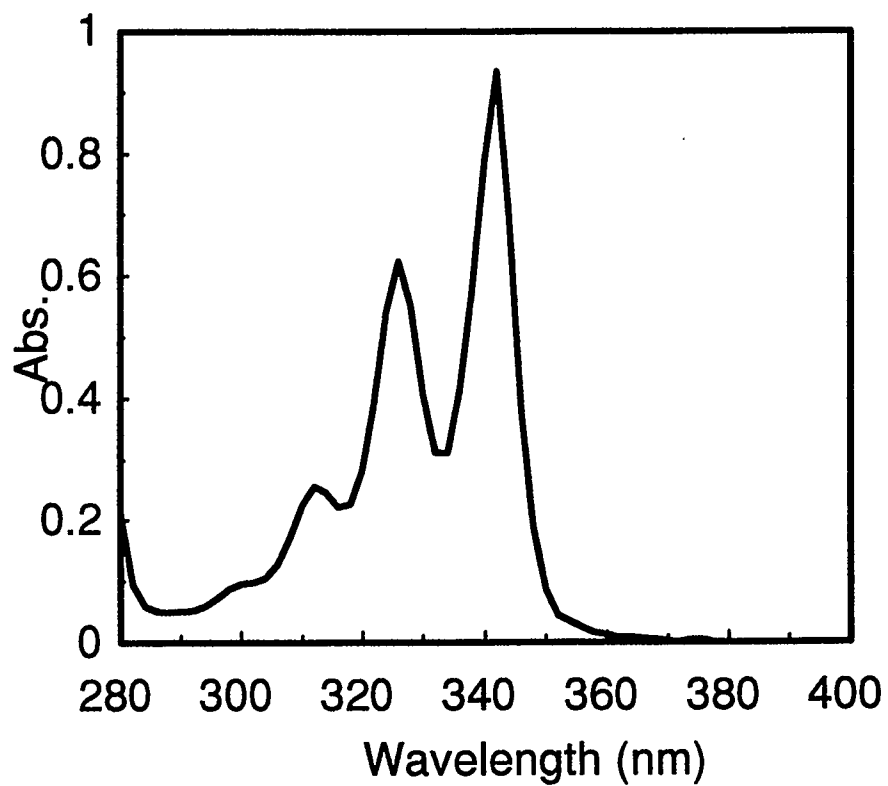


Figure III-16. UV-Visible absorption spectra of 1-pyrenemethanol in THF (5.01×10^{-3} mg/ml). The measured value of $\epsilon(342 \text{ nm}) = 4.34 \times 10^4 \text{ cm}^{-1} \cdot \text{M}^{-1}$.

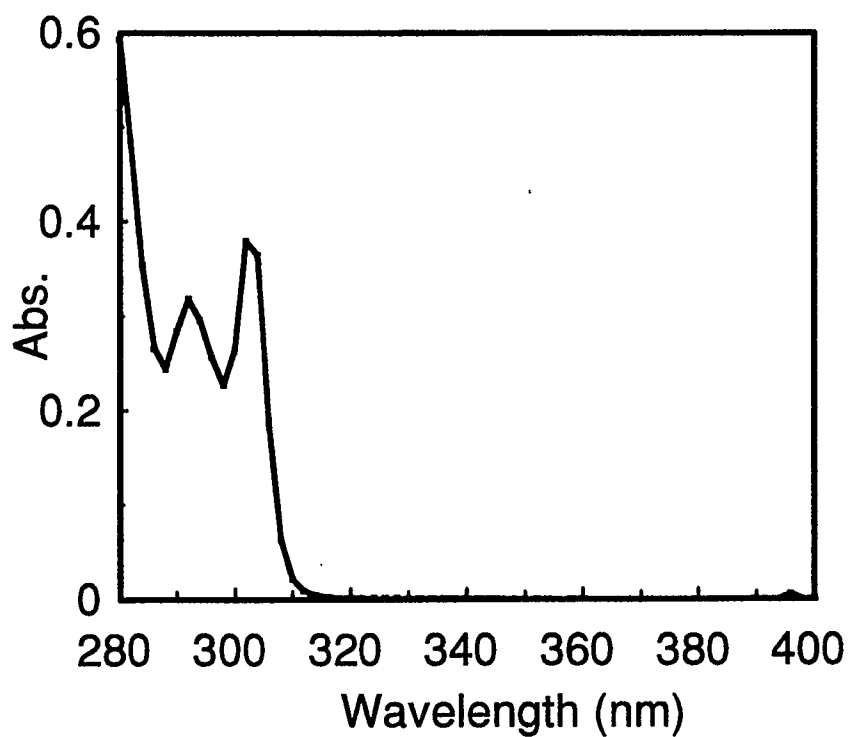


Figure III-17. UV-Visible absorption spectra of Fl (MMA)₃₅-H standard in THF (0.1995 mg/ml). The measured value of $\epsilon(304 \text{ nm}) = 6844 \text{ cm}^{-1} \cdot \text{M}^{-1}$.

CHAPTER IV: CHAIN EXCHANGE KINETICS of PMMA-PMAA MICELLES

IV-1. Introduction

The synthesis of poly(methyl methacrylate)-*b*-poly(methacrylic acid) of similar molar masses, with and without fluorene attached to the end of the PMMA block and pyrene labels attached to the end of the PMAA block was described in Section III-2.b.v. It will be shown below that these copolymers formed micelles with the PMAA block in the micelle cores in ethyl acetate / methanol solvent mixtures, for ethyl acetate volume fractions greater than 80 %. NET was used to detect the solvent systems where micellization occurred. The aggregation numbers of these micelles were determined by dilute solution viscometry and light scattering. The critical micelle concentrations (CMC) of PMMA-PMAA in solutions of 85 % and 90 % ethyl acetate were determined by measuring the increase in the fluorescence lifetime of pyrene upon incorporation into micelles.

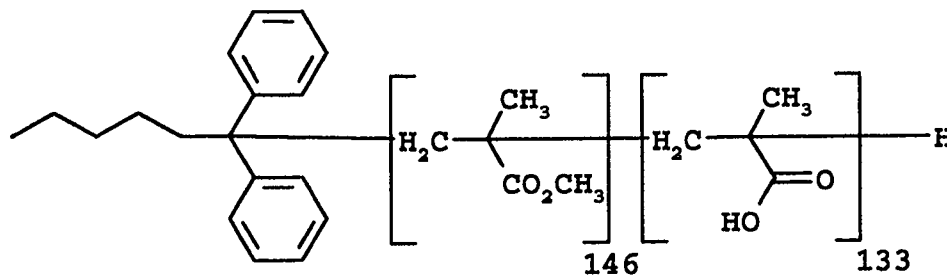
The goal of these experiments was to measure the rate of chain exchange between the pool of unimers and the micelles aggregates. A kinetic model is proposed for describing the rate of exchange (k_p) of copolymer chains between unimers and micelles in Section IV-2.a. This model has been confirmed by experiments on PMMA-PMAA in 85 % and 90 % ethyl acetate solutions that exploit the increase in the fluorescence emission intensity of pyrene upon incorporation into micelle cores.

IV-2. Theory

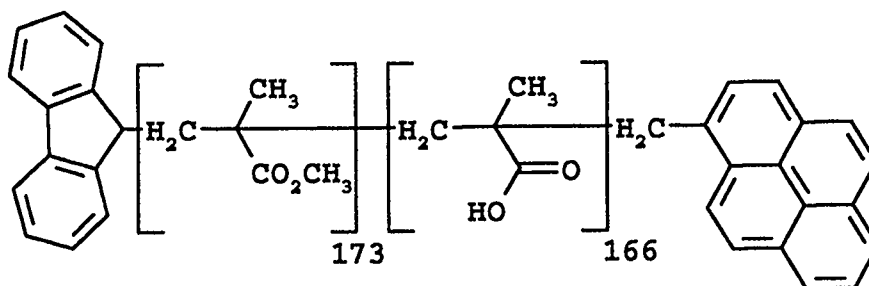
IV-2.a. Experimental Procedure

A new approach that determines the value of the micelle chain exchange rate, k_p , experimentally is described below and is a variation of a procedure previously proposed by Liu⁹⁴.

Schematics of the two copolymers used for these experiments are shown below:



Polymer IV-1. PMMA-PMAA



Polymer IV-2. FI-PMMA-PMAA-Py

The experiment involved mixing equal volumes of two solutions of the same solvent composition. The first solution was of micelle aggregates of the unlabelled copolymer (Polymer IV-1) whose concentration was:

$$c_M^0 = \frac{c - c^*}{p} \quad \text{IV-1}$$

where c is the unlabelled copolymer concentration, c^* is the CMC of the copolymer for the solvent system, and p is the aggregation number of the micelles. c_M^0 was chosen to be approximately equal to c^* . The second solution was of the labelled copolymer (Polymer IV-2) with a concentration c_y^0 which is below the CMC (c^*). c_y^0 was equal to ac^* where a was chosen to be approximately $0.2 c^*$.

Mixing the two solutions resulted in a unimer concentration $[U]$ of $(1+a)c^*/2$, since $[U] = ac^*$ for the Polymer IV-2 solution, $[U] = c^*$ for the Polymer IV-1 micelle solution and the volume increased by a factor of two. The concentration of unimers $[U]$ immediately after mixing was below c^* . The total unimer concentration was re-established to c^* again by a rapid dissociation of unimers from the existing micelles. This initial adjusting period, characterized by τ_1 , was short (on the order of 6 s or less), and the total number of micelles remained constant¹⁹⁻²¹.

At time $t \approx \tau_1$, the aggregation number of the micelles was slightly below that expected at complete equilibrium. Micelle size redistribution then proceeded. In this

process, a small number of micelles disintegrated and the majority increased in size. It was the kinetics of chain exchange, in this long time domain ($\tau_2 = 1/k_p$), between Polymer IV-2 chains, existing exclusively as unimers and micelles consisting of unlabelled polymer chains that was measured in these experiments.

The experiment involved PMMA-PMAA in ethyl acetate / methanol mixed solvent systems. Ethyl acetate is a good solvent for the PMMA block and a poor solvent for the PMAA block while methanol is a good solvent for the PMAA block and a poor solvent for the PMMA block. The solvent systems used for these experiments were selectively poor for the PMAA block.

The incorporation of labelled copolymer chains was monitored by measuring the increase in the steady state fluorescence emission intensity of pyrene. After mixing, unimers of Polymer IV-2 became incorporated into micelles of Polymer IV-1. The increased fluorescence emission intensity of pyrene was due to the reduced mobility of oxygen (see Section V-2.d) inside the PMAA core which resulted in a decreased efficiency of pyrene fluorescence quenching by oxygen. The fluorescence intensity of pyrene was monitored with respect to time. The value of k_p was obtained by analyzing the data.

IV-2.b. Model of Dynamic Chain Exchange of Diblock Copolymer Micelles

Chain exchange can involve micelles and unimers of Polymer IV-1 and Polymer IV-2, however the incorporation of a Polymer IV-1 chain into or its dissociation from a micelle had no effect on the pyrene fluorescence intensity. Thus only exchange involving

Polymer IV-2 chains was considered. The concentration of the labelled unimer chains c_y^0 was small relative to c_M^0 , and therefore the probability for the incorporation of two or more Polymer IV-2 chains into the same micelle was low. The dominant chain exchange process involving Polymer IV-2 was:



where M_p represents a micelle of p unlabelled copolymer chains and no labelled polymer chains, and $\sim\sim Py$ represents a labelled unimer chain. In this situation the measurable rate of the backward reaction, that is the expulsion of the labelled chain from the micelle is a factor of $p+1$ smaller than the rate of expulsion of all chains.

The rate of MPy formation is:

$$\frac{d[MPy]}{dt} = k_p[M][\sim\sim Py] - \frac{1}{p+1}k_{-p}[MPy] \quad \text{IV-3}$$

where $[M]$ is the molar micelle concentration at time t , $[MPy]$ is the concentration of micelles with an incorporated Polymer IV-2 chain, and $[\sim\sim Py]$ is the concentration of Polymer IV-2 unimers at time t . The second term on the right hand side can be neglected

where p is large. The aggregation number, p , is approximately 170 for these copolymer systems (see Section IV-3.a.).

The concentration of micelles with one incorporated labelled copolymer chain is denoted by $x = [MPy]$. It was assumed that there is no more than one labelled copolymer chain incorporated into one micelle. Following the procedure of Liu⁹⁴ it follows that:

$$[M] = c_M^0 - x \quad \text{IV-4}$$

and that the number of labelled unimer chains remaining at a time t during the experiment is:

$$[\sim\sim\sim Py] = c_y^0 - x \quad \text{IV-5}$$

Substituting in equations IV-7, and IV-6, into equation IV-5, and IV-5 becomes:

$$\frac{dx(t)}{dt} = k_p (c_M^0 - x)(c_y^0 - x) \quad \text{IV-6}$$

the solution to the above equation is known⁹⁵ to be:

$$x(t) = \frac{c_y^0(1 - e^{-kt})}{1 - \frac{c_y^0}{c_M^0}e^{-kt}} \quad \text{IV-7}$$

where:

$$k = (c_M^0 - c_y^0)k_p \quad \text{IV-8}$$

In this research the increase in the value of $I_{Py}(t)$, the fluorescence emission intensity of pyrene, was monitored.

The fluorescence quantum yield of pyrene associated with unimers and micelles is φ_u and φ_m , respectively. The fluorescence intensity of pyrene at t after mixing is then:

$$I_{Py}(t) = \kappa [\varphi_m x + \varphi_u (c_y^0 - x)] \quad \text{IV-9}$$

where κ is a parameter dependent on the instrument settings and the initial concentration of Polymer IV-2 but is constant throughout a mixing experiment. To fit the experimental

data the boundary condition at $t = 0, x = 0$ is applied to equation IV-9 which reduces to

$$I_{py}(0) = \kappa \phi_u c_y^0 \quad \text{IV-10}$$

Inserting equations. IV-10 and IV-7 into IV-9 and with some rearranging:

$$I_{py}(t) - I_{py}(0) = \frac{\kappa' (1 - e^{-kt})}{1 - \frac{c_y^0}{c_m} e^{-kt}} \quad \text{IV-11}$$

where $\kappa' = \kappa(\phi_m - \phi_u)c_y^0$. Therefore, pyrene fluorescence intensity increases if $\phi_m > \phi_u$.

Experimental data for $I_{py}(t)$ was then fitted to equation IV-11 to obtain k_p . For this experiment it was also necessary to determine the CMC of the copolymer. The CMC of the Polymer IV-1 in a suitable solvent mixture is determined by measuring the fluorescence lifetime, $\langle \tau \rangle$, of the attached pyrene as a function of copolymer concentration. Upon micellization, the value of $\langle \tau \rangle$ increases significantly for well chosen chromophores (see Section IV-2.d.). Pyrene is an excellent choice for a fluorescent chromophore in this experiment as it has a long intrinsic lifetime and it has a high molar absorptivity. As the labelled Polymer IV-1 is incorporated into a micelle structure from the unimer phase the steady state fluorescence intensity increases.

These polymers were observed to form micelles in mixtures of ethyl acetate and methanol when the ethyl acetate content was above 80 %. The MAA blocks with pyrene labels constitute the micelle core and the MMA blocks form the corona.

IV-3. Experimental

IV-3.a. Fluorescence Experimental Results on PMMA-PMAA Micelles

IV-3.a.i. Fluorescence Intensity Ratio (I_{Py}/I_{Fl}) to Determine Micellar Solvent Systems

In none of the cases was pyrene excimer emission observed. Figure IV-1 shows the steady state fluorescence emission spectra for Fl-PMMA-PMAA-Py solutions in 50 % ethyl acetate / 50 % methanol and 90 % ethyl acetate / 10 % methanol. Both of the samples were excited at 290 nm, however the sample in 90 % ethyl acetate shows more pyrene fluorescence. The values of I_{Py} / I_{Fl} calculated from spectra like that shown in Figure IV-1 are shown in Figure IV-2 as a function of ethyl acetate content. From the increase in the intensity ratio it can be seen that micelles were formed with an ethyl acetate content of 80 % or greater (cf. Section V-2.b).

IV-3.a.ii. Time Resolved Fluorescence Spectroscopy to Determine CMC

The pyrene fluorescence intensity decay spectra were recorded as a function of polymer concentration for both 85% and 90% ethyl acetate solutions, by exciting pyrene

at 326 or 343 nm and monitoring the emission at 387 nm. The time resolved intensity was fitted by the deconvolution method⁷¹ using a sum of three exponential terms:

$$F(t) = \sum_{i=1}^3 a_i e^{(-t/\tau_i)} \quad \text{IV-12}$$

where $F(t)$ is the chromophore response, and a_i and τ_i are the fitting parameters (see Figure IV-3). The average fluorescence lifetime τ was calculated by using equation II-23.

The calculated average lifetimes are shown in Figures IV-4 and IV-5 (85 %) and IV-6 and IV-7 (90 %) as a function of polymer concentration. Upon the onset of micellization the average lifetime of pyrene increases significantly. The CMC for the 85 % ethyl acetate solutions was determined to be $1.30 \cdot 10^{-2}$ mg/ml (Figure IV-5) and for the 90 % ethyl acetate solution $1.24 \cdot 10^{-2}$ mg/ml (Figure IV-7).

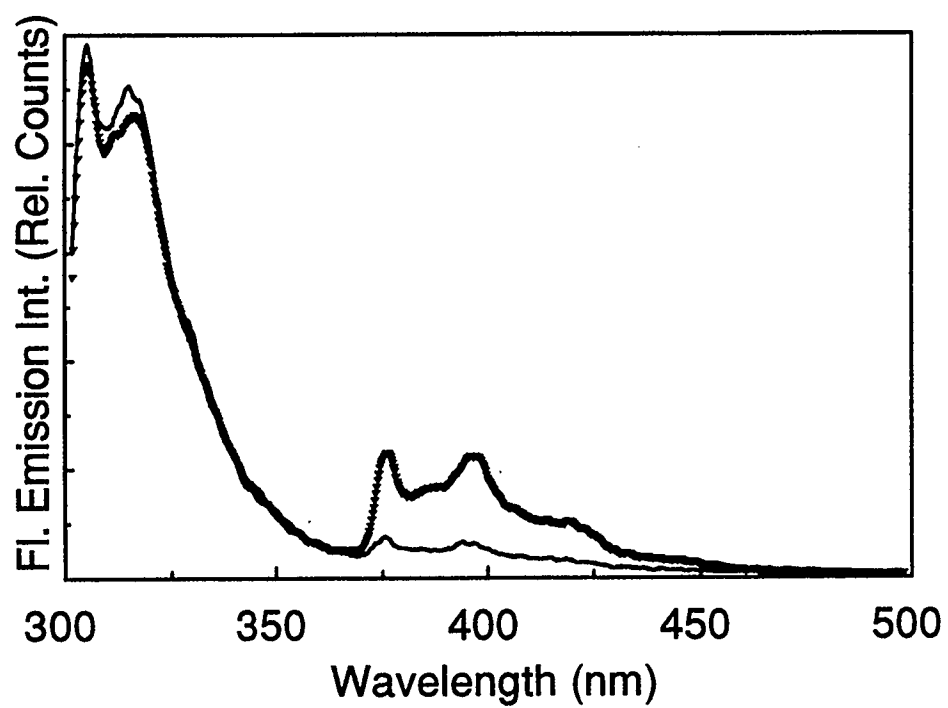


Figure IV-1. Steady state fluorescence emission spectra of FI-PMMA-PMAA-Py in 90 % ethyl acetate / 10 % methanol (triangles) and in 50 % ethyl acetate / 50 % methanol (lighter line). Fluorene is selectively excited at 290 nm.

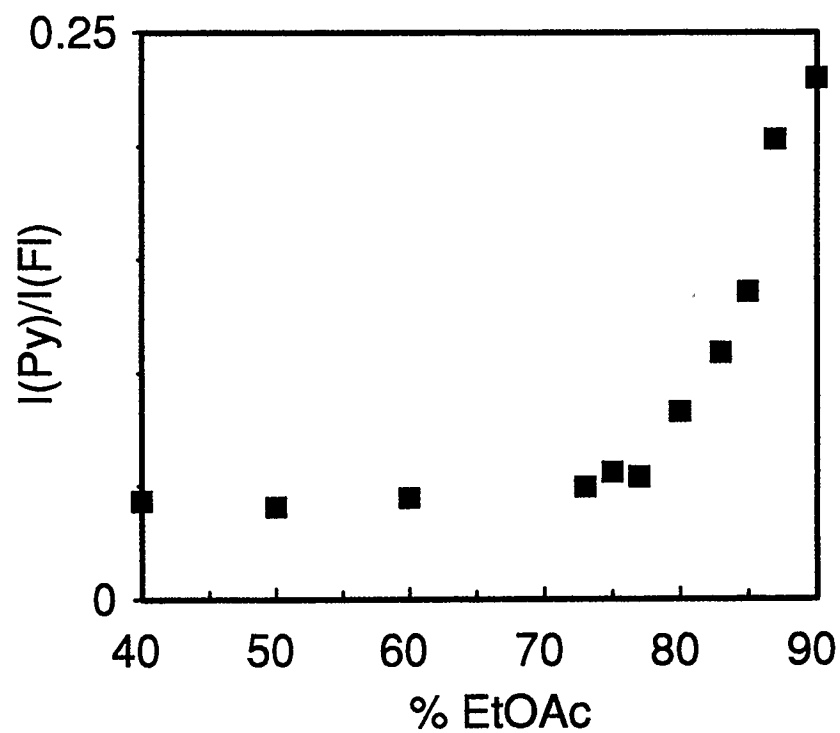


Figure IV-2. Ratio of the fluorescence intensity areas of pyrene to fluorene chromophores ($I_{\text{Py}}/I_{\text{FI}}$) as a function of the solvent composition.

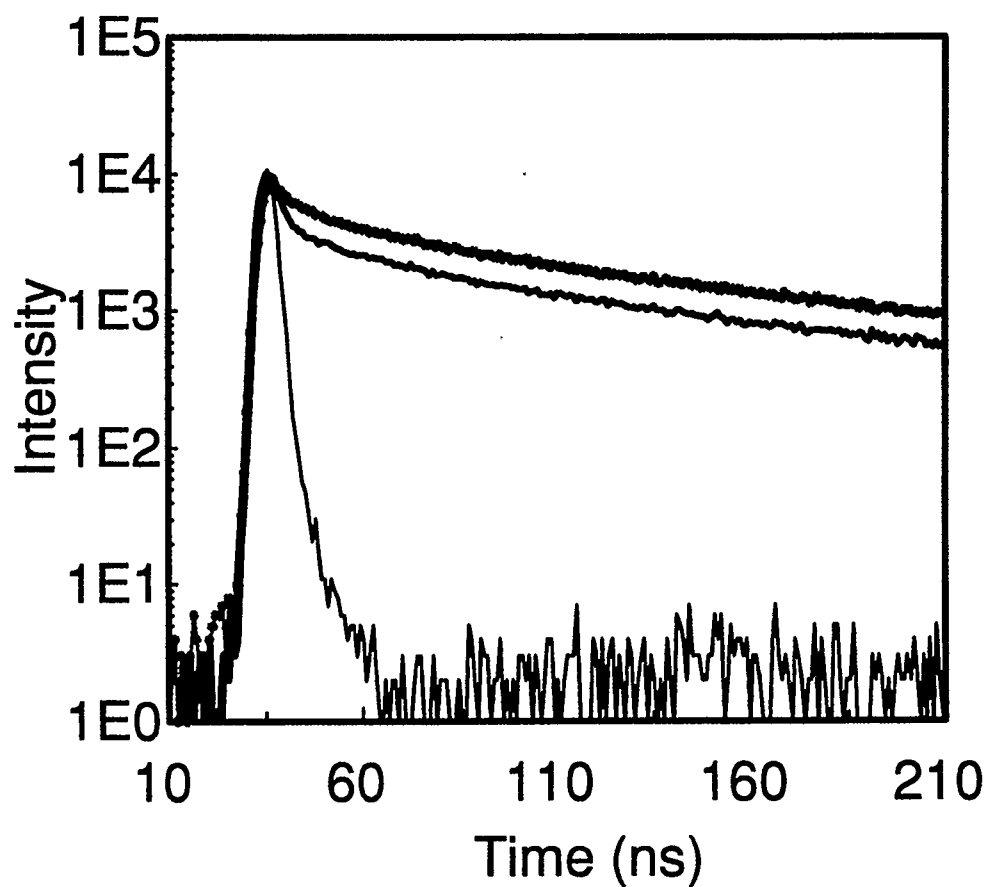


Figure IV-3. TCSPC fluorescence emission decay spectra of FI-PMMA-PMAA-Py micelles in 85 % ethyl acetate / 15 % methanol, 0.015 mg/ml (grey circles) where $\langle\tau\rangle = 37.3$ ns and 0.0056 mg/ml (dark line), $\langle\tau\rangle = 9.7$ ns. The lamp profile is also shown (thin line).

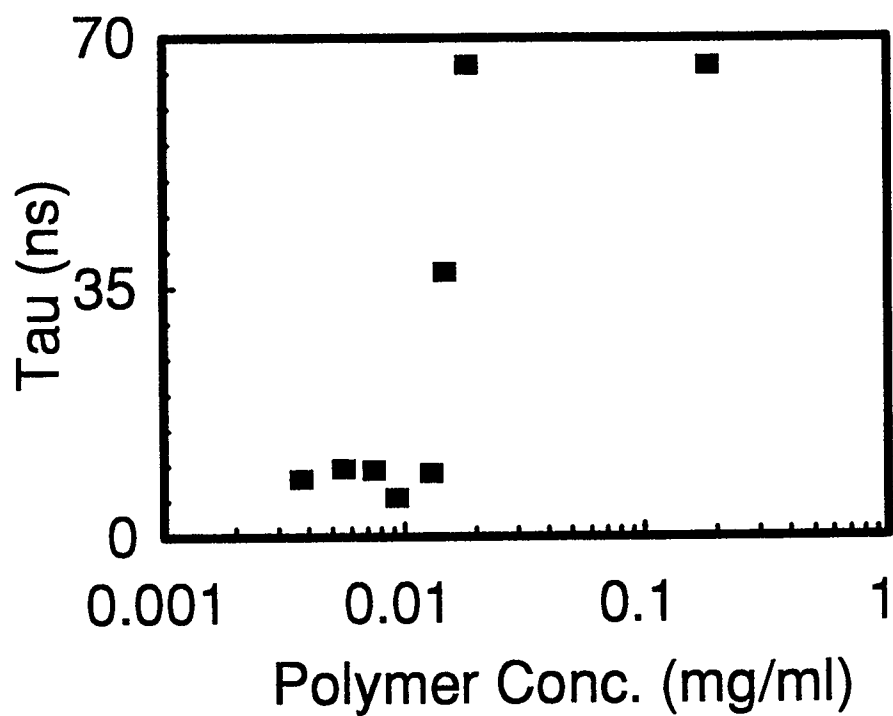


Figure IV-4. Fluorescence lifetime of pyrene chromophores of Fl-PMMA-PMAA-Py as a function of copolymer concentration in 85 % ethyl acetate / 15 % methanol. Data was collected with 0.8247 ns / channel.

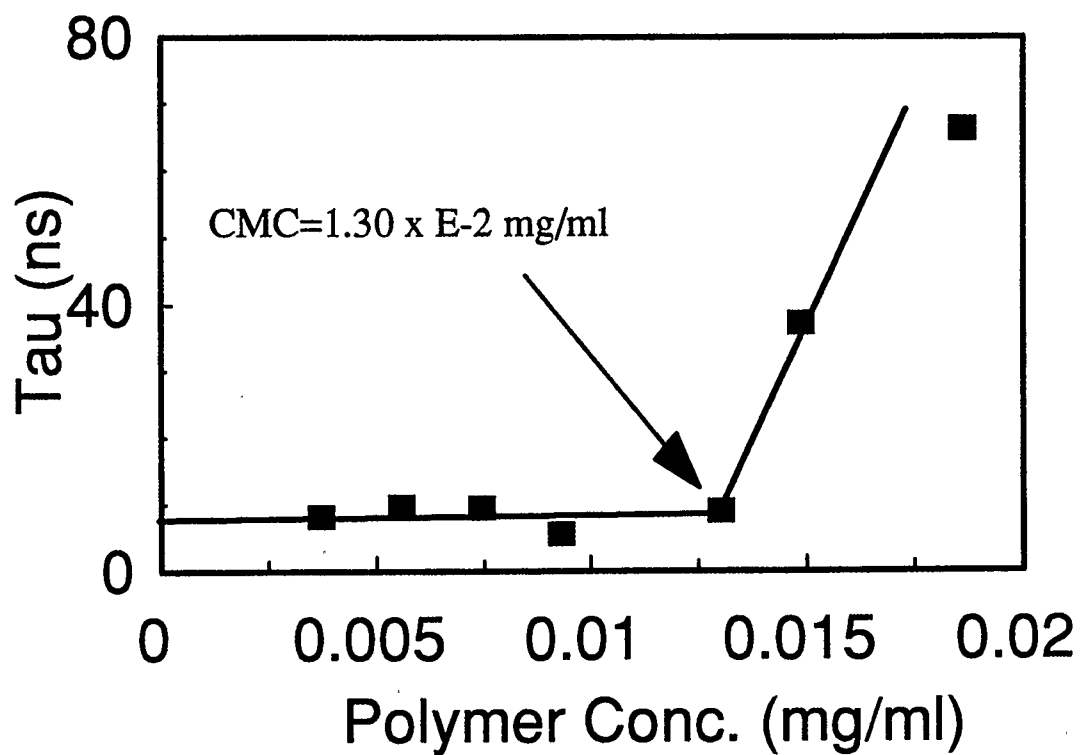


Figure IV-5. Fluorescence lifetime of pyrene chromophores of FI-PMMA-PMAA-Py in 85 % ethyl acetate / 15 % methanol as a function of copolymer concentration presented on a linear scale.

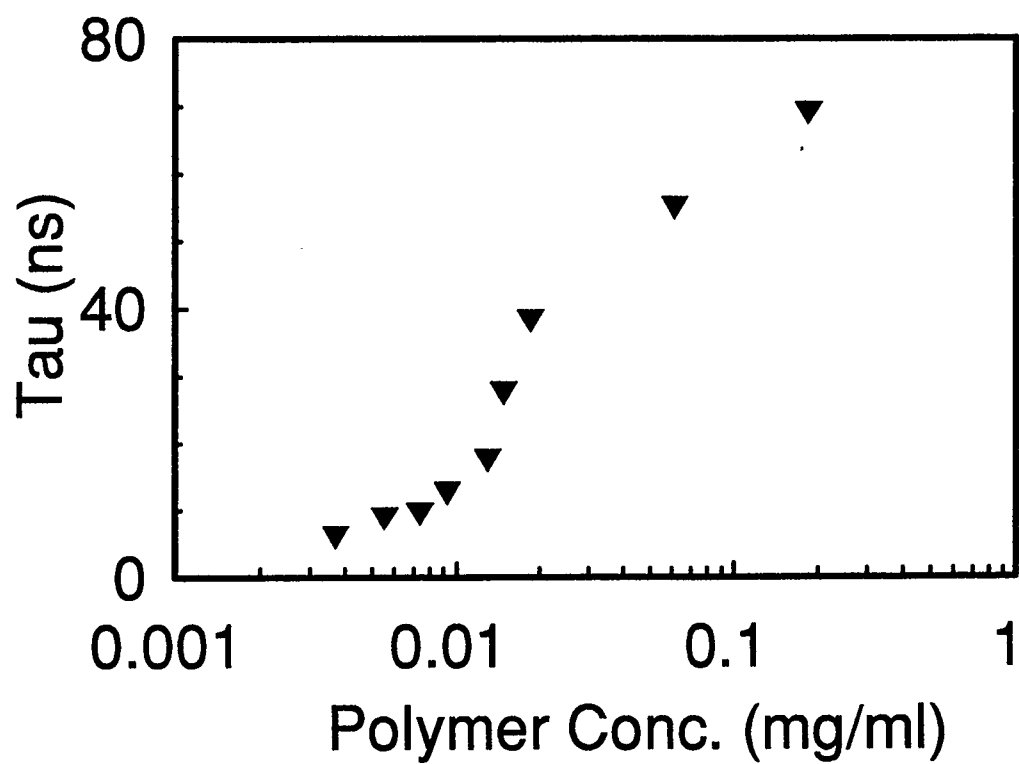


Figure IV-6. Fluorescence lifetime of pyrene chromophores of FI-PMMA-PMAA-Py as a function of copolymer concentration in 90 % ethyl acetate / 10 % methanol. Data was collected with 0.8247 ns / channel.

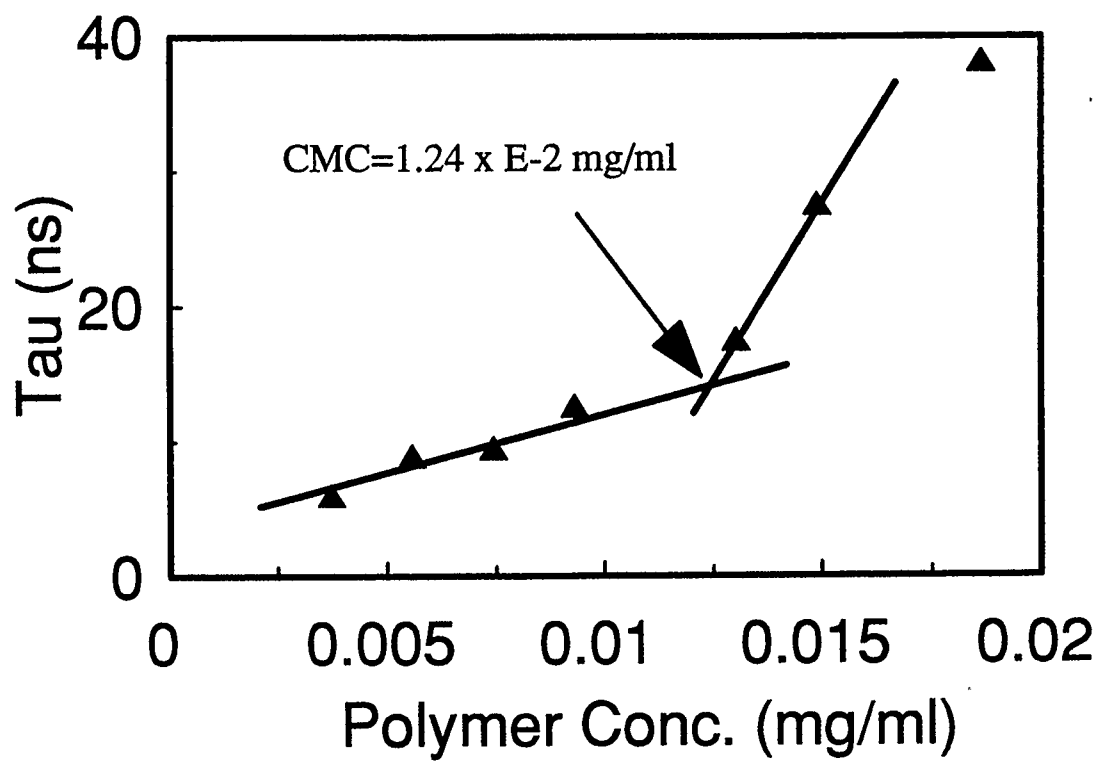


Figure IV-7. Fluorescence lifetime of pyrene chromophores of FI-PMMA-PMAA-Py in 90 % ethyl acetate / 10 % methanol as a function of copolymer concentration presented on a linear scale.

IV-3.b. Characterization of Micelles

Dilute solution viscometry and dynamic light scattering were used for the characterization of PMMA-PMAA copolymer micelles. Viscometry experiments were done on the unlabelled copolymer only and the results are shown in Figures IV-8 (85 % ethyl acetate) and IV-9 (90 % ethyl acetate). The intrinsic viscosities of the unlabelled copolymer are shown in Table IV-1.

The dynamic light scattering experiments were performed on 1 mg/ml solutions of both the labelled and the unlabelled copolymer samples at solvent compositions of 85 % and 90% ethyl acetate. The scattering angle θ was between 15 and 45 degrees and the temperature was 21 ± 0.5 °C. The argon laser light source was operated at a wavelength $\lambda = 532$ nm. The aggregation number p was determined by using equation II-8.

The aggregation numbers are the same for 90 % and 85 % ethyl acetate solutions at about 170 polymer chains per micelle. The hydrodynamic radius for the labelled copolymer was about 10 % larger than that of the unlabelled copolymer. This result is consistent with the GPC data that shows the molecular weight of the labelled copolymer to be about 21 % larger than the unlabelled copolymer and that generally polymers with higher molar masses form larger micelles.

Table IV-1. Characterization of unlabelled PMMA-PMAA diblock copolymer micelles

% EtOAc	q (10^5 cm^{-1})	η_{solvent} (cp)	Γ (10^4 s^{-1})	R_h (\AA)	$[\eta]$ (ml/g)	p
90	3.121	.436	2.58	189	9.14	171
85	3.116	.433	2.48	198	10.41	172

Table IV-2. Characterization of labelled PMMA-PMAA-Py diblock copolymer micelles

% EtOAc	q (10^5 cm^{-1})	η_{solvent} (cp)	Γ (10^4 s^{-1})	R_h (\AA)
90	3.121	.436	2.32	210
85	3.116	.433	2.25	217

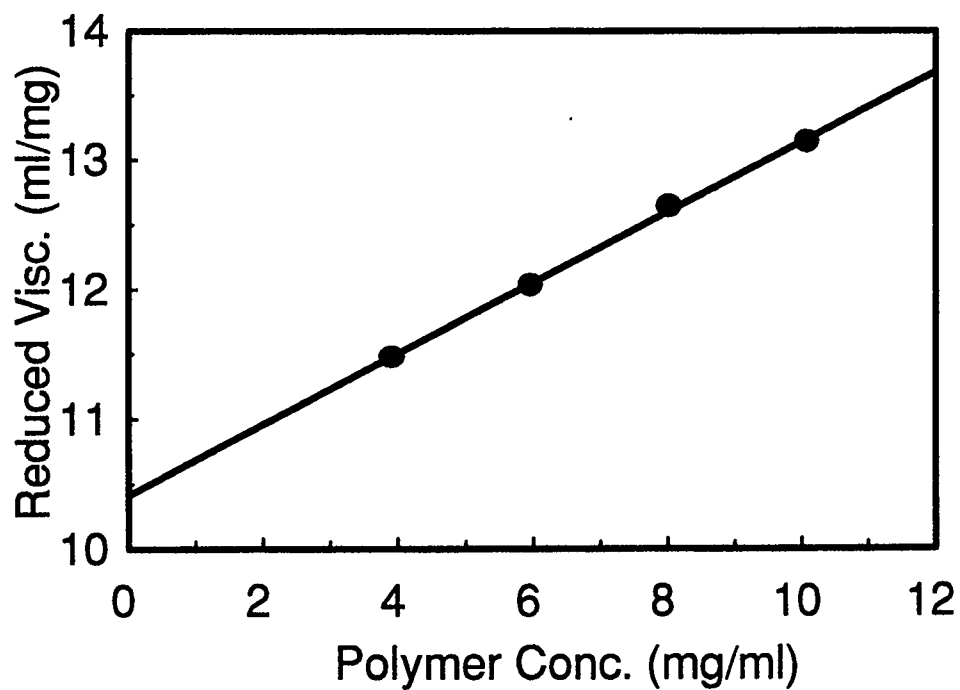


Figure IV-8. Reduced viscosity of PMMA-PMAA (unlabelled) micelles in 85 % ethyl acetate / 15 % methanol versus copolymer concentration. The intrinsic viscosity of this system was 10.4 ml/mg.

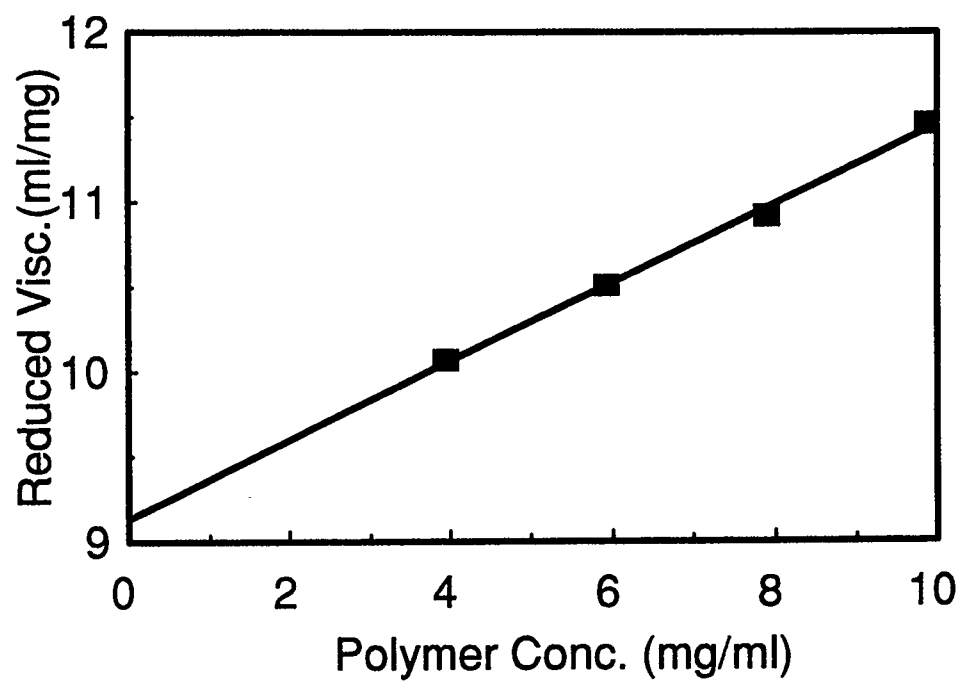


Figure IV-9. Reduced viscosity of PMMA-PMAA (unlabelled) micelles in 90 % ethyl acetate / 10 % methanol versus copolymer concentration. The intrinsic viscosity of this system was 9.1 ml/mg.

IV-4. Measurement of the Dynamic Chain Exchange Rate

IV-4.a. Experimental Procedures and Results

The values of I_{Py} / I_{Fl} shown in Figure IV-2 indicate that both 85 % and 90 % ethyl acetate solutions are micellar. For experiments in 90 % ethyl acetate, three sets of kinetic experiments with different c_M^0 and c_y^0 combinations were tried and the values are shown in Table IV-3. One kinetic experiment in 85 % ethyl acetate system was done. At the end of each of the experiment runs the copolymer mixtures were heated to 45 °C for four hours to check if complete incorporation of the labelled Polymer IV-1 into the micelles was achieved at room temperature. It was found that further heating did not increase $I_{py}(t)$ thus the incorporation was almost complete after each of the kinetic runs. In all cases, c_y^0 were much lower than c^* .

The experimental steady state fluorescence intensity of $I(t)$ of pyrene as a function of time after sample mixing is shown in Figure IV-10. The experimental data was fitted to equation IV-11 using κ' and k of equation IV-8 as the adjustable variables. The fit was done by an iterative fitting programme written by Dr. G. Liu.

This programme fits the data by minimizing the error function

$$\chi^2 = \left(\frac{1}{N}\right) \sum_{i=1}^N [I_{ex}(i) - I_{th}(i)]^2 \quad \text{IV-13}$$

where N is the total number of data points in a set; $I_{ex}(i)$ are the experimental pyrene fluorescence emission intensity values and $I_{th}(i)$ are the corresponding calculated values from equation. IV-11. To enable a meaningful comparison between the resultant χ^2 from different experimental runs, $I_{ex}(i)$ were all normalized with respect to the highest $I_{ex}(i)$ value in each data set.

The resultant k values are tabulated in Table IV-3. Using equation. IV-8, the k_p values are calculated. The k_p values were consistent for various initial values of c_M^0 and c_y^0 . The value of k_p did increase as the ethyl acetate content decreased and this is consistent with the expectation that the PMAA core might be less compact in the 85 % ethyl acetate mixture.

The fit between equation. IV-11 and the experimental data was tested by rearranging equation IV-11 to present the data and the fit in a semi logarithmic fashion.

$$\left(1 - \frac{\left(I_{Py}(t) - I_{Py}(0) \right) \left(1 - \frac{c_y^0}{c_m^0} e^{-kt} \right)}{\kappa'} \right) = e^{-kt} \quad \text{IV-14}$$

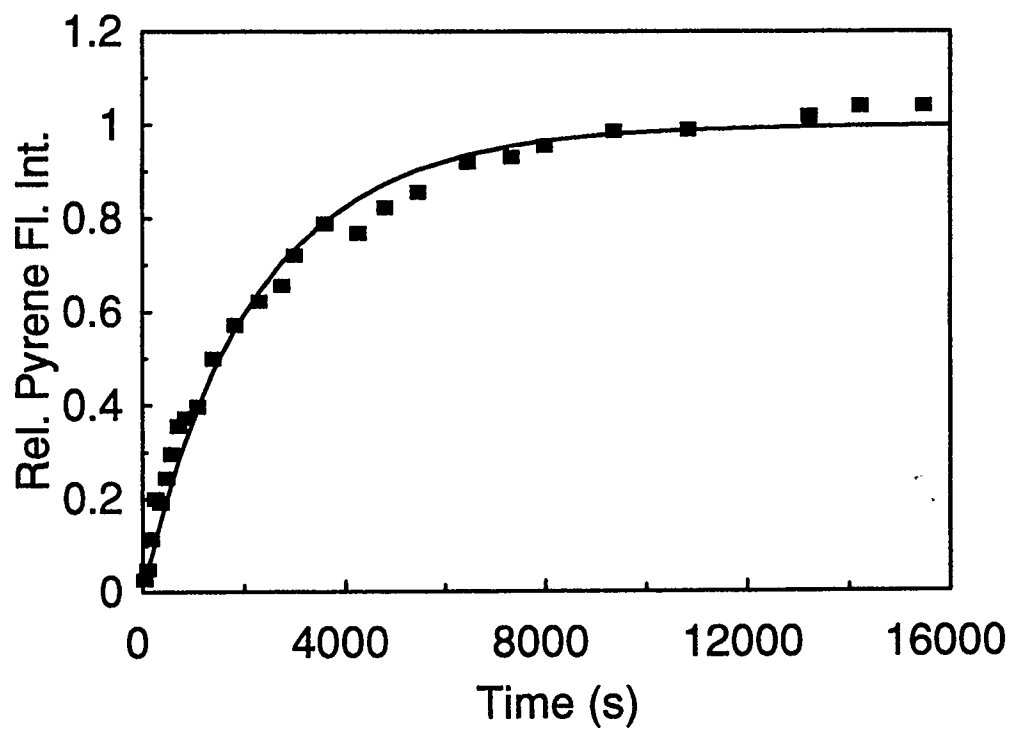


Figure IV-10. Relative pyrene fluorescence intensity versus time for micelle chain exchange experiment in 90 % ethyl acetate / 10 % methanol. The above data was fitted to equation. IV-11. $c_M^0 = 1.80 \times 10^{-7}$ M and $c_y^0 = 3.09 \times 10^{-8}$ M.

Taking the natural logarithm of both sides of equation IV-14 gives:

$$-\ln \left(1 - \frac{(I_{Py}(t) - I_{Py}(0)) \left(1 - \frac{c_y^0}{c_m^0} e^{-kt} \right)}{\kappa'} \right) = kt = A(t) \quad \text{IV-15}$$

Plotting the values of $A(t)$ versus time should give a straight line with a slope of k . The plot of $A(t)$ versus time for the experimental data in Figure IV-10 is presented in Figure IV-11. The fit at longer times ($> 4000s$) was not ideal, and experimental errors are suspected. The most likely cause of error was a photochemical reaction that was observed to occur with pyrene. Exposure to the light source for longer periods of time resulted in a decrease in the fluorescence emission intensity of pyrene which was probably the result of partial sample decomposition. Other sources of error include the mismatch in the size of the unlabelled and labelled copolymer (Section III-3.d) and neglect of the back reaction. G. Liu has done a computer simulation of the chain exchange experiment with and without the back reaction and estimates that the error introduced by neglect of the back reaction is no more than 4 %.

The time scale used in this study has been large (~ 5 hours) and during this time period instrument shift was possible. The time scale can be greatly shortened by carrying out similar studies at elevated temperatures to speed up the chain exchange kinetic process and to improve data accuracy.

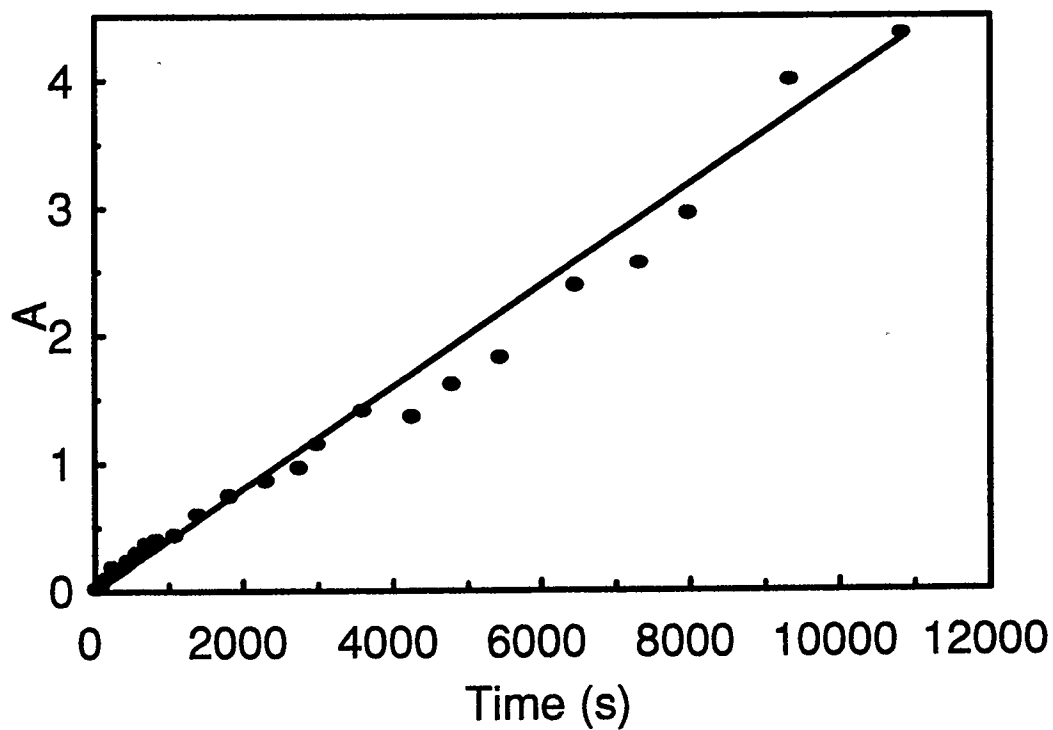


Figure IV-11. Values of $A(t)$ (dots) and line of kt ($k = 3.99 \times 10^{-4} \text{ s}^{-1}$, line) versus time for micelle chain exchange experiment in 90 % ethyl acetate / 10 % methanol ($c_M^0 = 1.80 \times 10^{-7} \text{ M}$ and $c_y^0 = 3.09 \times 10^{-8} \text{ M}$). The above data shows the quality of the fit to equation.

IV-11. A linear regression analysis of the above data points gives a slope of $3.83 \times 10^{-4} \text{ s}^{-1}$ (difference of 4.0 %, line not shown).

Table IV-3. Dynamic Chain Exchange Results

% EtOAc	c^* (M)	c_M^0 (M)	c_y^0 (M)	k (s⁻¹)	k_p (M⁻¹s⁻¹)	χ^2
85 %	$3.95 \cdot 10^{-7}$	$3.01 \cdot 10^{-7}$	$5.41 \cdot 10^{-8}$	$9.13 \cdot 10^{-4}$	$3.70 \cdot 10^3$	$1.3 \cdot 10^{-3}$
90% i)	$3.77 \cdot 10^{-7}$	$2.97 \cdot 10^{-7}$	$5.46 \cdot 10^{-8}$	$4.90 \cdot 10^{-4}$	$2.02 \cdot 10^3$	$2.1 \cdot 10^{-3}$
ii)	$3.77 \cdot 10^{-7}$	$2.97 \cdot 10^{-7}$	$3.12 \cdot 10^{-8}$	$5.40 \cdot 10^{-4}$	$2.03 \cdot 10^3$	$2.5 \cdot 10^{-3}$
iii)	$3.77 \cdot 10^{-7}$	$1.80 \cdot 10^{-7}$	$3.09 \cdot 10^{-8}$	$3.99 \cdot 10^{-4}$	$2.68 \cdot 10^3$	$1.5 \cdot 10^{-3}$

IV-5. SUMMARY

PMMA-PMAA was found to form micelles in ethyl acetate / methanol mixtures where the ethyl acetate content is greater than 80 %. PMMA-PMAA and Fl-PMMA-PMAA-Py micelles with similar n and m numbers have also been characterized in 85 % ethyl acetate / 15 % methanol and 90 % ethyl acetate / 10 % methanol by light scattering and viscometry. The CMC of Fl-PMMA-PMAA-Py was found by measuring the fluorescence lifetime of the pyrene chromophores attached to the PMAA block. It was found to be 3.95×10^{-7} M (1.30×10^{-2} mg/ml) in 85 % ethyl acetate / 15 % methanol and 3.77×10^{-7} M (1.24×10^{-2} mg/ml) in 90 % ethyl acetate / 10 % methanol.

The dynamic chain exchange rates of these systems were measured by monitoring the steady state fluorescence emission intensity. The values of the rate exchange constant k_p were found by fitting the pyrene fluorescence intensity curve to equation IV-11 and were determined to be $3700 \text{ M}^{-1}\text{s}^{-1}$ for 85 % ethyl acetate system and about $2030 \text{ M}^{-1}\text{s}^{-1}$ for 90 % ethyl acetate system. The results amongst the 90 % ethyl acetate systems with differing concentrations measured the same value for k_p within experimental error and two of the results were almost exactly the same. The value for k_p was smaller for the 90 % ethyl acetate system compared to that of the 85 % ethyl acetate system. This result is expected because the 90 % ethyl acetate system should have a more compact micelle core because the solvent system has less solvating power for the PMAA block. Using the newly proposed method for micelle dynamics studies, the chain exchange rate constants were measured for the first time. The model explained experimental data well.

CHAPTER V: PMMA-PHEMA COPOLYMER MICELLES

V-1. Introduction

In chapter IV the rate of micelle chain exchange was measured by monitoring an increase in the quantum yield of pyrene as labelled copolymer chains were incorporated into micelles. In this chapter the properties of diblock copolymer micelles of FI-PMMA-PHEMA-Py in dilute solutions of ethyl acetate and methanol are examined. The reasons for this study are twofold. The first is that PMMA-PHEMA would be a suitable copolymer for chain exchange study if a matching unlabelled copolymer were synthesized and the second is to examine the mechanisms of the increase in the quantum yield of pyrene upon incorporation into micelles.

Pyrene fluorescence properties are used to detect micelle formation. It has been already suggested that the reason for the increase on the quantum yield of pyrene fluorescence is reduced diffusion of oxygen within the cores of copolymer micelles. This can be tested by comparing the increase in the fluorescence intensity of pyrene before and after the removal of atmospheric oxygen from micelle solutions. Experiments on the micellization of the diblock copolymer FI-PMMA-PHEMA-Py show that :

1. FI-PMMA-PHEMA-Py formed micelles in mixtures of ethyl acetate and methanol where the ethyl acetate content was above 90 % such that the HEMA blocks with attached pyrene labels constituted the micelle core and the MMA blocks, end labelled

with fluorene, formed the corona. Micelle formation by PMMA-PHEMA was characterized by dynamic light scattering and dilute solution viscometry to obtain the hydrodynamic radius and the aggregation numbers.

2. Upon the onset of micellization of FI-PMMA-PHEMA-Py there was an increase in the measured rate of non-radiative energy transfer from fluorene to pyrene where fluorene was selectively excited. The reason for this increase was likely due to an increase in the fluorescence lifetime of pyrene and to a reduction in the distance between the two types of chromophores.
3. The percentage increase in the fluorescence lifetime of pyrene upon micellization was found to be less when the dissolved oxygen was removed from the system.

V-2. Results and Discussion

Methanol is a good solvent for HEMA and a poor solvent for MMA, while ethyl acetate is a good solvent for MMA and a poor solvent for HEMA. FI-PMMA-PHEMA-Py was found to be well solvated in a 1:1 mixture of methanol and ethyl acetate. In the experiments described below the micellization properties of PMMA-PHEMA are examined as the concentration of the ethyl acetate is increased from 50 % to 99.5 % v/v.

V-2.a. Characterization of Micelles by Viscometry and Light Scattering

The formation of micelles by PMMA-PHEMA in dilute solutions of ethyl acetate and methanol was demonstrated by viscometry and dynamic light scattering

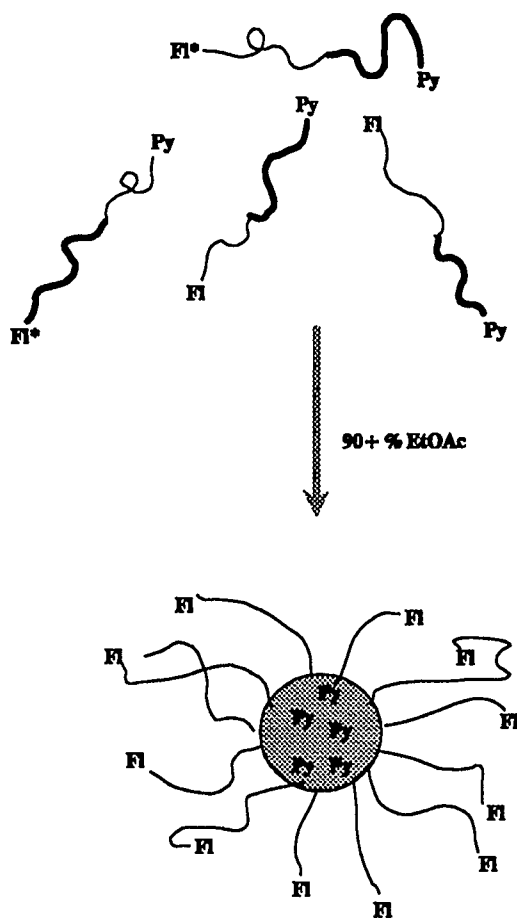


Figure V-1. Schematic diagram of the micellization of FI-PMMA-PHEMA-Py in ethyl acetate / methanol. The HEMA blocks form the core of the micelle when the proportion of ethyl acetate is greater than 90 % and is surrounded by a corona of well solvated MMA blocks. The pyrene labels are embedded within the micelle core and the fluorene chromophores are at the end of the corona chains.

measurements. Micellar solutions of copolymers give lower values for intrinsic viscosity than those of well solvated solutions³⁴. A typical set of results is presented in Figure V-2 where the reduced viscosities are shown as a function of polymer concentration for 95 % and for 50 % ethyl acetate in methanol solutions. The intrinsic viscosity of the copolymer at each of the solvent compositions is found by extrapolating the reduced viscosity to the limit of zero concentration (y-axis intercept). The 95 % ethyl acetate solution of PMMA-PHEMA had an intrinsic viscosity of 7.79 ml/mg versus 9.15 ml/mg for the 50 % ethyl acetate solution. This level of decrease in the intrinsic viscosity is similar to that of other investigators upon micellization^{34,96}. The complete set of results for this polymer are shown in Table V-1.

These viscometry measurements were used in conjunction with dynamic light scattering results to obtain aggregation numbers of the micelle dispersions for several systems. The hydrodynamic radius of micelles was calculated from light scattering measurements. Equation II-17 is substituted into equation II-19 and after rearranging equation V-1 is obtained:

$$R_h = \left(\frac{kTq^2}{6\pi\eta\Gamma} \right) \quad \text{V-1}$$

The dynamic light scattering experiments were performed on 2 mg/ml solutions at various solvent compositions (Table V-1). The aggregation number p , of the micelles was found utilizing equation II-8 (see Section II-2.a.).

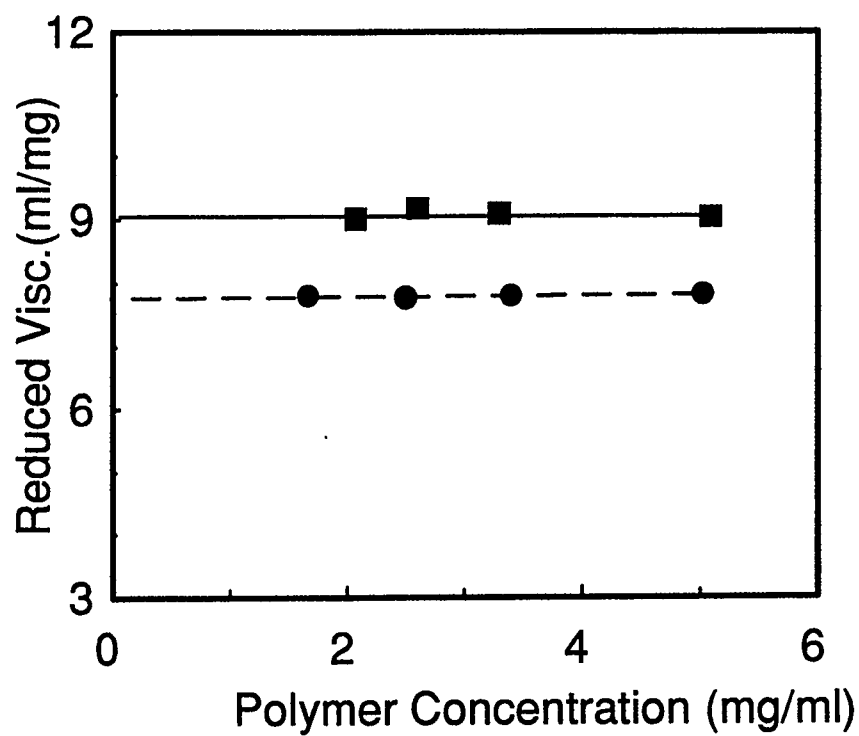


Figure V-2. Reduced viscosity as a function of copolymer concentration for FI-PMMA-PHEMA-Py in 95 % ethyl acetate (circles) and in 50 % ethyl acetate (squares) in methanol. The viscosity measurements were done at 22.0 °C. The intrinsic viscosity is determined as the y-axis intercept of the reduced viscosity.

The aggregation numbers were consistent from 99.5 % to 95 % ethyl acetate at about 64 polymer chains per micelle. The hydrodynamic radii were also consistent over this range at about 120 Å. Diblock copolymer micelle aggregation numbers do not vary greatly with the quality of the solvent. The reasons for this behavior have not been delineated. This phenomenon has also been observed with other diblock copolymer micelle systems⁹⁷ studied in our laboratory.

V-2.b. Steady State Fluorescence Experiments on PMMA-PHEMA Micelles

Fluorene and pyrene are an energy donor-acceptor pair (cf. Section II-2.h.ii.) and the value of R_0 is relatively large⁹⁸ (~32 Å). The fluorescence emission spectra of fluorene and the UV-VIS absorption spectra of 1-pyrenemethanol are shown in Figure V-3 and significant overlap occurs between the two spectra.

The ratio of I_{Py} / I_{Fl} was expected to increase upon micellization due to a reduction in the distance between the two types of chromophores (see Figure V-1). The distance between the two chromophores in the well solvated case is the end to end distance of the polymer. Upon micellization, energy transfer should occur between the excited fluorene and the pyrene chromophore on the core/corona interface nearest to the excited fluorene. The transition from well solvated polymer to micelles has been studied with the use of non-radiative fluorescence energy transfer and the results.

Table V-1. Characterization of Diblock Copolymer Micelles of PMMA-PHEMA.

% EtOAc	q (10^5 cm^{-1})	η_{solvent} (cp)	Γ (10^4 s^{-1})	R_h (Å)	$[\eta]$ (mg/ml)	p^a
99.5	3.096	.4445	3.90	119.9	7.30	65.0
98.0	3.094	.4420	3.93	118.6	7.60	60.4
96.5	3.093	.4399	3.81	122.7	7.89	64.5
95.0	3.092	.4386	3.83	122.3	7.79	64.7
90	3.086	.4363	4.55	103.1	8.07	37.4
50	-----	-----	weak signal	-----	9.15	-----

a - p is the aggregation number of the micelles.

The experimental conditions were as given in section II-4.c.. The ratio of the fluorescence intensity of pyrene to that of fluorene (I_{Py}/I_{Fl}) was measured by selectively exciting fluorene at 290 nm. Fluorene fluorescence emission occurred from 300 nm to 370 nm and that of pyrene was from 370 nm to 480 nm. In Figure V-4 a set of steady state fluorescence emission spectra are shown for FI-PMMA-PHEMA-Py solutions at the concentration of 0.022 g/l (9.6×10^{-7} M) as a function of ethyl acetate content. In none of the cases was pyrene excimer emission observed. The integrated areas of fluorene to pyrene fluorescence emission are plotted in Figure V-5.

Changing the ethyl acetate volume fraction from 50 % and 85 %, did not result in any significant change in I_{Py}/I_{Fl} . The change in I_{Py}/I_{Fl} with the ethyl acetate content in the 85 % to 99.5 % region is shown in Figure V-6 for three different polymer concentrations. All of the spectra show some pyrene fluorescence emission even when micelles are not formed. This is due to a small amount of direct absorption by pyrene at 290 nm. For the most dilute polymer solution shown (0.0224 g/l) an abrupt increase occurs at 95 % ethyl acetate and for the other two polymer concentrations the increase occurs at \approx 90 % ethyl acetate. The increase in the value of I_{Py}/I_{Fl} as the ethyl acetate content became greater than 90 % was indicative of the onset of micellization.

There are three possible reasons identified for the increase in I_{Py}/I_{Fl} . The first is an increase in the rate of energy transfer efficiency (k_{et}) which varies with the distance between the two chromophores as per equation IV-1.

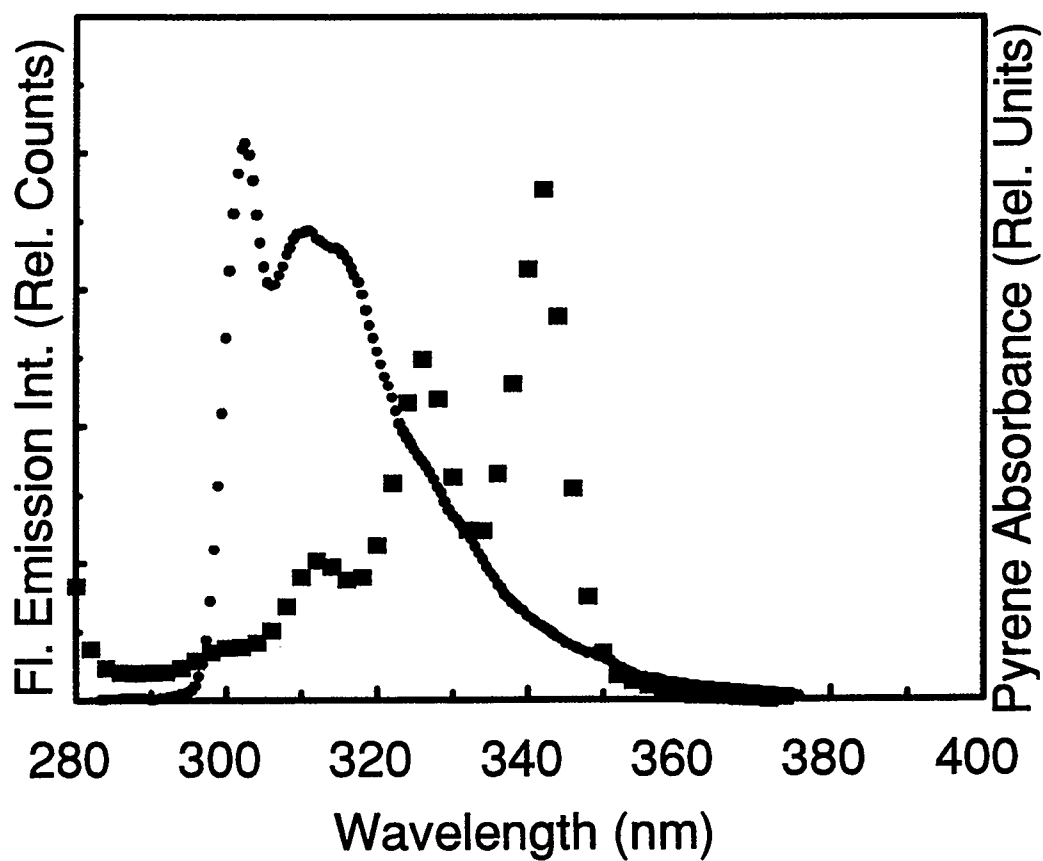


Figure V-3. The overlap of the fluorescence emission of fluorene (dots) with the absorption spectra of 1-pyrenemethanol (squares). The fluorescence emission spectra is uncorrected (excitation = 265 nm).

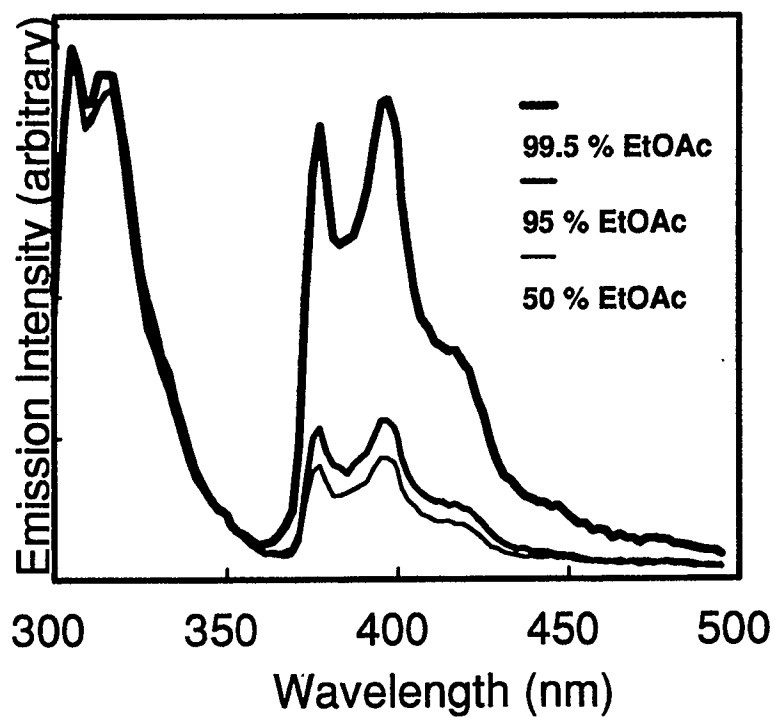


Figure V-4. Steady state fluorescence spectra of FI-PMMA-PHEMA-Py in ethyl acetate / methanol as a function of ethyl acetate content. Excitation wavelength selectively excites fluorene ($\lambda_{ex} = 290$ nm). Polymer concentration is 0.022 mg/ml for all samples.

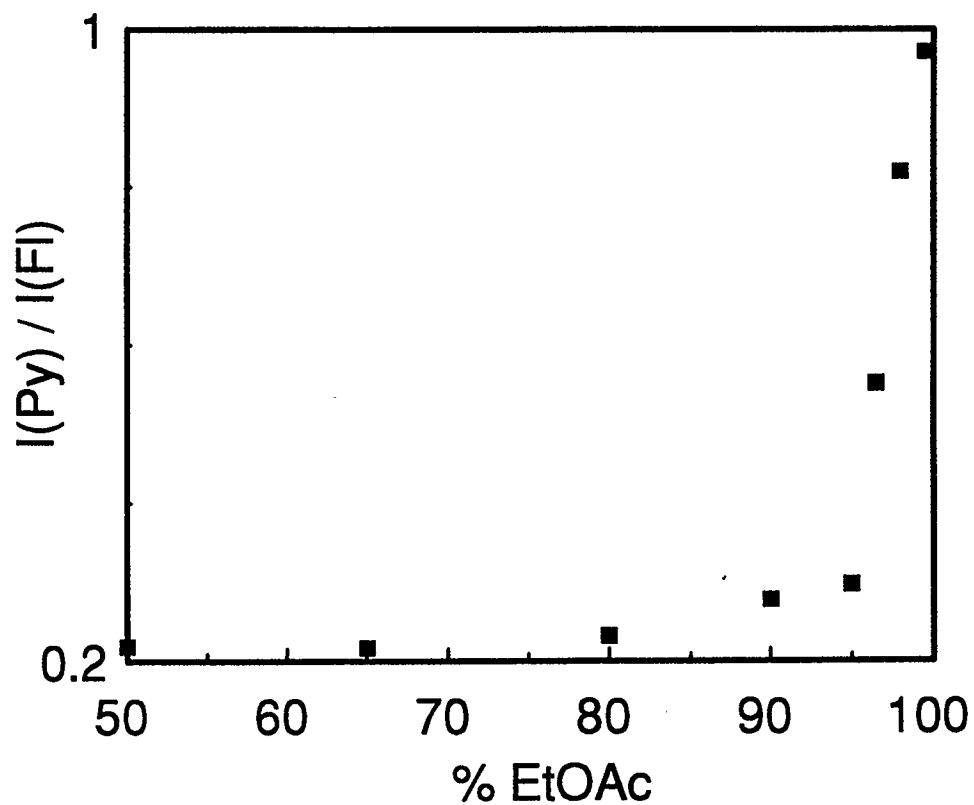


Figure V-5. Ratio of the fluorescence intensity areas of pyrene to that of fluorene for Fl-PMMA-PHEMA-Py in ethyl acetate / methanol as a function of ethyl acetate content. Excitation wavelength (λ_{ex}) is 290 nm. Polymer concentration is 0.022 mg/ml for all samples. Fluorene fluorescence is integrated from 300 to 365 nm and that of pyrene from 365 to 475 nm.

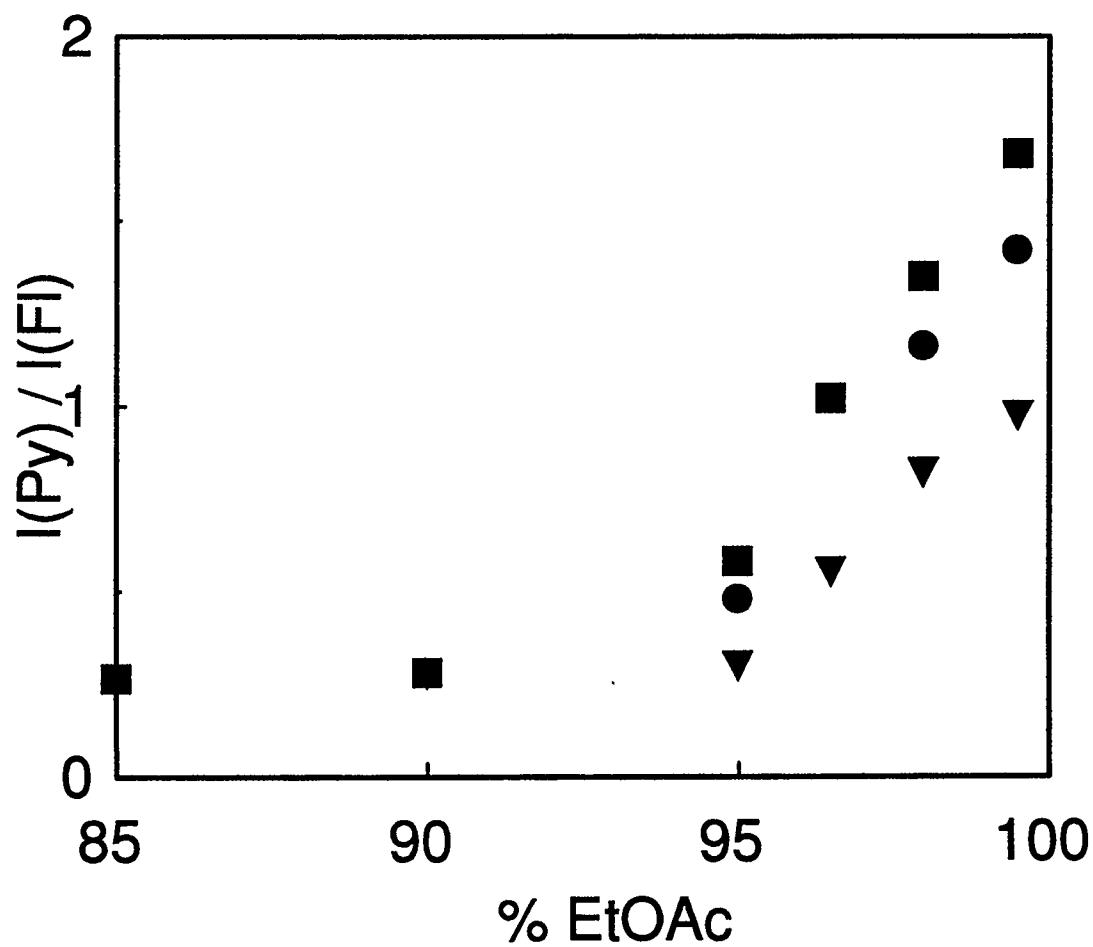
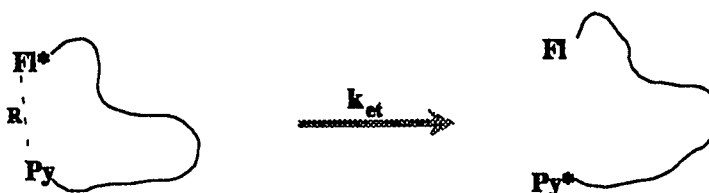


Figure V-6. Fluorescence intensity ratio ($I_{\text{Py}}/I_{\text{Fl}}$) for Fl-PMMA-PHEMA-Py for copolymer concentrations 0.022 mg/ml (triangles), 0.044 mg/ml (circles), and 0.110 mg/ml (squares).

reduction in oxygen quenching of pyrene fluorescence. Less oxygen quenching results in an increase in the steady state pyrene fluorescence intensity since the quantum yield of pyrene excitation is effectively increased. This is experimentally demonstrated in section V-2.d. below.

The third contributing factor is energy migration amongst the fluorene chromophores. Fluorene is able to transfer its exciton energy to other fluorene molecules because its fluorescence emission spectra overlaps with its with its light absorption spectra. For well solvated FI-PMMA-PHEMA-Py in dilute solution the amount of this type of transfer is negligible because the fluorene chromophores will on average be too far apart. Micellization of the copolymer aggregates many of the copolymer chains together and the fluorene chromophores attached to the corona chains will be closer than R_0 for energy migration. The exciton energy of fluorene can migrate from fluorene to fluorene until a favourable fluorene - pyrene interaction occurs and the exciton energy is transferred to pyrene. The overall result is an increase in the pyrene fluorescence intensity.



$$k_{et} = \frac{\left(\frac{R_0}{R}\right)^6}{\tau_D}$$

V-2.c. Time Correlated Single Photon Counting Fluorescence Spectroscopy

In the two sections above the formation of diblock copolymer micelles in certain solvent systems was measured by dilute solution viscometry, dynamic light scattering, and steady state fluorescence energy transfer. In order to further elucidate the reasons for the change in the properties of the fluorescent chromophores attached to PMMA-PHEMA, the fluorescence lifetime of the pyrene labels was measured.

The UV-Visible and fluorescence emission spectra of pyrene are shown in Figure V-7. It shows absorption maxima at 326 and 343 nm for 1-pyrenemethanol and fluorescence emission maxima at 387 and 398 nm. For time correlated single photon counting (TCSPC) experiments pyrene was excited at 343 nm and its fluorescence emission was monitored at 387 nm. A TCSPC fluorescence emission decay spectra for this polymer is shown in Figure V-8. Most of the fluorescence experiments were done under atmospheric conditions. Some experiments were done under an argon atmosphere using the freeze-thaw method to remove oxygen. This was done to determine the effect of oxygen quenching on (I_{Py}/I_{Fl}) . These experiments are described in section V-2.d. below. Freeze-thaw cycles were normally avoided because the process may induce copolymer micellization or change the aggregation number of existing micelles.

Pyrene fluorescence intensity decay was recorded as a function of both solvent composition and of polymer concentration. The time resolved fluorescence intensity curves were fitted by the deconvolution method⁷¹ using a sum of three exponential terms (equation IV-12). The average fluorescence lifetime τ was calculated by equation II-23.

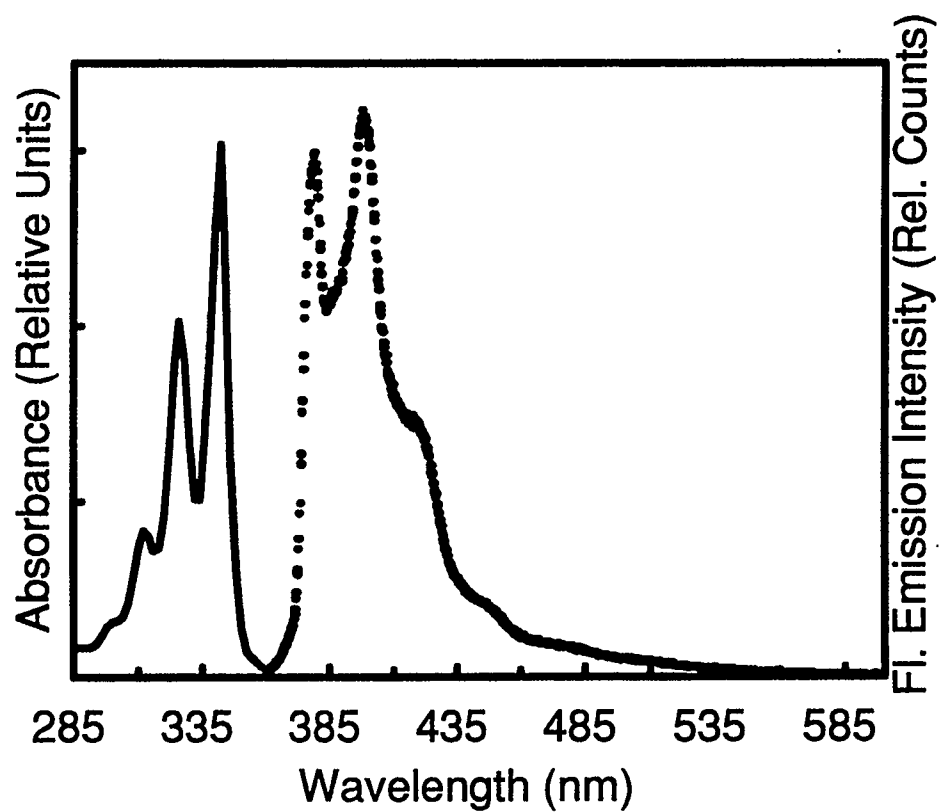


Figure V-7. The UV-Visible absorption (solid line) spectra of 1-pyrenemethanol in THF and fluorescence emission spectra of FI-PMMA-PHEMA-Py (circles) in 1:1 ethyl acetate / methanol. Pyrene was excited at 343 nm and the fluorescence emission spectra was uncorrected.

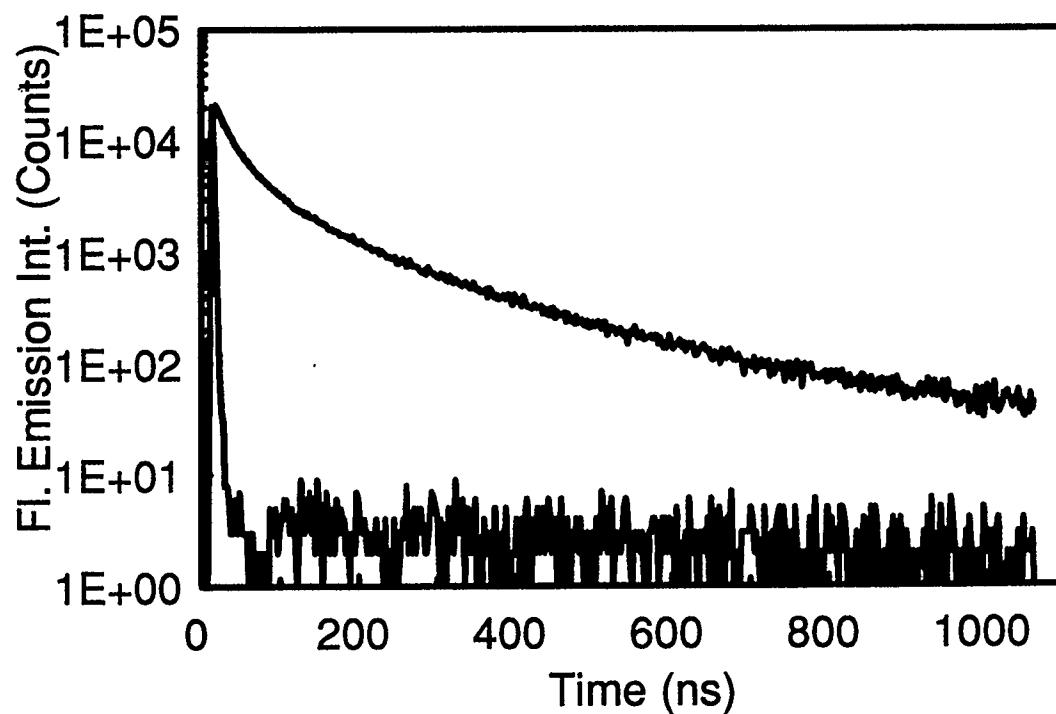


Figure V-8. Fluorescence emission decay curve of pyrene attached to FI-PMMA-PHEMA-Py. The pyrene chromophores are in copolymer micelle cores. Solution is 1.52 mg/ml of copolymer in 95 % EtOAc. The solution was not de-oxygenated and the measured average fluorescence lifetime is 43.9 ns. The profile of the flash lamp source is also shown.

The calculated average lifetimes are shown in Figure V-9 as a function of solvent composition at a polymer concentration of 0.022 mg/ml. Upon the onset of micellization the average lifetime of pyrene increases. For solvent mixtures of between 50 % to 85 % ethyl acetate the average lifetime is fairly constant at 24 ns but increases up to 90 ns in the micellar regime. The general form of these sets of results mirrors very closely those of the steady state fluorescence results and this suggests that one of the reasons for the increase in the observed I_{Py}/I_{Fl} is an increase in the fluorescence lifetime of pyrene.

The calculated average pyrene fluorescence lifetimes are shown in Figure V-10 as a function of solvent composition and polymer concentration. The magnitude of the increase in the fluorescence intensity ratio (I_{Py}/I_{Fl}) upon micellization increases as the concentration of the copolymer increases. Figure V-11 shows the fluorescence lifetime of pyrene in 95 % and 50 % ethyl acetate copolymer solutions as a function of copolymer concentration. The well solvated copolymer has a pyrene fluorescence lifetime that remains roughly constant. At 0.022 mg/ml the fluorescence lifetime was 24 ns and it decreases to 19 ns at 5.0 mg/ml. This decrease in the fluorescence lifetime is likely due to an increased amount of fluorene fluorescence quenching by the carbonyl groups on the polymer backbones of other polymer chains. At higher copolymer concentrations this interaction is more likely for the well solvated case. The pyrene fluorescence lifetime in the 95 % ethyl acetate experiments was always greater than that of the corresponding 50 % ethyl acetate solution and the fluorescence lifetime increased with higher copolymer concentration. This is consistent with the closed association model of diblock copolymer

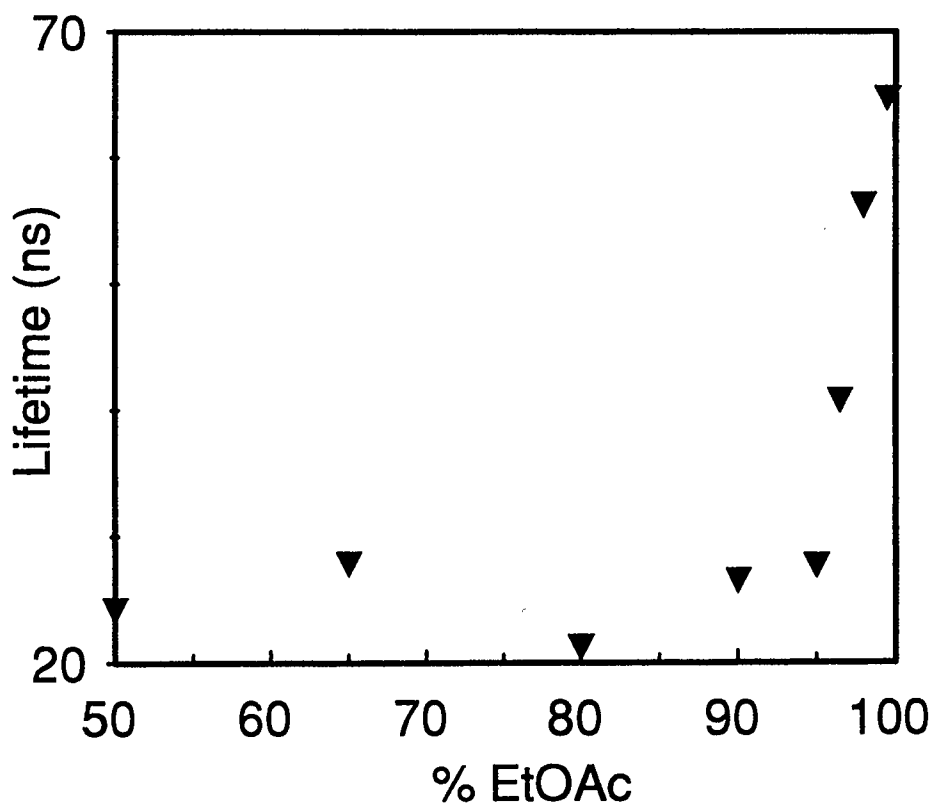


Figure V-9. Fluorescence lifetimes of pyrene attached to FI-PMMA-PHEMA-Py in ethyl acetate/methanol as a function of ethyl acetate content. Excitation wavelength selectively excites pyrene ($\lambda_{ex} = 343$ nm, $\lambda_{em} = 387$ nm). Polymer concentration is 0.022 mg/ml for all samples. Samples were measured under ambient conditions.

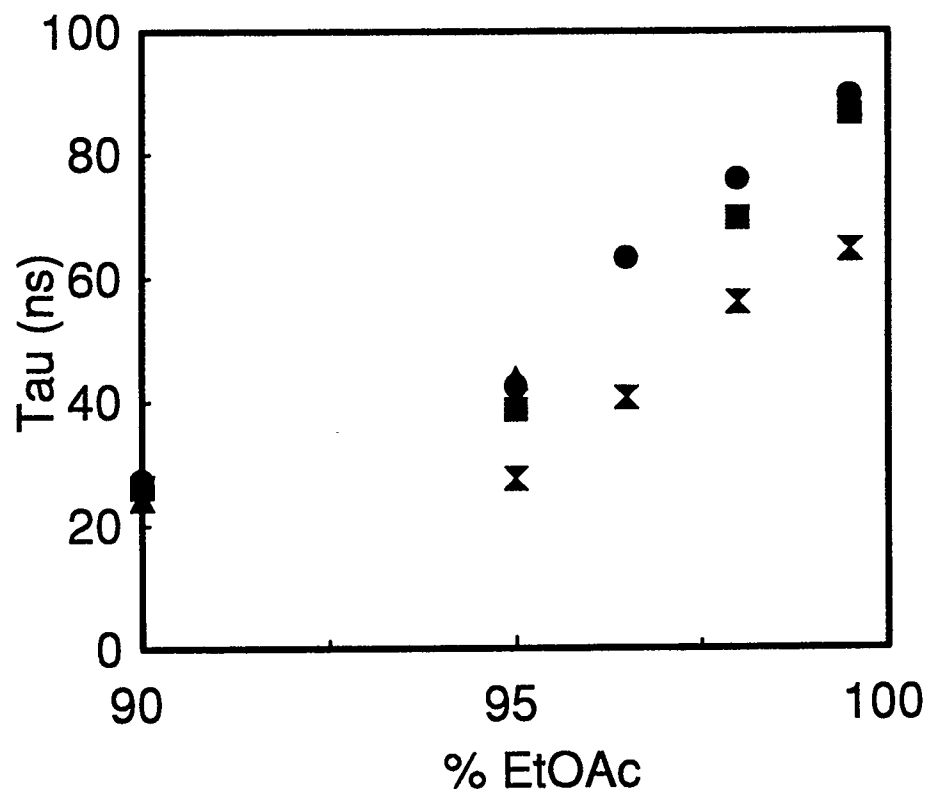


Figure V-10. Pyrene average fluorescence lifetimes vs. ethyl acetate content. Results from copolymer concentrations are 0.022 mg/ml (ties), 0.044 mg/ml (squares), 0.110 mg/ml (circles) and 1.52 mg/ml (triangles).

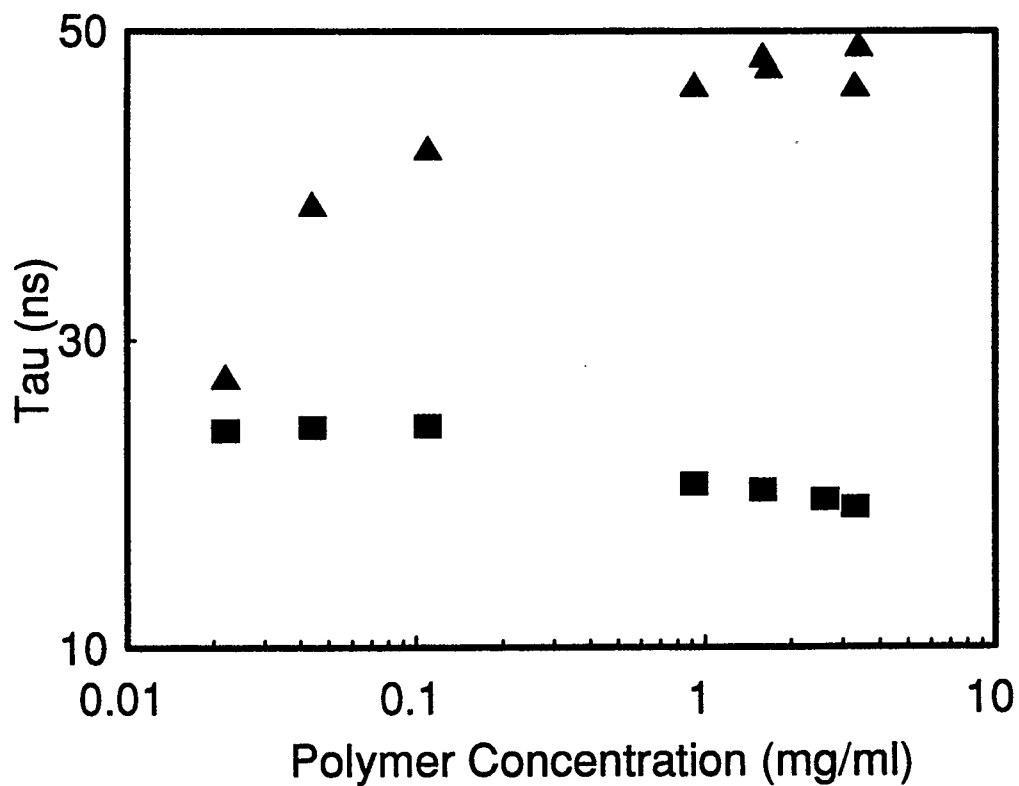


Figure V-11. Fluorescence lifetime of pyrene versus FI-PMMA-PHEMA-Py polymer concentration for 95 % ethyl acetate micelle solutions (triangles) and for 50 % ethyl acetate polymer solutions (squares). Excitation = 343 nm, emission = 387 nm. The lifetime of pyrene increases with concentration for the 95 % ethyl acetate solutions as a greater percentage of the polymer is in the micellar phase.

micellization. It is assumed that below the CMC the copolymer chains will be molecularly dispersed and above the CMC all of the additional copolymer will aggregate into micelle structures. Thus at higher concentrations a higher percentage of the copolymer chains will be aggregated into micelles and their associated pyrenes would have longer fluorescence lifetimes. Since the overall pyrene fluorescence lifetime is a weighted average of all the contributing chromophores, at copolymer concentrations the pyrene lifetime should be higher. The pyrene fluorescence lifetime converges to 50 ns for 95 % ethyl acetate solutions.

V-2.d. Oxygen Quenching of Fluorescence in PMMA-PHEMA Micelles

The fluorescence emission intensity ratio (I_{Py}/I_{Fl}) was shown, in Section V-2.c, to increase in proportion to the value of the fluorescence lifetime of pyrene. The role that dissolved oxygen plays in the above experiments is demonstrated by removing oxygen and repeating the experiments. Oxygen was replaced with argon with three freeze/pump/thaw cycles. Pyrene fluorescence lifetimes (Table V-3) and I_{Py}/I_{Fl} (Table V-2) were measured for copolymer samples in 50 % and 95 % ethyl acetate solutions were measured under atmospheric conditions and under argon. The lifetime of pyrene under argon increases upon the onset of micellization by 25 %. Under atmospheric conditions the corresponding increase is 264 %. This is also reflected in the steady state fluorescence results. The ratio of the fluorescence intensities (I_{Py} / I_{Fl}) increases 106 % under argon and increases 498 % under atmospheric conditions. It is concluded that oxygen quenching plays a significant

Table V-2. Effect of Oxygen on the Fluorescence Intensity Area Ratios. Polymer concentration = 0.116 mg/ml. Excitation wavelength (λ_{ex} = 290 nm). Argon samples were subjected to three times freeze-thaw treatment to remove atmospheric oxygen.

	50 % EtOAc (I_{Py}/I_{Fl})	99.5 % EtOAc (I_{Py}/I_{Fl})	Ratio Increase (%)
atmospheric O ₂	.281	1.68	498
Argon	1.61	3.31	106

Table V-3. The Effect of Oxygen on the Lifetime of Pyrene Fluorescence. Polymer concentration = 0.116 mg/ml, λ_{ex} = 343 nm, λ_{em} = 387 nm. Argon samples were subjected to three times freeze-thaw treatment to remove atmospheric oxygen.

	Pyrene lifetime (τ) 50 % EtOAc	Pyrene lifetime (τ) 99.5 % EtOAc	% increase in pyrene lifetime
atmospheric O ₂	24.5 ns	89.3 ns	264
Argon	168.1 ns	210.6 ns	25

role in the increase in the pyrene fluorescence lifetime which results in an increase in I_{Py}/I_{Fl} for copolymer micelles. Diffusion of oxygen to pyrene chromophores in the cores of micelles is reduced and this results in an increased pyrene fluorescence lifetime and intensity. There is an increase in the fluorescence intensity area ratio for micelles under argon atmosphere. The increase in the fluorescence lifetime under these conditions is 25 % but the increase in the intensity area ratio is 106 %. This extra increase is the result of the reduced distance between the two chromophores upon micellization.

V-3. Summary

PMMA-PHEMA micelles formed in 90 % or greater ethyl acetate were well characterized by viscometry, and light scattering. The aggregation numbers and hydrodynamic radius were measured for a number of solvent systems. It has been shown that non-radiative energy transfer between the two chromophores and time dependent fluorescence can also be used to detect the formation of micelles in selective solvents. The above series of experiments show large changes in the observed I_{Py}/I_{Fl} upon the onset of micellization. The reasons for the increase in pyrene fluorescence intensity upon the onset of micellization are reduced oxygen quenching in the core of micelles, an increased energy transfer rate between fluorene and pyrene and an increase in the energy migration between fluorene chromophores. The increased rate of energy transfer is the result of a reduced distance between fluorene and pyrene upon the formation of micelles. The fluorescence

properties of the pyrene chromophores on FI-PMMA-PHEMA-Py can be used to explain the similar behavior of pyrene on the other copolymers used in this research.

In summary, micelles of this copolymer in ethyl acetate and methanol have been well characterized. Selective solvent systems have been determined and micellization of PMMA-PHEMA occurs in systems containing more than 90 % ethyl acetate in methanol. The fluorescence properties of FI-PMMA-PHEMA-Py are well suited for chain exchange kinetics studies. The fluorescence quantum yield of the pyrene chromophore increased significantly upon incorporation into copolymer micelles. For these studies to proceed it would be necessary to synthesize a matching unlabelled copolymer and to determine the CMC of the copolymer in the solvent system of choice.

CHAPTER VI: PS-PHEMA MICELLES

VI-1. Introduction

The chain exchange rate of PMMA-PMAA micelles in ethyl acetate / methanol was measured in Chapter IV by following the increase in the fluorescence emission intensity of pyrene. Some of the factors that contributed to the increase in fluorescence intensity upon micellization were delineated in Chapter V. In this chapter, the properties of PS-PHEMA micelles will be examined.

PS-PHEMA micelles are interesting because micelles are formed over a wider range of solvent mixture ratios and therefore the effect of the solvent quality on the micelle chain exchange rate could be examined over a much greater range with this system. PS-PHEMA formed micelles in cyclohexane / THF from 20 to 75 % v/v cyclohexane, with the HEMA block in the core.

PS-PHEMA micelle chain exchange experiments were done by procedures similar to those described in Chapter IV. PS-PHEMA micelles were characterized by dilute solution viscometry and dynamic light scattering. TCSPC fluorescence measurements on pyrene chromophores, attached at the junction point between the two blocks of the copolymer, were made at several solvent mixture ratios to confirm the solvent compositions that result in micelle formation. The CMC of Polymer VI-1b (Section III-3.c.) in 20 % cyclohexane was also found by TCSPC fluorescence measurements. Micelle chain exchange rates were monitored by the pyrene fluorescence emission intensity and

were done at both room and elevated temperatures. Energy transfer measurements were also used in micelle chain exchange experiments between micelles labelled with energy donors and energy acceptors respectively.

VI-2. Theory

VI-2.a. Dynamic Chain Exchange Experiments by Pyrene Fluorescence Intensity

The theory and experimental procedure follows closely that of sections IV-2.a and IV-2.b. In this experiment, pyrene was at the junction between the two blocks of the copolymer. Pyrene however was still expected to increase in quantum yield upon incorporation into micelles from the unimer pool. It was the rate of this increase that was measured. The pyrene fluorescence emission intensity data was fitted to equation IV-13 with the fitting parameters κ' and k . The CMC was determined by TCSPC measurements of the pyrene chromophore as a function of copolymer concentration.

VI-3. Experimental

VI-3.a. Characterization of Micelles

THF is a good solvent for both PS and PHEMA while cyclohexane is a poor solvent for PHEMA and a theta solvent at 34.5 °C for PS. Dilute solution viscometry and dynamic light scattering were used for the characterization of Polymer VI-1a and Polymer VI-2a micelles in a range of cyclohexane / THF solvent systems. These results are presented in Tables VI-1 and VI-2 and Figure VI-1 and VI-2. The dynamic light

scattering experiments were performed on 2 mg/ml solutions. The experiments were done at 22 ± 0.5 °C, using a 514.5 nm source and at a scattering angle θ of 135°. The hydrodynamic radii were calculated using eqn. V-1 and the aggregation numbers were calculated using eqn. II-8.

The aggregation numbers for PS-PHEMA(100) and for PS-PHEMA(300) were reasonably constant over most of the range of solvent compositions. For PS-PHEMA(100) the aggregation number was about 85 and for PS-PHEMA(300) it was 135. A small amount of phase separation occurred for the samples of PS-PHEMA(100) in 70 and 75 % cyclohexane.

VI-3.b. Time Resolved Fluorescence Spectroscopy

The pyrene fluorescence intensity decay spectra were recorded as a function of solvent composition for Polymer VI-1b. The copolymer concentration was about 1 mg/ml to ensure that any micellar solutions were well above the CMC of the copolymer and that the signal intensity was strong. The results are presented in Figure VI-3 and they show that the polymer was in a micellar phase for solutions between 10 % to 60 % cyclohexane. The pyrene chromophores were excited at 343 nm and the emission decay was monitored at 387 nm. The time resolved intensity was fitted by the deconvolution using a sum of three exponential terms (see equation IV-14). The average fluorescence lifetime τ was calculated as per equation II-23.

Upon the onset of micellization the average lifetime of pyrene increases significantly. This experiment confirms the results of the viscometry experiments as an

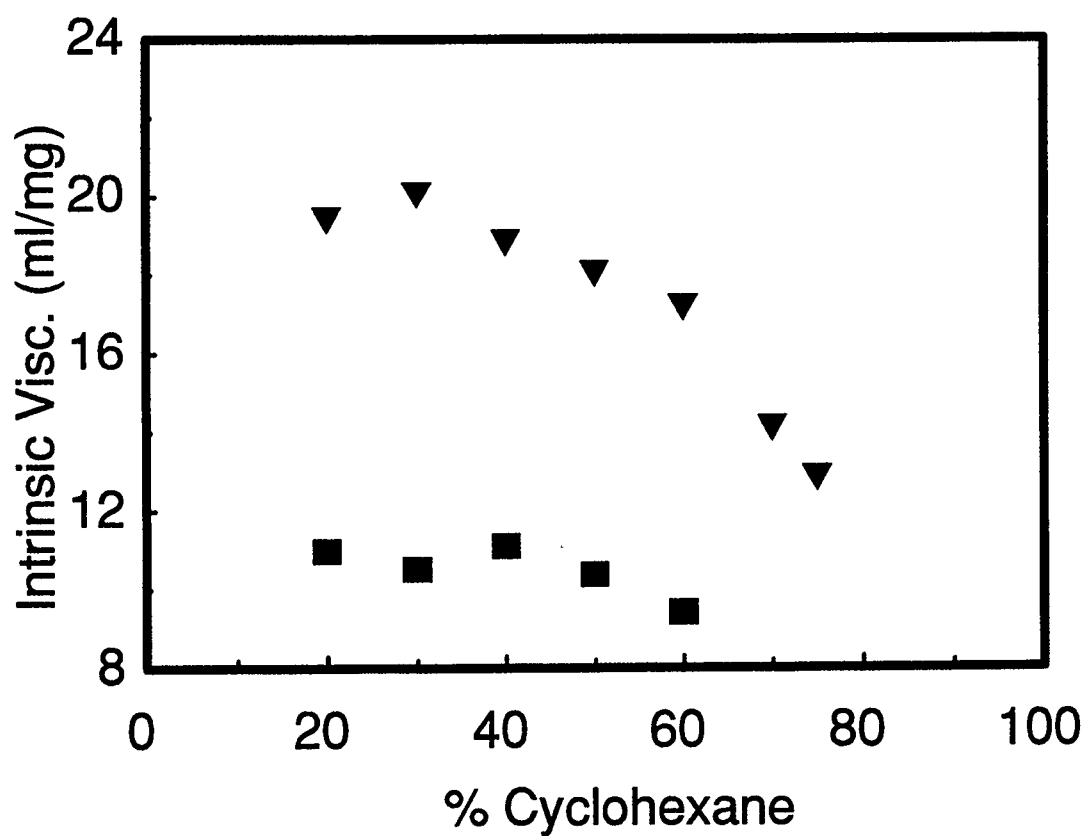


Figure VI-1. Intrinsic viscosity versus solvent composition for PS-PHEMA. Polymer VI-1a (squares) and Polymer VI-2a (triangles) are shown.

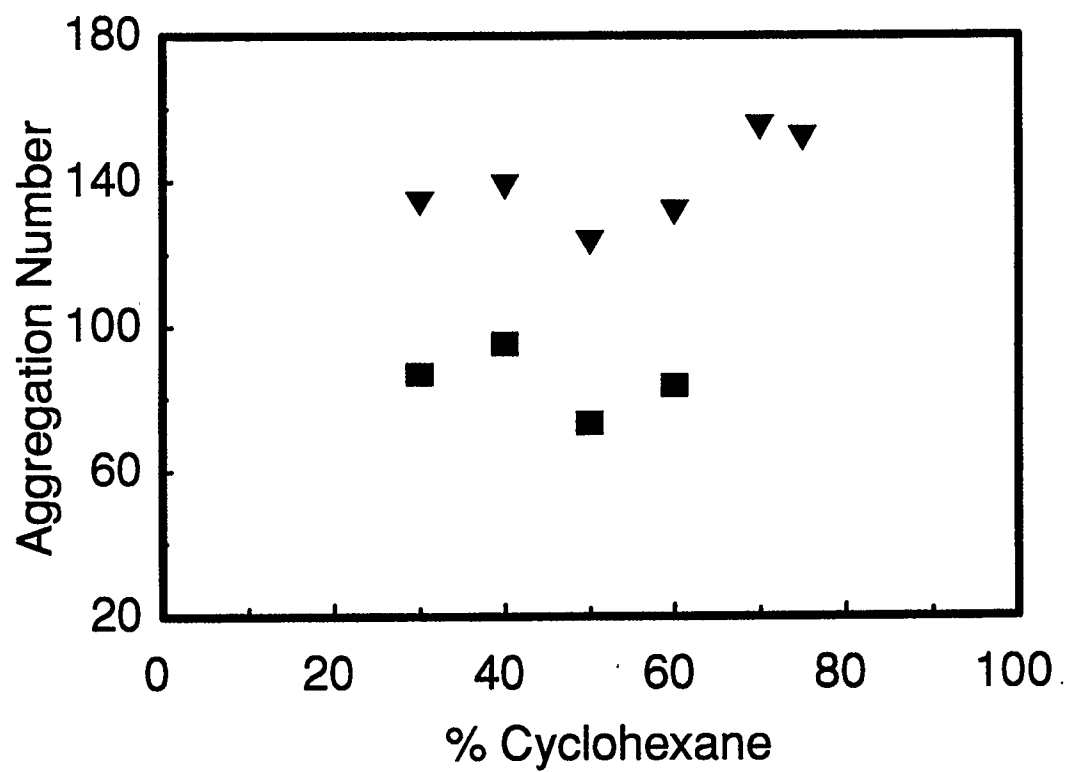


Figure VI-2. Aggregation number versus solvent composition. Polymer VI-1a (squares) and Polymer VI-2a (triangles) are shown.

increase in the fluorescence lifetime of pyrene is seen for samples in 20 to 60 % cyclohexane.

The results of chapter IV indicated that diblock copolymer micelles in less selective solvent systems experience faster chain exchange with unimers. Therefore, for chain exchange experiments with PS-PHEMA, the first kinetic experiments were attempted with 20 % cyclohexane micellar solutions. It was necessary to determine the CMC of the copolymer in the solvent system to be used to set the experimental conditions properly. The CMC was determined by measuring the fluorescence lifetime of pyrene chromophores of Polymer VI-1b as a function of copolymer concentration in 20 % cyclohexane / 80 % THF. The results are shown in Figure VI-4. The CMC of this solvent system and copolymer was about 0.01 mg/ml.

VI-3.c. Dynamic Chain Exchange Rate Experimental Results

Dynamic chain exchange experiments with PS-PHEMA were done in a similar manner to those done in chapter IV. The smaller chain diblock copolymer was chosen because faster chain exchange was expected. For this set of experiments the CMC was previously determined to be 0.01 mg/ml (5×10^{-7} M).

The concentration of the labelled unimer solution was 1.16×10^{-3} mg/ml (5.25×10^{-8} M, ~ 0.1 CMC) and that of the unlabelled micelle solution was 0.16 mg/ml (5.6×10^{-6} M, 10 CMC) The experiment was run for 24 hours with only just perceptible gains in the fluorescence intensity of pyrene. At this point the sample along with a magnetic stirring bar were sealed in a glass ampoule. The sample was heated with stirring at 51 °C for 1

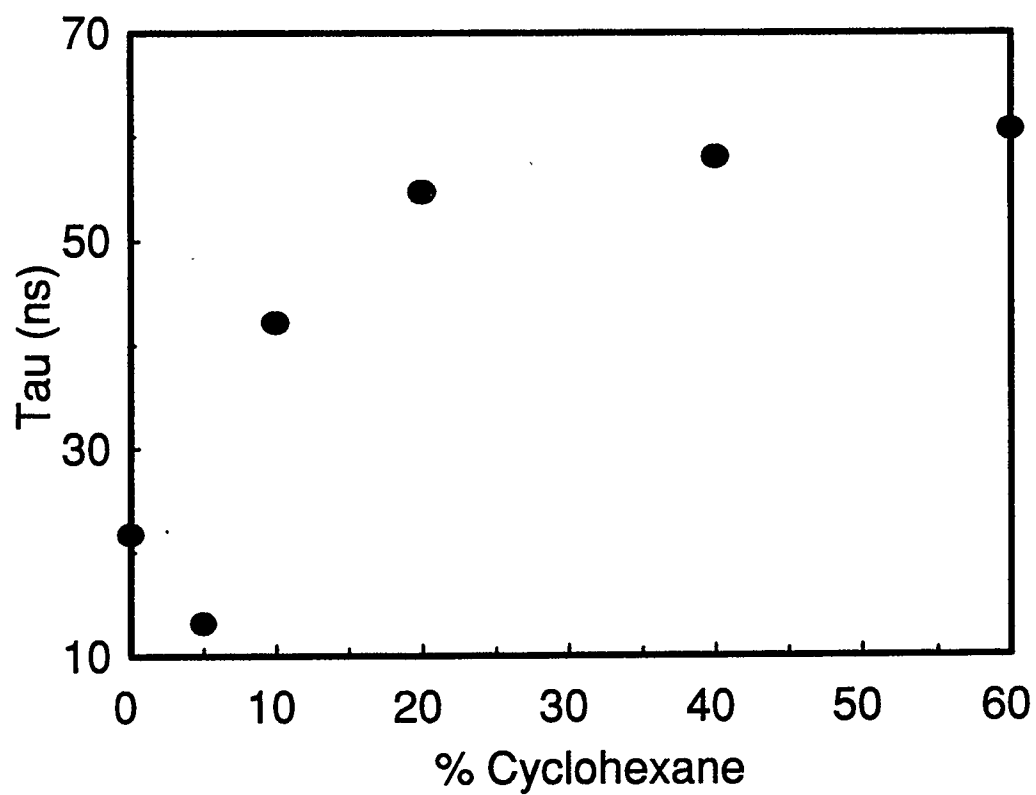


Figure VI-3. Average lifetime of pyrene chromophore on Polymer VI-1b versus solvent composition. The copolymer is in a micellar solution for samples with 20 % to 60 % cyclohexane.

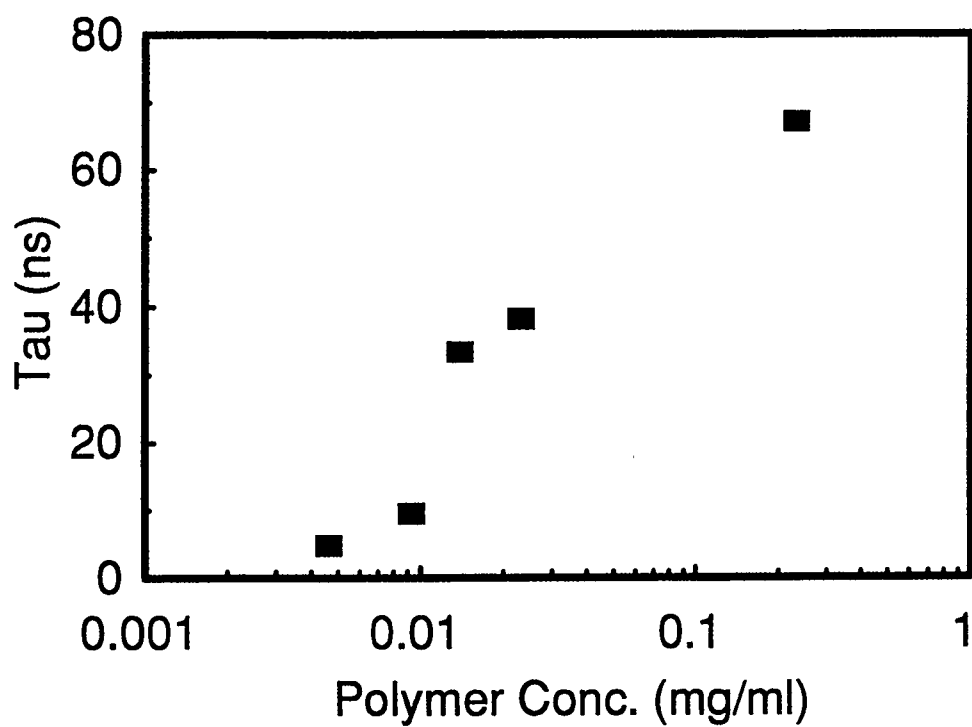


Figure VI-4. Average fluorescence lifetime of pyrene chromophores of Polymer VI-1b versus copolymer concentration for 20 % cyclohexane / 80 % THF solutions.

Table VI-1. Characterization of Unlabelled PS-PHEMA Diblock Copolymer Micelles for Polymer VI-3a. [PS-PHEMA(300)]

% C6H12	q (10^5 cm^{-1})	η_{solvent} (cp)	Γ (10^4 s^{-1})	R_h (\AA)	$[\eta]$ (ml/g)	p
75	3.213	.7267	1.059	290	12.84	152
70	3.211	.6972	1.062	301	14.10	155
60	3.207	.6474	1.127	305	17.18	132
50	3.202	.6064	1.161	303	18.04	123
40	3.197	.5731	1.207	320	18.83	139
30	3.193	.5448	1.253	323	20.06	134
20	3.188	.5215	1.252	337	19.42	157

Table VI-3. Characterization of Unlabelled PS-PHEMA Diblock Copolymer Micelles for Polymer VI-1a. [PS-PHEMA(100)]

% C6H12	q (10^5 cm^{-1})	η_{solvent} (cp)	Γ (10^4 s^{-1})	R_h (\AA)	$[\eta]$ (ml/g)	p
60	3.207	.6474	2.50	137	9.42	84
50	3.202	.6064	2.69	136	10.38	73
40	3.197	.5731	2.55	151	11.12	95
30	3.193	.5448	2.80	144	10.53	87
20	3.188	.5215	3.22	131	10.99	62

hour. The sample was then allowed to cool to room temperature for 30 minutes and exposed to the atmosphere to ensure that the equilibrium amount of oxygen was dissolved again in the sample. The fluorescence intensity of pyrene measured to be about 60 % of the anticipated gain expected of full labelled unimer chain incorporation.

VI-3.d. Dynamic Chain Exchange in 10 % Cyclohexane Solution

The above experiment was repeated in 10 % cyclohexane / 90 % THF solution. The average fluorescence lifetime of pyrene in 10 % cyclohexane was measured to be 42.2 ns and therefore the copolymer was in a micellar dispersion. The CMC of PS-PHEMA in 10 % cyclohexane was measured and found to be about the same as in 20 % cyclohexane. The experiment was set up in the same manner as section VI-3.a. above. Again, there was little measurable change in the pyrene fluorescence intensity over a number of hours. It was concluded that at room temperature there was little chain exchange.

VI-3.e. Micelle Chain Exchange by Energy Transfer

Chain Exchange between micelles of PS-PHEMA (Polymer VI-1a.) labelled by pyrenebutyric anhydride and labelled by fluorene acetic anhydride were measured by the increase in the fluorescence energy transfer in an experiment that was similar to that of others^{23,24}. This experiment was conducted in 75 % THF / 25 % cyclohexane. The sample of PS-PHEMA(FI) was labelled randomly with the fluorene chromophore on 2.4 %

of the HEMA blocks and the sample labelled with pyrene chromophores was labelled randomly on 4.0 % of the HEMA blocks.

Micellar solutions of the differently labelled copolymers were prepared separately. The fluorene labelled copolymer solution was prepared at a concentration of 0.23 mg/ml and the pyrene labelled copolymer solution was prepared at a concentration of 0.046 mg/ml. Both solutions were well above the CMC for this solvent composition. The two solutions were mixed and the fluorescence emission intensity of both fluorene and pyrene were monitored periodically. The fluorene chromophores were selectively excited at 290 nm. Very little change was observed after two hours of stirring at room temperature. The mixed sample was then heated at 50 °C for 1.25 hours and the steady state fluorescence was measured again in the same manner as before. The amount of pyrene fluorescence increased indicating some unimer chain exchange.

VI-4. Summary

VI-4.a. PS-PHEMA Micelle Characterization

For solutions with cyclohexane content of 20 to 75 % the sizes of Polymer VI-2a micelles are larger than those of Polymer VI-1a, which is in agreement with the prediction of scaling theories¹⁵. Scaling theories have been used to derive relations between the length of a diblock copolymer and the size of “hairy” and “crew-cut” micelles. In a “hairy” micelle, the core block is much shorter than the corona one and the radius R of a

micelle is chiefly determined by the thickness of the corona, which scales as

$$R \propto m^{4/25} n^{3/5} \quad \text{VI-2}$$

where m and n represent the number of units in the core and corona block, respectively.

In a crew-cut micelle, the radius R , now governed by the core size, scales according to :

$$R \propto m^{2/3} \quad \text{VI-3}$$

With our samples, the lengths of the core and corona blocks are comparable and no simple scaling relations exist between R and n and m . One would intuitively expect R to increase with n and m .

As the solvent quality for the PHEMA block worsens, the hydrodynamic radius R_h decreases for Polymer VI-2a micelles but remains constant for Polymer VI-1a micelles. These results seem to contradict the theoretical prediction of Munch and Gast^{8,9}. Their numerical analysis showed that as the solvent quality for the core block worsened, the corona thickness increased, the core diameter decreased, and the overall radius of the micelle, e.g. R_h , increased. The possible reason for the discrepancy is that our experimental situation is different from what was examined by Munch and Gast. They examined the effect of adding a solvent which was a poor solvent for the core forming block and a good solvent for the corona block on the change of micelle sizes.

Cyclohexane at room temperature borders between a theta and a poor solvent for PS. The theta temperature is 34.5 °C. As more cyclohexane is added to the polymer solution, the corona layer may not expand as much as it would in a good solvent. This hypothesis seems to explain the R_h results of Polymer VI-1a micelles. The molar mass of the PS block of Polymer VI-1a is only $\sim 1.0 \times 10^4$ g/mole. Cyclohexane may be reasonably good for PS with such a low molar mass. Upon the addition of cyclohexane, the PS block of Polymer VI-1a may expand more significantly than in the Polymer VI-2a case, which makes R_h of Polymer VI-1a micelles relatively constant at all cyclohexane concentrations.

Examination of R_h distribution of Polymer VI-1a and VI-2a micelles revealed that Polymer VI-2a formed more stable micelles. While Polymer VI micelles had a single peak R_h distribution at all solvent compositions examined, Polymer VI-1a was seen to form a small amount of aggregates with sizes larger than those of micelles at cyclohexane content above 60 %.

VI-4.b. Dynamic Chain Exchange Experiments

Dynamic chain exchange experiments at room temperature showed that little or no chain exchange occurred. When the samples were heated to 50 °C exchange did occur, both for the pyrene intensity experiment and for the energy transfer. This indicates that at lower temperatures exchange proceeds at a very slow rate and that the rate is quite sensitive to temperature. Experiments by other investigators in our research group show

that PS-PHEMA does not coat onto silica surfaces. Only diblock copolymers with some cinnamoyl pendant groups coated out.

The results of the energy transfer experiment (section VI-3.e) indicate that chain exchange would occur at elevated temperatures for micelle solutions in 75 % cyclohexane even though little or no exchange occurs at room temperature.

VII. CONCLUSIONS

The dynamics of the unimer - micelle equilibrium are a fundamental property of diblock copolymer micelles. The primary goals of this research were to confirm the rate law and to measure the polymer chain exchange constant. Steady state fluorescence emission intensity of pyrene was used to monitor the rate for PMMA-PMAA chains to migrate between the unimer and micelles in ethyl acetate / methanol directly and the values of k_p were found to be independent of the concentration of the micelle aggregates and that of the labelled unimer. The chain exchange rates values followed the expected trend of faster exchange in the less selective solvent (85 % ethyl acetate) than in the more selective solvent system (90 % ethyl acetate).

The exchange of PS-PHEMA in cyclohexane / THF was found to be much slower than that of the PMMA-PMAA systems at room temperature and in fact was only detectable at elevated temperatures. The reason for the slower exchange rate is not entirely clear. The CMC of PS-PHEMA in 20 % cyclohexane / 80 % THF was very close ($\sim 1.4 \times 10^{-2}$ mg/ml) to that of PMMA-PMAA in either 85 or 90 % ethyl acetate in methanol ($\sim 1.3 \times 10^{-2}$ mg/ml). Any differences in the systems are not reflected in the CMC values. The answer probably lies in the nature of the micelle cores themselves. The HEMA cores of the PS-PHEMA micelle system would have hydrogen bonding between different polymer units. There would be interactions between the alcohol, carbonyl and ester groups. Hydrogen bonding could have also occurred between the carboxylic acid

groups of the PMAA block cores of the PMMA-PMAA micelles. The strength of the hydrogen bonding in the case of the PS-PHEMA was likely stronger than that of the PMAA block due to the fact that there was methanol in the solvent system with the PMMA-PMAA micelles. Methanol would be preferentially absorbed into the cores of PMMA-PMAA micelles and would form hydrogen bonds with the PMAA polymer block. The interaction of PMAA with methanol would reduce the strength of interaction between groups on the polymer chain and reduce the attraction of the acid groups for each other. The result would be an increased rate of chain expulsion due to a lower energy barrier.

Micelle chain exchange experiments with PS-PHEMA at elevated temperatures should be attempted in the future. Care would have to be taken to ensure strict temperature control since the solubility of the fluorescence quencher oxygen in solvents is very sensitive to temperature. The problem of oxygen solubility could be circumvented by excluding oxygen and using a non-volatile and soluble fluorescence quencher such as an amine. The diffusion rate of soluble non-volatile fluorescence quenchers is also expected to be much slower in the cores of micelles and hence the fluorescence emission method for measuring the chain exchange rate should be viable.

The equilibrium dynamic properties of diblock copolymer micelles have important implications for the adsorption kinetics of these polymers onto surfaces. Adsorption from a selective solvent results in the formation of a polymer brush where one of the polymer blocks finds it thermodynamically favourable to adsorb. Diblock copolymer solutions with concentrations above the CMC will form micelles and this will complicate the

adsorption kinetics of the copolymer unto the surface. This is because it is the unimer phase that is adsorbed and micellization of the copolymer reduces the amount of unimer chains available for polymer adsorption.. Thus the rate that polymer chains are expelled from micelles will dictate the rate of surface adsorption of polymer.

Where k_p can be measured the value of k_p can be calculated if the concentration of the copolymer in the solvent phase and the CMC are known. The importance of the value of k_p has been demonstrated in our laboratory by coating experiments with PS-PHEMA and PS-PHEMA esterified with cinnamoyl chloride (PS-PCEMA). PS-PCEMA was found to adsorb onto silica surfaces from 60 % cyclohexane however unesterified PS-PHEMA did not and this may have been the result of the low rate of micelle chain exchange for PS-PHEMA.

The CMC of diblock copolymers in selective solvents has been determined by TCSPC fluorescence emission decay spectra. This technique for CMC determination has not been reported before. The magnitude of the change in the fluorescence lifetime of the chromophore upon micellization is also a good indication as to the amount of the change expected during the kinetic experiments.

Pyrene was proven to be a good choice for the fluorescent probe for these experiments. Pyrene has a high absorptivity and quantum yield which allows it to be used at the low concentrations required for these experiments. It also has a long intrinsic lifetime and this makes pyrene sensitive to changes in the diffusivity of oxygen.

Many other experiments are possible with the new fluorescence technique. It would be interesting to see the effect of elevated temperatures, and of the solvent composition at these elevated temperatures, on the exchange rate of PS-PHEMA in THF / cyclohexane solvent mixtures. It would be interesting to observe the differences in the chain exchange rates of this system as the solvent composition is changed from 20 % cyclohexane to 75 % cyclohexane. It is predicted that solvent systems with more cyclohexane would exhibit slower chain exchange rates at any particular temperature since they are more selective for the core forming PHEMA blocks.

PMMA-PMAA has an easily measurable exchange rate at room temperature in both 85 % and 90 % ethyl acetate. It would be possible to formulate relationships between the dimensions of the diblock copolymers and the exchange rates if polymers of different block lengths were synthesized. In particular these types of studies should be done on copolymers that form "hairy" micelles and "crew cut" micelles. The kinetic data on the hairy micelles should delineate the effect that the corona size has on the exchange rate and kinetic data on the crew cut micelles could provide the same for the core size.

It is highly desirable to find a diblock copolymer that will coat out on surfaces from an aqueous dispersion. The problem to date has been the very low rates of chain exchange that copolymer micelles exhibit in aqueous medium. It would be interesting to find copolymers that have detectable rates of chain exchange in water as this would point the way to a workable system.

In conclusion, a new experimental technique has been developed that can directly measure the chain exchange rate of diblock copolymer micelles. This procedure should prove useful in providing a more complete understanding of these systems both from a theoretical point of view and for practical applications.

BIBLIOGRAPHY

1. Price, C.; Stubbersfield, R. B.; El-Kafrawy, S.; Kendall, K.D. *Br. Polym. J.* 1989,21, 391.
2. Kotaka, T.; Tanaka, T.; Inagaki, H. *Polym. J.* 1972, 3, 327.
3. Bluhm, T. L.; Malhotra, S.L. *Eur. Polym. J.* 1986, 22, 249.
4. Quintana, J.R.; Villacampa, M.; Munoz, M.; Andrio, A.; Katime, A. *Macromolecules* 1992, 25, 3125.
5. Quintana, J.R.; Villacampa, M.; Munoz, M.; Andrio, A.; Katime, A. *Macromolecules* 1992, 25, 3129.
6. Quintana, J.R.; Villacampa, A.; Katime, I.A. *Macromolecules* 1993, 26, 601.
7. Elias, H.-G. In *Light Scattering from Polymer Solutions*; Huglin, M.B. Ed.; Academic Press: London, 1972.
8. Munch, M.R.; Gast, A.P. *Macromolecules* 1988, 21, 1360.
9. Munch, M.R.; Gast, A.P. *Macromolecules* 1988, 21, 1366.
10. Evans, D.F.; Ninham, B.W. *J. Phys. Chem.* 1986, 90, 226.
11. Zhu, J.; Eisenberg, A.; Lennox, R.B. *Macromolecules* 1992, 25, 6547.
12. Hunter, R.J. *Foundations of Colloid Science*; Clarendon: Oxford, 1986.
13. Tuzar, Z.; Kratochvil P., *Surf. Colloid. Sci.* 1992, 15, 1.
14. Halperin, A; Alexander, S. *Macromolecules* 1989, 22, 2403.
15. Halperin, A.; Tirrell, M.; Lodge, T.P. *Adv. Polym. Sci.* 1992, 100, 31.
16. Milner, S. *Science* 1991, 251, 905.
17. Liu, G.; Hu, N.; Xu, X.; Yao, H. *Macromolecules* 1994, 27, 3892.

18. Liu, G.; Xu, X.; Skupinska, K.; Hu, N; Yao, H. *J. Appl. Polym. Sci.* **1994**, 53, 1699. .
19. Aniansson, E.A.G.; Wall, S.N. *J. Phys. Chem.* **1974**, 78, 1024.
20. Aniansson, E.A.G.; Wall, S.N. *J. Phys. Chem.* **1975**, 79, 857.
21. Aniansson, E.A.G.; Wall, S.N.; Almgren, M.; Hoffman, H.; Kielmann, I.; Ulbricht, W.; Zana, R.; Lang, J.; Tondre, C. *J. Phys. Chem.* **1976**, 80, 905.
22. Bednar, B.; Edwards, K.; Almgren, M.; Tormod, S.; Tuzar, Z. *Makromol. Chem. Rapid Comm.* **1988**, 9, 785.
23. Prochazka, K.; Bednar, B.; Muktar, E.; Svoboda, P.; Trnena, J.; Almgren, M. *J. Phys. Chem.* **1991**, 95, 4563.
24. Wang, Y.; Kausch, C.M.; Chun, M.; Quirk, R.P.; Mattice, W.L. *Macromolecules* **1995**, 28, 908.
25. Duhamel, J.; Yekta, A.; Ni, S.; Khaykin, Y.; Winnik, M.A. *Macromolecules* **1993**, 26, 6255.
26. Tian, M.; Qin, A.; Ramireddy, C.; Webber, S.E.; Munk, P.; Tuzar, Z.; Prochazka, K. *Langmuir* **1993**, 9, 1741.
27. Honda, C.; Hasegawa, Y.; Hirunuma, R.; Nose, T. *Macromolecules* **1994**, 27, 7660.
28. Goodman, I. In *Developments in Block Copolymers, Vol 1*; Goodman, I. Ed.,, Applied Science Publishers: London and New York, 1982.
29. Riess, G.; Hurtrez, G.; and Bahadur, P. In *Encyclopedia of Polymer Sciences and Engineering, Vol. 2*, Mark, H. F.; Bikales, N.M.; Overberger Ch, G.; Menges, G. Eds.; 2nd edition, Wiley: New York, 1985, pp.324-436.
30. Morton, M. *Macromolecular Reviews* **1967**, 2, 71.
31. Szwarc, M. *Ions and Ion Pairs in Organic Reactions*; Wiley-Interscience: New York, 1972 and 1974; Vols.1 and 2.

32. Huggins, M.L. *J. Am. Chem. Soc.* **1942**, 64, 2716.
33. Flory, P. J. *J. Chem. Phys.* **1949**, 17, 303.
34. Krause, S. *J. Phys. Chem.* **1964**, 68, 1948.
35. Bovey F.A.; Tiers, G.V.D. *J. Polym. Sci.* **1960**, 44, 173.
36. Moore, J. C. *J. Polym. Sci.* **1964**, A2, 835.
37. Varshney, S.K.; Zhong, X.F.; Eisenberg, A. *Macromolecules* **1993**, 26, 701.
38. Zimm, B.H. *J. Chem. Phys.* **1948**, 16, 1093.
39. Zimm, B.H. *J. Chem. Phys.* **1948**, 16, 1099.
40. Mark, H. *Der feste Korper*; Hirxel: Leipzig, 1938, Pg.103.
41. Bushuk, W.; Benoit, H. *Can. J. Chem.* **1958**, 36, 1616.
42. Stockmayer, W.H.; Moore, L.D.; Fixman, M.; Epstein, B.N. *J. Polym.Sci.* **1955**, 16, 517.
43. Einstein, A., *Ann. Physik*, **1905**, 17, 549. and **1906**, 19, 289, 371. and **1911**, 34, 591.
44. Kuhn, W., *Kolloid-Z*, **1933**, 62, 260. and **1934**, 68, 2. and **1936**, 76, 258.
45. Young, R.J.; Lovell, P.A. *Introduction to Polymers, 2nd edition*; Chapman and Hall: New York, 1991, pg178-194.
46. Flory, P.J. *Principles of Polymer Chemistry*; Cornell University Press: Ithaca, New York, 1953.
47. Qin, A.; Tian, M.; Ramireddy, C.; Webber, S.; Munk, P.; Tuzar, Z. *Macromolecules* **1994**, 27, 120.
48. Kiserow, D.; Chan, J.; Ramireddy, C.; Munk, P.; Webber, S.E. *Macromolecules* **1992**, 25, 5338.
49. Khougaz, K.; Gao, Z.; Eisenberg, A. *Macromolecules* **1994**, 27, 6341.

50. Plestil, J.; Baldrian, J. *Makromol. Chem.* **1975**, 176, 1009.
51. Bluhm, T.L.; Whitmore, M.D. *Can. J. Chem.* **1985**, 63, 249.
52. Broadbent, G.; Brown, D.S.; Dawkins, J.V. *Polym. Comm.* **1987**, 28, 282.
53. Brown, D.S.; Dawkins, J.V.; Farnell, A.; Taylor, G. *Eur. Polym. J.* **1987**, 23, 463.
54. Candau, F.; Guenet, J.M.; Boutillier, J.; Picot, C. *Polymer* **1979**, 20, 1227.
55. Tuzar, Z.; Sikora, A.; Petrus, V.; Kratodhvil, P. *Makromol.Chem.* **1977**, 178, 2743.
56. Tuzar, Z.; Petrus, V.; Kratodhvil, P. *Makromol.Chem.* **1974**, 175, 3181.
57. Price, C. *Pure Appl. Chem.* **1983**, 55, 1563.
58. Price, C.; Hudd, A.L.; Booth, C.; Wright, B. *Polymer* **1982**, 23, 650.
59. Gilbert, F.A. *Disc. Farad. Soc.* **1955**, 20, 68.
60. Price, C.; Kendall, K.D.; Stubbersfield, R.B. *Poly. Comm.* **1983**, 24, 326.
61. Major, M.; Torkelson, J.M.; Brearley, A.M. *Macromolecules* **1990**, 23, 1700.
62. Almgren, M.; Alsins, J.; Bahadur, P. *Langmuir* **1991**, 7, 446.
63. Prochazka, K.; Kiserow, D.; Ramireddy, C.; Tuzar, Z.; Munk, P.; Webber, S.E. *Macromolecules* **1992**, 25, 454.
64. Prochazka, K.; Vajda, S.; Fidler, V.; Bednar, B.; Mukhtar, E.; Holmes, S. *J.Mol. Struct.* **1990**, 219, 377.
65. Chan, J.; Fox, S.; Kiserrow, D.; Ramireddy, C.; Munk, P.; Webber, S.E. *Macromolecules* **1993**, 26, 7016.
66. Calderara, F.; Hruska, Z.; Hurtrez, G.; Lersh, J.-P.; Nugar, T.; Riess, G. *Macromolecules* **1994**, 27, 1210.
67. Watanabe, A.; Matsuda, M. *Macromolecules* **1985**, 18, 273.
68. Watanabe, A.; Matsuda, M. *Macromolecules* **1986**, 19, 2253.

69. Yeung, A.; Frank, C.W. *Polymer* **1990**, 31, 2101.
70. Lakowicz, J.R. *Principles of Fluorescence Spectroscopy*; Plenum Press: New York and London, 1983.
71. O'Connor, D.V.; Phillips, D. *Time-Correlated Single Photon Counting*; Academic Press: London, 1984.
72. Forster, Th. In *Modern Quantum Chemistry*; Sinanoglu, O. Ed.; Academic Press: New York, 1965.
73. Collins, F.C.; Kimball, G.E. *J. Colloid Sci.* **1949**, 4, 425.
74. Chu, S.G.; Munk, P. *Macromolecules* **1978**, 11, 879.
75. Aminabhavi, T.M.; Munk, P. *Macromolecules* **1979**, 12, 607.
76. Zhulina, E.B.; Birshtein, T.M. *Vysokomol. Soedin.* **1985**, 27, 511.
77. Leibler, L.; Orland, H.; Wheeler, J.C. *J. Chem. Phys.* **1989**, 90, 5843.
78. Izzo, D.; Marques, C.M. *Macromolecules* **1993**, 26, 7189.
79. Cao, T.; Munk, P.; Ramireddy, C.; Tuzar, Z.; Webber, S.E. *Macromolecules* **1991**, 24, 6300.
80. de Gennes, P.-G. In *Solid State Physics*; Liebert, L., Ed.; Academic: New York, 1978; Suppl. 14.
81. Noolandi, J.; Hong, K.M. *Macromolecules* **1982**, 15, 482.
82. Noolandi, J.; Hong, K.M. *Macromolecules* **1983**, 16, 1443.
83. Whitmore, M. D.; Noolandi, J. *Macromolecules* **1985**, 185, 657.
84. Leibler, L.; Orland, H.; Wheeler, J.C. *J. Chem. Phys.* **1983**, 79, 3550.
85. Nagarajan, R.; Ganesh, K. *J. Chem. Phys.* **1989**, 90, 5843.
86. Hirao, A.; Kato, H.; Yamaguchi, K.; Nakahama, S. *Macromolecules* **1986**, 19, 1295.

87. Duhamel, J.; Yekta, A.; Hu, Y.Z.; Winnik, M.A. *Macromolecules* **1992**, 25, 7024.
88. Adkins, H.; Thompson, Q.E. *J. Amer. Chem. Soc.* **1949**, 71, 2242.
89. Quirk, R.P.; Shrock, L.E. *Macromolecules* **1991**, 24, 1237.
90. Varshney, S.K.; Hautekeer, J.P.; Fayt, R.; Jerome, R.; Teyssie, Ph. *Macromolecules* **1990**, 23, 2618.
91. Jung, M.E.; Lyster, M.A. *J. Amer. Chem. Soc.* **1976**, 99, 968.
92. Blumstein, R.; Murphy, G.J.; Blumstein, A.; Watterson, A.C. *J. Polym. Sci. Polym. Lett.* **1973**, 15, 21.
93. Swindells, J.F. In *Handbook of Chemistry and Physics* ; 60th Ed. Weast, R.C. Ed.; CRC Press: Boca Raton, 1980, pg. F-51.
94. Liu, G. *Can. J. Chem.* in press, Nov. 1995.
95. Castellan, G.W. *Physical Chemistry*, 2nd ed.; Addison - Wesley Publishing Company: Reading, Mass., 1971.
96. Kotaka, T.; Tanaka, T.; Inagaki, H. *Polymer J.* **1972**, 3, 327.
97. Liu, G.; Smith, C.K.; Hu, N.; Tao, J. accepted by *Macromolecules*.
98. Berlman, I.B. *Handbook of Fluorescence Spectra of Aromatic Molecules*; Academic Press: New York, 1971.